

THE UTILIZATION OF GRANULAR MEDIA FILTRATION AND RAPID
FLOCCULATION IN A MODIFIED JAR TEST PROCEDURE FOR DRINKING
WATER TREATMENT

by

Charles Sean King

A thesis submitted to the faculty of
The University of North Carolina at Charlotte
in partial fulfillment of the requirements
for the degree of Master of Science in
Engineering

Charlotte

2017

Approved by:

Dr. James Amburgey

Dr. Olya Keen

Dr. James Bowen

©2017
Charles Sean King
ALL RIGHTS RESERVED

ABSTRACT

CHARLES SEAN KING. The Utilization of Granular Media Filtration and Rapid Flocculation in a Modified Jar Test Procedure for Drinking Water Treatment. (Under the direction of DR. JAMES AMBURGEY)

Jar testing is one of the most common tools that water treatment facilities use to determine the treatment conditions necessary to meet finished water quality goals. A six-place stirrer is normally used for jar testing to provide identical mixing conditions while coagulant dose and pH vary in each jar to create “floc” that is removed via sedimentation. There are some utilities that are unable to utilize jar testing, since the current jar testing procedures do not identify optimum treatment conditions for their water supply. This is particularly true for those utilities treating low-turbidity, low-TOC waters because low coagulant doses can produce small floc that does not settle efficiently (even though it is removed efficiently by filters). A modified jar test procedure was developed with the goal of providing consistent and reliable results for all treatment facilities without having to make site-specific changes to the mixing speeds and times to try to match the plant performance. Instead of sedimentation, the modified jar test procedure uses a novel granular media filter along with a standardized mixing protocol and titrations to predict and control the pH of the coagulated water. Contour mapping of jar test data was utilized to provide a detailed visual description of zones of effective treatment. Research found that the application of direct filtration (instead of traditional sedimentation) reduced testing time and showed better correlation to treatment plant performance. A method of optimizing coagulant dose and coagulated pH based on titrations is proposed, which is

based on an alternating, single-variable optimization method with experimentally determined starting points. Treatment with coagulant only (i.e., without prior pH adjustment) limits the range of coagulation conditions a water treatment plant can operate at. Coagulants are acidic and their addition during treatment causes both the pH and coagulant dose to change simultaneously. Treating water with coagulant only provides only one diagonal path for treatment to occur across a two-dimensional area of pH and coagulant dose combinations, which sometimes misses optimal treatment conditions entirely.

ACKNOWLEDGMENTS

First, I would like to thank Dr. James Amburgey for his guidance over the course of my graduate school career as my advisor and committee chair. He has been the major contributor in my growth as a researcher and water treatment professional. His knowledge has been invaluable throughout this process. I genuinely appreciate the time he has taken to ensure the thoroughness of my research. I would also like to thank my committee members, Dr. James Bowen and Dr. Olya Keen, for their time, insight, and feedback with regards to this research as well as in the classroom.

I have the deepest gratitude for the contributions that Amir Alansari has made to this project. He was a major contributor from the initial stages, with his development and design of the filtration apparatus to being someone that I could bounce ideas and concerns off of. He that took time out of his busy schedule to routinely answer any questions or help solve any problems that arose during this research.

I would like to thank the entire staff at the Mt. Holly and Kannapolis utilities departments. The opportunities that were provided to me by allowing me to gain field experience at a full-scale facility has been vital to not only my research, but to my future as a professional. Specifically, I would like to thank Brian Wilson, Anna Ostendorff, Gina Miller, Alex Anderson, and Gerald Faulkner for their time and patience.

I would like to thank Dr. William Saunders and Mr. David Naylor for their advice during and prior to my time in the MSE program. They were both were very influential in my decision to pursue this endeavor.

For my family, there are no words that I can say that would describe the deep appreciation that I have. They have all have given me the support and self-assurance that I needed to accomplish the goals I have set for myself. I must give a special thank you to my grandfather, Bob King, for giving me the confidence to quit a well-paying job to pursue a more fulfilling path.

Finally, for my wife Elizabeth, I do not know where to begin. Her strength throughout this entire process has been unwavering. Her encouragement has been second to none. To say that I could not have done this without her would be untrue, but I would not have done this without her. She has been my eternal motivation during my time at the university. I will be forever grateful and indebted to her.

TABLE OF CONTENTS

LIST OF TABLES	x
LIST OF FIGURES	xi
LIST OF ABBREVIATIONS	xviii
CHAPTER 1: INTRODUCTION	1
CHAPTER 2: BACKGROUND	4
2.1 Coagulation	4
2.1.1 Coagulant Demand	7
2.1.1.1 Particulate Contaminants	7
2.1.1.2 Dissolved Natural Organic Matter	7
2.2 Jar Test	8
2.2.1 Sample Size and Container Geometry	9
2.2.2 Mixing in the Jar Test	10
2.2.2.1 Rapid Mix	10
2.2.2.2 Flocculation	12
2.2.3 Dosage Selection Criteria	14
CHAPTER 3: METHODS AND PROCEDURES	16
3.1 Filter Apparatus and Jar Test instrument	16
3.2 Filter Set-up and Maintenance	18
3.3 Jar Testing Procedure	19
3.3.1 Initial Setup and Titration Procedures	19
3.4 Sample Waters	23

3.5 SUVA and Dissolved Organic Carbon	25
3.6 Flocculation Mixing Analysis	27
3.7 Filter Loading Rate	32
3.7.1 Deep Filter Apparatus	32
3.7.2 Bench-Scale	34
CHAPTER 4: RESULTS AND DISCUSSION	35
4.1 Titration	35
4.2. Filter Loading Rate Optimization	39
4.2.1 Deep-Bed Filter Apparatus	39
4.2.2 Bench Scale Filtration Optimization	40
4.3 Mt. Holly Water	44
4.3.1 Natural Water #1	44
4.4 Natural Water #2	48
4.5 Model Water #2	58
4.5.1 Flocculation Procedure Optimization	58
4.5.1.1 Photometric Dispersion Analysis	58
4.5.1.2 Particulate Removal	63
4.6 Model Water #3	82
4.7 Coagulation Diagram Comparisons	87
4.7.1 Natural Water #2 Coagulation Diagram	87
4.7.2 Model Water #2 Coagulation Diagram	89
4.7.3 Model Water #3 Operational Diagram	93

4.8 Alternating Single-Variable Optimization Method	94
4.8.1 Hypothetical Jar Test	95
4.8.2 Bench-Scale Evaluation of the Alternating Single-Variable Method	109
CHAPTER 5: SUMMARY AND CONCLUSIONS	120
5.1 Summary	120
5.2 Conclusions and Recommendations	121
5.2.1 Conclusions	121
5.2.2 Recommendations	123
5.3 Recommendations for Further Research	124
REFERENCES	125
APPENDIX A: RESULTS FROM BENCH-SCALE FLOCCULATION ANALYSIS	128
APPENDIX B: JAR TEST PROCEDURE	139

LIST OF TABLES

Table 3.1. Syringe volume with corresponding coagulant dosages.....	21
Table 3.2. Jar Test Procedure Summary with mixing intensities and duration.	22
Table 3.3. Water quality parameters of experimental waters.	24
Table 3.4. Experimental waters and their respective descriptive names.	24
Table 3.5. Flow and loading rates used during flow rate analysis.....	34
Table 4.1. Temperature and pK_w	56
Table 4.2. Summary of the results from the series of hypothetical jar tests with results that fell within a zone of maximum observed treatment efficiency highlighted.	109
Table 4.3. Summary of the minimum observed filtered turbidity and its corresponding percent turbidity removal for each LITF with direct filtration contour plot.....	119

LIST OF FIGURES

Figure 2.1. Chemical reactions in alum coagulation (Pernitsky, 2003).....	5
Figure 2.2. Operational diagram for alum coagulation (Edwards & Amirtharajah, 1985).	6
Figure 2.3. Gator jar drawing with design dimensions. The water level is at a volume of 2 L. (Cornwell & Bishop, 1983)	10
Figure 2.4. Effects of flocculation speed on floc growth with a constant rapid mix speed of 200 rpm for 60 s. (Yu et al., 2011).....	13
Figure 3.1. Filter drawing without filter stand or jar tester.....	17
Figure 3.2. Jar test instrument with filtration apparatus.	18
Figure 3.3. Shimadzu TOC-L calibration curve from TOC Control L software.	27
Figure 3.4. PDA Apparatus Schematic.	30
Figure 3.5. Schematic of deep filter apparatus.	33
Figure 4.1. Operational coagulation diagram graphed with an alum-only titration curve from model water #2.	36
Figure 4.2. Acid titration curve without coagulant addition with raw water pH for model water #2.	37
Figure 4.3. Titration curve at a coagulant dose of 30 mg/L as Alum with initial coagulated pH for model water #2.....	38
Figure 4.4. Summary of titrant volume addition for a series of seven jar test experiments (42 individual jars) using model water #2.	38
Figure 4.5. Flow rate comparisons with deep filter apparatus at a coagulated pH of 5.5 using model water #1.	40
Figure 4.6. Flow rate comparisons with deep filter apparatus at a coagulated pH of 6.5 using model water #1.	40
Figure 4.7. Flow rate testing on bench top filter apparatus reported as filtered turbidity at a coagulated pH of 5.5 using model water #1.	42

Figure 4.8. Flow rate testing on bench top filter apparatus reported as percent turbidity removal at a coagulated pH of 5.5 using model water #1.	42
Figure 4.9. Flow rate testing on bench top filter apparatus reported as filtered turbidity at a coagulated pH of 6.5 using model water #1.	43
Figure 4.10. Flow rate testing on bench top filter apparatus reported as percent turbidity removal at a coagulated pH of 6.5 using model water #1.	44
Figure 4.11. Final turbidity comparisons for settled and filtered jar tests at Mt. Holly Water Treatment Plant.	45
Figure 4.12. Percent turbidity removal comparisons for settled and filtered jar tests at Mt. Holly Water Treatment Plant.	45
Figure 4.13. Coagulated pH for jar testing at the Mt. Holly Water Treatment Facility.	46
Figure 4.14. Model Water #1 filtered turbidity at a constant coagulated pH.	47
Figure 4.15. Comparison of filtered water turbidity for Mt. Holly natural and model water.	48
Figure 4.16. Coagulated pH values for natural water #2 contour plot using LITF with sedimentation. Each represents a singular jar from a series of jar tests and has a filtered turbidity associated with it.	49
Figure 4.17. Contour plot of percent turbidity removal for natural water #2 using LITF with sedimentation. ★ represents Kannapolis Water Treatment Plant's typical operating conditions.	50
Figure 4.18. Contour plot of percent turbidity removal for natural water #2 using LITF with sedimentation graphed with an alum-only titration curve.	51
Figure 4.19. Comparison of direct filtration to filtration following settled particle resuspension for natural water #2.	52
Figure 4.20. Contour plot of percent turbidity removal for natural water #2 using LITF with sedimentation. ★ represents Kannapolis Water Treatment Plant's typical operating conditions.	53
Figure 4.21. Contour plot of percent turbidity removal for natural water #2 using LITF with direct filtration graphed with an alum-only titration curve.	54

Figure 4.22. Contour plot of percent turbidity removal for natural water #2 using LITF with direct filtration and the 95% removal boundary from LITF with sedimentation.....	55
Figure 4.23. Contour plot of percent turbidity removal for natural water #2 using LITF with sedimentation with a theoretical temperature shift to 30 °C graphed with an alum-only titration curve.....	57
Figure 4.24. PDA analysis for moderate DOC/SUVA model water with single-stage flocculation. (Dose = 50 mg/L as Alum, pH = 7.0).....	59
Figure 4.25. PDA analysis for model water #2 with tapered flocculation. (Dose = 50 mg/L as Alum, pH = 7.0).....	61
Figure 4.26. Summary of PDA analysis for model water #2. (Dose = 50 mg/L as Alum, pH = 7.0).....	61
Figure 4.27. PDA analysis comparisons between sweep (Dose= 50 mg/L as Alum, pH = 7.0) and charge neutralization (Dose = 5.0 mg/L as Alum, pH = 5.0) mechanisms for model water #2.....	63
Figure 4.28. Effect of mixing intensities on filtered turbidity under sweep coagulation conditions using model water #2. (Dose = 50 mg/L as Alum, pH = 7.0).....	64
Figure 4.30. Summary of the results for the three jar test procedures evaluated at coagulant doses of 50 and 10 mg/L as Alum.	66
Figure 4.31. Summary of results for the three jar test procedures evaluated at coagulated pH values of 6.5 and 5.5.	67
Figure 4.32. Contour plot of percent turbidity removal for model water #2 using LITF with sedimentation overlaid with an alum-only titration curve.....	69
Figure 4.33. Contour plot of percent turbidity removal for model water #2 using LITF with direct filtration graphed with an alum-only titration curve.	71
Figure 4.34. Contour plot of percent turbidity removal for model water #2 using LITF with direct filtration and the 90% removal boundary from LITF with sedimentation.....	72
Figure 4.35. Contour plot of percent turbidity removal for model water #2 with flocculation at an intensity of 174 s ⁻¹ and direct filtration graphed with an alum-only titration curve.....	74

Figure 4.36. Contour plot of percent turbidity removal for model water #2 with flocculation at an intensity of 174 s^{-1} with direct filtration and the 95% removal boundary from LITF with direct filtration.....	75
Figure 4.37. Contour plot of percent turbidity removal for model water #2 using LITF with a combination of sedimentation and filtration graphed with an alum-only titration curve.....	76
Figure 4.38. Contour plot of percent turbidity removal for model water #2 using LITF with a combination of sedimentation and filtration and the 95% removal boundary from LITF with direct filtration.....	78
Figure 4.39. Contour plot of percent turbidity removal for model water #2 using LITF with a combination of sedimentation and filtration and the 95% removal boundary from LITF with direct filtration, LIFT with sedimentation, and 174 s^{-1} with direct filtration.....	80
Figure 4.40. The four contour plots created from model water #2 using LITF with sedimentation (A), LITF with direct filtration (B), single-stage flocculation with direct filtration (C), and LITF with sedimentation and filtration (D).....	Error!
Bookmark not defined.	
Figure 4.41. Maximum observed removals from LITF and single-stage flocculation with direct filtration. Areas of treatment not identified by LITF, but identified by single-stage flocculation are highlighted in red.....	82
Figure 4.42. Contour plot of percent turbidity removal for model water #3 using LITF with direct filtration graphed with an alum-only titration curve.	84
Figure 4.43. Contour plot of the zone of maximum treatment efficiency for model water #3 with flocculation at an intensity of 174 s^{-1} with direct filtration and 95% removal boundary from LIFT with direct filtration.....	85
Figure 4.44. Original contour data for model water #3 using LITF with direct filtration at a target coagulated pH of 5.5 with duplicate results with standard deviation from LITF and single-stage flocculation with direct filtration.	86
Figure 4.45. Coagulated pH values from jar test data for model water #3 from the original, LITF, and single-stage flocculation data sets.	87
Figure 4.46. Operational diagram with the contour plot from natural water #2 with sedimentation as the particulate removal mechanism. Zone of observed turbidity removals $\geq 70\%$ is shaded yellow.....	88
Figure 4.47. Operational diagram with the contour plot from natural water #2	

with filtration as the particulate removal mechanism. Zone of maximum observed turbidity removals is shaded red.	89
Figure 4.49. Operational coagulation diagram with the contour plot from LITF with direct filtration for model water #2. Zone of maximum observed turbidity removals is shaded red.	91
Figure 4.50. Operational coagulation diagram with the contour plot from single-stage flocculation at an intensity of 174 s^{-1} with direct filtration for model water #2. Zone of maximum observed turbidity removals is shaded red.	92
Figure 4.51. Operational coagulation diagram with the contour plot from LITF with sedimentation and filtration for model water #2. Zone of maximum observed turbidity removals is shaded red.	93
Figure 4.52. Operational coagulation diagram with the contour plot from LITF with direct filtration for model water #3. Zone of maximum observed turbidity removals is shaded red.	94
Figure 4.53. Hypothetical jar tests for model water #2 with flocculation at an intensity of 174 s^{-1} at an initial coagulated pH of 6.0. The selected alum dose and coagulated pH has been circled.	97
Figure 4.54. Hypothetical jar tests for model water #2 with flocculation at an intensity of 174 s^{-1} at an initial coagulated pH of 6.5. The selected alum dose and coagulated pH has been circled.	98
Figure 4.55. Hypothetical jar tests for model water #2 with flocculation at an intensity of 174 s^{-1} at an initial coagulated pH of 7.0. The selected alum dose and coagulated pH has been circled.	99
Figure 4.56. Hypothetical jar tests for model water #2 using LITF at an initial coagulated pH of 6.0. The selected alum dose and coagulated pH has been circled.	100
Figure 4.57. Hypothetical jar tests for model water #2 at an initial coagulated pH of 6.5. The selected alum dose and coagulated pH has been circled.	101
Figure 4.58. Hypothetical jar tests for model water #2 using LITF at an initial coagulated pH of 7.0. The selected alum dose and coagulated pH has been circled.	102
Figure 4.59. Hypothetical jar tests for model water #3 using LITF at an initial coagulated pH of 6.0. The selected alum dose and coagulated pH has been circled.	103

Figure 4.60. Hypothetical jar tests for model water #3 at an initial coagulated pH of 6.5. The selected alum dose and coagulated pH has been circled.	104
Figure 4.61. Hypothetical jar tests for model water #3 using LITF at an initial coagulated pH of 7.0. The selected alum dose and coagulated pH has been circled.	105
Figure 4.62. Hypothetical jar tests for natural water #2 using LITF at an initial coagulated pH of 6.0. The point of optimum alum dose and coagulated pH has been circled.	106
Figure 4.63. Hypothetical jar tests for natural water #2 using LITF at an initial coagulated pH of 6.5. The selected alum dose and coagulated pH has been circled.	107
Figure 4.64. Hypothetical jar tests for natural water #2 at an initial coagulated pH of 7.0. The selected alum dose and coagulated pH has been circled.	108
Figure 4.66. Jar test results at an alum dose of 50 mg/L for model water #4.	110
Figure 4.65. Jar test results at a target coagulated pH of 6.5 for model water #4.	111
Figure 4.67. Jar test results at a target coagulated of pH 6.25 for model water #4.	112
Figure 4.68. Jar test results at a coagulant dose of 40 mg/L as Alum for model water #4.	113
Figure 4.69. Jar test results at a target coagulated pH of 6.00 for model water #4.	113
Figure 4.70. Target coagulated pH values and alum doses from the series of jar test used to determine effective coagulation conditions. Selected dose and pH has been circled.	114
Figure 4.71. Jar test results at a target coagulated pH of 6.00, with an alum dose above selected effective dose, for model water #4.	115
Figure 4.72. Contour plot created from a series of optimization jar tests for model water #4. A zone boundary irregularity has been circled.	117
Figure 4.73. Contour plot created from a series of optimization jar tests for model water #4 graphed with the measured coagulated pH from each jar test from the series. The selected alum dose and coagulated pH has been circled.	118

Figure A.1. The effects of different flocculation procedures on percent turbidity removals for model water #2 across a range of coagulated pH values at a constant coagulant dose of 50 mg/L as Alum.	129
Figure A.2. The effects of different flocculation procedures on percent turbidity removals for model water #2 across a range of alum doses at a target coagulated pH of 6.5.	130
Figure A.3. The effects of different flocculation procedures on percent turbidity removal for model water #2 across a range of coagulated pH at a constant coagulant dose of 10 mg/L as Alum.	131
Figure A.4. The effects of different flocculation procedures on percent turbidity removal for model water #2 across a range of alum doses at a target coagulated pH of 5.5.	132
Figure A.5. Percent turbidity removal with flocculation at an intensity of 174 s^{-1} with direct filtration at Alum doses of 50 mg/L and 10 mg/L.	133
Figure A.6. Percent turbidity removal with flocculation at an intensity of 174 s^{-1} with direct filtration at target coagulated pH values of 6.5 and 5.5.	134
Figure A.7. Percent turbidity removal using LITF with direct filtration at coagulant doses of 50 and 10 mg/L as Alum.	135
Figure A.8. Percent turbidity removal using LITF with direct filtration at target coagulated pH values of 6.5 and 5.5.	136
Figure A.9. Percent turbidity removal using LITF with sedimentation and filtration at coagulant doses of 50 and 10 mg/L as Alum.	137
Figure A.10. Percent turbidity removal using LITF with sedimentation filtration at target coagulated pH values of 6.5 and 5.5.	138

LIST OF ABBREVIATIONS

DI	deionized
DOC	dissolved organic carbon
FI	flocculation index
HITF	high-intensity tapered flocculation
ID	inner diameter
IMS	integrated media support
LITF	low-intensity tapered flocculation
NPT	national pipe thread
OD	outer diameter
PDA	photometric dispersion analysis
PVC	polyvinyl chloride
RMS	root mean square
TOC	total organic carbon

CHAPTER 1: INTRODUCTION

Conventional surface water treatment involves a multistep process to destabilize and remove colloidal particles, along with dissolved natural organic matter (NOM). This is generally achieved through coagulation (and rapid mixing), flocculation (or gentle mixing), sedimentation, and filtration. Coagulants, typically metal salts, are added to raw water supplies just prior to rapid mix to aid in contaminant removal. The optimization of a treatment plant's coagulation conditions is important in order to maximize treatment efficiency, reduce operating cost, and minimize residual metal concentrations in finished water (H.E. Hudson Jr. & Wagner, 1981; Teefy, Farmerie, & Pyles, 2011).

Jar testing is one of the most common tools that water treatment facilities use to determine the treatment conditions necessary to meet finished water goals. One study found that out of the eight methods identified for determining and monitoring coagulation conditions, jar testing was the second most prevalent method applied, following only the use of historical data (Logsdon & Hess, 2002). Of the 37 participating treatment facilities, 29 applied jar testing to their coagulation optimization process. Only 4 utilities surveyed used one method of coagulation monitoring and determination, with the majority of facilities applying three to five different techniques. A jar test allows treatment plant conditions to be replicated at the bench scale. A time efficient and accurate test is necessary, since raw water conditions can change rapidly due to rain events and seasonal variation. Along with turbidity (or light scatter due to suspended particles) and natural organic matter (NOM), additional water quality parameters that have the potential to shift

treatment condition goals are alkalinity, pH, and temperature. Currently jar testing procedures consist of coagulation, flocculation, and sedimentation to predict treatment at a given plant. Each stage of the jar test is designed to replicate plant mixing conditions and detention times as accurately as possible (Budd et al., 2004; H.E. Hudson Jr. & Wagner, 1981; Teefy et al., 2011). Testing is carried out with either a 4 or 6 jar apparatus to allow multiple scenarios to be evaluated simultaneously. The treated water turbidity is measured following sedimentation to assess the potential treatment effectiveness. Although general guidelines are applied to jar test development, the existing protocols require that the jar test procedure itself be optimized to produce results that best fit the plant at which they are being employed (Budd et al., 2004).

Conventional jar testing, where sedimentation is utilized as the primary particulate removal mechanism, has been shown to not be applicable for certain water types (Brink, Choi, AL-Ani, & Hendricks, 1988). This is especially true for low turbidity waters where low contact opportunity prevents the formation of a settleable floc. Floc are the particles that form during drinking water treatment between the aluminum hydroxide that occurs after alum addition and the particulate contaminants. It was necessary to develop a procedure that could be useful at all treatment facilities and provide results that would better indicate effective coagulation conditions.

The primary objective of this research was to develop a new jar test procedure that could be used at all treatment facilities without site specific customization to compare coagulation conditions in terms of filtration efficiency (instead of sedimentation efficiency) in a timely manner. The development of a new jar test procedure could reduce limitations in its ability to accurately match plant conditions (Teefy et al., 2011). A uniform

flocculation procedure could be universally applied without the need for customization to each facility while also saving time.

CHAPTER 2: BACKGROUND

2.1 Coagulation

Coagulation, as it applies to surface water treatment, is the process in which colloidal particles and dissolved NOM (or more specifically DOC) are reacted with coagulants to aid in their removal by subsequent treatment processes. Coagulation is accomplished through two mechanisms: charge neutralization and sweep flocculation (Dempsey, Ganho, & O'Melia, 1984; Edzwald, 1993; Stumm & O'melia, 1968). Charge neutralization can be defined by the presence of a stoichiometric relationship between negatively charged contaminants and positively charged intermediate hydrolyzed metal species from the coagulant with the potential of restabilization. Whereas sweep flocculation requires excess coagulant that produces an amorphous precipitate with a near neutral surface charge that physically removes contaminants (Bratby, 2006; Stumm & O'melia, 1968). Typically, contaminant concentration determines the most effective treatment mechanism for a given raw water supply (Stumm & O'melia, 1968). Each mechanism consists of different chemical reactions and these reactions are dependent upon whether the coagulant is interacting with colloidal particles or NOM (Pernitsky, 2003). Figure 2.1 provides a summary of these reactions. The pathway in the figure that contains $\text{Al(OH)}_{3(\text{am})}$ as the active coagulant species is that of sweep flocculation, as the contaminants are either enmeshed or adsorbed (mechanisms A and B) by the precipitate. The lower pathway has intermediate hydrolysis species acting in coagulation, which are

responsible for particle destabilization/precipitation (mechanisms C and D) through chemical bonds of positively charged species with the contaminants present.

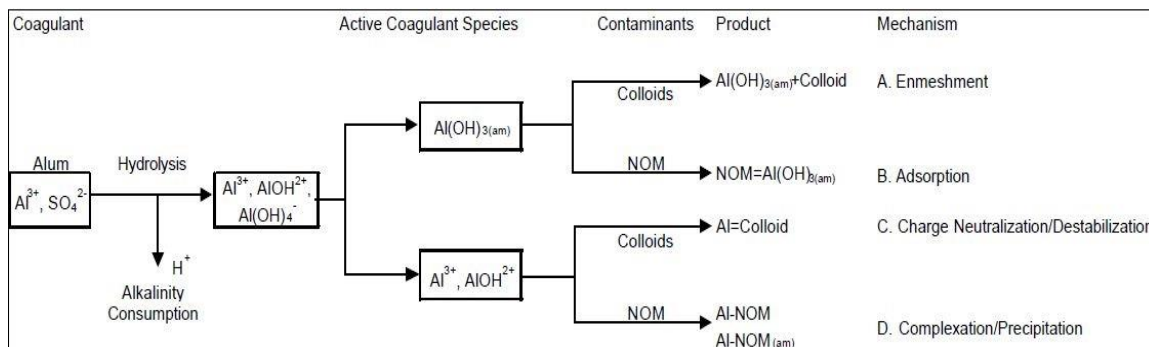


Figure 2.1. Chemical reactions in alum coagulation (Pernitsky, 2003).

Coagulant/contaminant interaction mechanisms can be defined by coagulated pH (i.e., the pH of the water after coagulation) and the coagulant dose. An operational diagram for alum coagulation was developed based on typical treatment conditions to aid in the identification of potential zones of treatment of colloidal particles (Amirtharajah & Mills, 1982). A later version of this diagram can be seen in Figure 2.2 (Edwards & Amirtharajah, 1985). Charge neutralization is described to occur from a pH slightly above 4.0 to 6.5 with a lower and upper bound of approximately 1.0 and 50 mg/L as alum, respectively. The multiple boundaries for the “restabilization zone” reflect the varying stoichiometry as contaminants differ in multiple water sources. Most water treatment plants operate near one of the boundary lines in this zone when possible. Additional work with the coagulation of NOM has also been investigated, and the boundary variability was also present (Dempsey et al., 1984; Edwards & Amirtharajah, 1985). In both instances, there are times where the restabilization zone may not be observed. The irregularities are attributed primarily to colloid and NOM concentrations. According to the operation diagram, sweep coagulation occurs from 15 to >100 mg/L as alum along the pH range of 5.75 to 8.5 with

an optimum zone centered on a pH of 7.5 and a coagulant dose of 40 mg/L. The red (charge neutralization) and blue (sweep flocculation) boxes are charge neutralization and sweep flocculation were observed to occur by the researcher. This is based on observations at both the bench and full-scale. This is included for reference only. The yellow line is the upper pH limit as defined by other research (Edzwald, 2014).

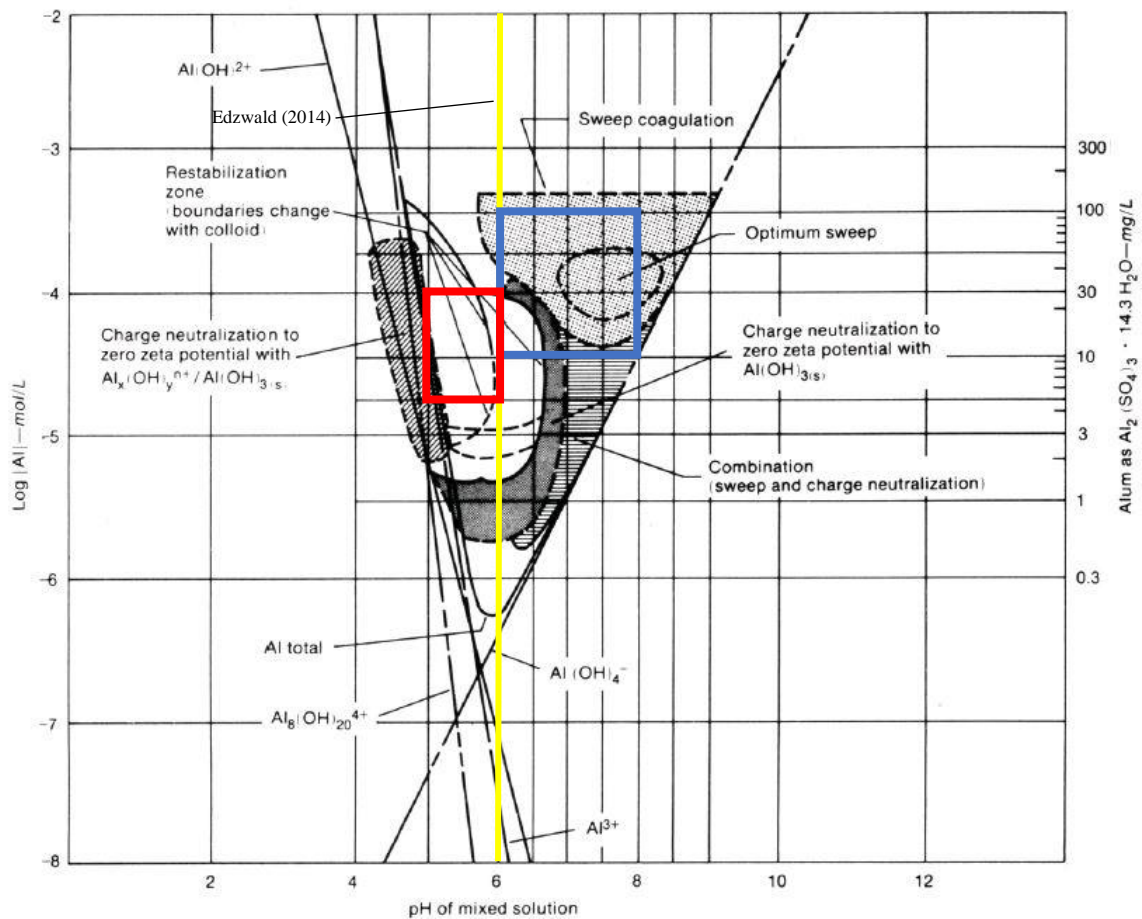


Figure 2.2. Operational diagram for alum coagulation (Edwards & Amirtharajah, 1985).

2.1.1 Coagulant Demand

2.1.1.1 Particulate Contaminants

Colloidal suspensions in raw water supplies consist of both inorganic and organic particulates and are quantified by measuring the water's turbidity, reported in Nephelometric Turbidity Units (NTU) (Au, Alpert, & Pernitsky, 2011). Inorganic particles consist of clay, iron and aluminum oxides, silica, calcites, and others as a result of runoff and erosion. Organic particles found in suspension are typically viruses, bacteria, protozoa and algae. The negative surface charge associated with colloidal particles found in natural waters is in the range of 0.1 to 1 $\mu\text{eq}/\text{mg}$ (Edzwald, 1993; Pernitsky, 2003).

2.1.1.2 Dissolved Natural Organic Matter

Natural organic matter as it applies to coagulant demand comes in the form of humic substances (humic and fulvic acids), which have origins from decaying plant matter. The physical properties of interests in terms of contaminant removal are their high molecular weight, hydrophobicity, and the charge associated with their functional groups (Au et al., 2011; Randtke, 1988). Quantifying NOM can be done through the measurement of a water supplies DOC as approximately 45% of DOC is composed of humic substances (Edzwald, 1993). A surrogate method of measurement the employs the method of UV absorbance at 254 nm may be more reliable when evaluating the amount of coagulant consuming organics present (Edzwald, Becker, & Wattier, 1985). Specific UV absorbance (SUVA) is the amount of UV light absorbed per meter, per mg/L of DOC. A water's SUVA can be used as a predictor of the composition of NOM present in a supply and if a significant effect on coagulant demand can be expected (Edzwald & Van Benschoten, 1990).

The charge density on NOM is typically within the range of 10 – 15 $\mu\text{eq}/\text{mg}$ DOC, which is significantly higher than values (0.1 to 1 $\mu\text{eq}/\text{mg}$) reported for colloidal particles (Edzwald & Van Benschoten, 1990). This greater charge density leads to NOM being the controlling factor in coagulant demand and treatment for most water treatment facilities (Edzwald, 1993).

2.2 Jar Test

The need to evaluate coagulation at the bench-scale led to the development of the jar test apparatus by Wilfred Langlier as described in his 1921 publication *Coagulation of Water with Alum by Prolonged Agitation* (Hendricks, 2011). Later recommendations for the utilization of a jar test method to provide repeatable results insisted that continuous stirring of the sample water was necessary (Black, Rice, & Bartow, 1933; Peterson & Bartow, 1928). Also, it was concluded that a sample volume of 2 liters provided the best estimates for coagulant dose (Black et al., 1933). This was based on both experimental analysis and a review of the findings in previous literature. After this early research, Phipps & Bird made available the first “off-the-shelf” jar test unit (Hendricks, 2011). While many early findings were made involving the use of the jar test, these are not pertinent to this research, but an in depth summary of the literature can be found in *Review of the Jar Test* (Black, Buswell, Eidsness, & Black, 1957).

Developing a standardized jar test procedure for water treatment facilities was seen as essential by researchers and attempts to do so were discussed in 1957 (Black et al., 1957). This research involved a detailed questionnaire sent to various individuals across the drinking water industry, including manufacturers, plant laboratories, consulting

engineers, and university researchers. The findings showed that, although the majority of the time the jar test method used followed the same general steps, there was no consistency among individual steps in the methods. Black and his fellow researchers stated that five aspects of the jar test needed to be evaluated to develop a standardized procedure: 1) the size of the sample, 2) the size and shape of the container, 3) peripheral speed and time of the rapid mix, 4) peripheral speed and time of slow mix, and 5) criteria for establishing optimum dosage.

2.2.1 Sample Size and Container Geometry

As previously mentioned, literature suggest that volume is critical in order to produce reliable coagulant dose estimates. The American Water Works Association (AWWA) and Phipps & Bird allow for either 1 or 2 L sample sizes to be used, but both recommend a 2 L sample (American Water Works Association, 2011); Phipps & Bird, 2017). This corresponds with previous recommendations which have been shown to produce more consistent and reliable results for coagulant control.

The development and utilization of 2 L, square jars further improved the jar test when compared to the traditional round beaker (H.E. Hudson Jr. & Wagner, 1981). These jars were constructed from sheets of acrylic. A drawing of the jar with dimensions can be seen in Figure 2.3. A sample port was also added to the jars, 10 cm below the water surface. The square jars, also known as Gator Jars because they were developed at the University of Florida, allowed for a number a number of benefits including:

- 1) Square jars provide better mixing conditions
- 2) Rotational velocity is stopped more quickly than round jars
- 3) Samples can be collected without disturbing the flocculation process
- 4) Acrylic has a lower heat conductivity than glass.

(American Water Works Association, 2011; H.E. Hudson Jr. & Wagner, 1981)

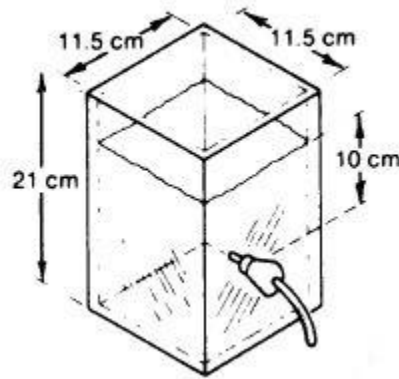


Figure 2.3. Gator jar drawing with design dimensions. The water level is at a volume of 2 L. (Cornwell & Bishop, 1983)

2.2.2 Mixing in the Jar Test

Current recommendations are that the mixing in the jar test procedure replicate that of the plant based on the full-scale velocity gradients (G, s^{-1}) and the detention times of each treatment stage (American Water Works Association, 2011). The Camp number, Gt , is commonly used to quantify mixing in water treatment where t is the detention time of the reactor in seconds. Apparatus and chemical manufactures typically have their own procedure that they recommend (Phipps & Bird, 2017; Tintometer Group, 2016; Water Specialist Technologies LLC, 2017). There has been little investigation into creating a standardized jar testing mixing procedure.

2.2.2.1 Rapid Mix

Evidence shows that there is the potential to optimize both the duration and intensity of the rapid mix phase of treatment for any given coagulant dose (Letterman, Quon, & Gemmell, 1973). Residual turbidity appears to be affected by the duration of

mixing more so than intensity, but the optimum combination of intensity and duration is a function of alum dose (Letterman et al., 1973). Rapid mix duration has the potential to affect the subsequent flocculation process, which is associated with the existence of an optimum mixing period (Letterman et al., 1973). It has been shown that increasing rapid mix duration can reduce the observed flocculation index (FI) plateau values, along with causing a rise in measured residual turbidity values (Yu, Gregory, Campos, & Li, 2011; Yukselen & Gregory, 2004).

The FI is obtained when an aggregated solution is analyzed on a continuous flow basis, photometrically (Gregory, 2009). A high intensity light is transmitted through the solution and the variability caused by the constant flow of particles is broken down into two components, a dc component and a fluctuating ac component, by a photodiode (Rank Brothers LTD, 2017). The FI is defined as the ratio of the average dc value to the root mean square (rms) of the ac component (dc/rms) (Gregory, 2009). Particle growth can be correlated to FI value, but no distinct particle size can be derived from a given FI value. This analytical technique is a means monitoring the effect of changing conditions.

Optimum durations of rapid mix often exceeds that of the alum hydrolysis and precipitation reactions, with hydrolysis occurring within a second and precipitation taking up to 7 seconds (Amirtharajah & Mills, 1982; Letterman et al., 1973) A duration of 10 seconds has been noted as being sub-optimum in a batch-mix reactor, but adverse effects on residual turbidities can occur with more than 60 seconds of mixing (Yu et al., 2011).

Findings indicate that the importance of high intensity mixing may be dependent upon the coagulation mechanism, as the fast reaction kinetics that occur during the hydrolysis of the coagulant requires a quick and uniform dispersal intermediate species

(Amirtharajah & Mills, 1982). The velocity gradients used in this study were $16,000 \text{ s}^{-1}$ ($Gt = 16,000$), 100 s^{-1} ($Gt = 20,000$), and 300 s^{-1} ($Gt = 18,000$). It was concluded that the high intensity ($G = 16,000 \text{ s}^{-1}$) only showed significant improvements in the charge neutralization zones of treatment, while treatment conditions that indicated sweep flocculation was the primary coagulation mechanisms showed no difference in turbidity removal effectiveness regardless of applied G value (Amirtharajah & Mills, 1982). It has been hypothesized that the application of mechanical, high-intensity mixing may be unnecessary, particularly in most instances where treatment facilities are relying on the sweep flocculation mechanism (Edzwald, 2014). During sweep flocculation, the chemical conditions are of more importance than rapid mixing. Hydraulic mixing (by means of weirs, Venturi meters, open-channel static mixers) may provide sufficient mixing to achieve uniform coagulant dispersion and allow for the elimination of high-intensity, mechanical mixing

2.2.2.2 Flocculation

Flocculation is the process of particle agglomeration through slow mixing, which requires a significantly lower mixing speed than that of rapid mix over a longer duration of time (Hendricks, 2011). Bench top testing has been shown to rely on uniform stirring during the flocculation step in order to produce accurate, repeatable data that correspond to full-scale treatment (Black et al., 1933).

The effects of mixing time on flocculation can be observed in Figure 2.4, where regardless of flocculation intensity each sample reaches their respective FI plateau values at approximately the same time (Yu et al., 2011). Only the data from 0 to 800 seconds (13.3

minutes) is important for this discussion. It can be seen that while the values for the FI vary greatly with mixing speed; all test runs reach their plateau values within approximately 2 minutes of one another. This plateau is indicative of there being an equilibrium between floc growth and break up (Yu et al., 2011). Researchers noted the slight decline in steady state values at slow mixing speeds of 80 and 100 rpm and hypothesized that this may be due to not all floc breakup being reversible. The higher mixing speeds magnified this problem.

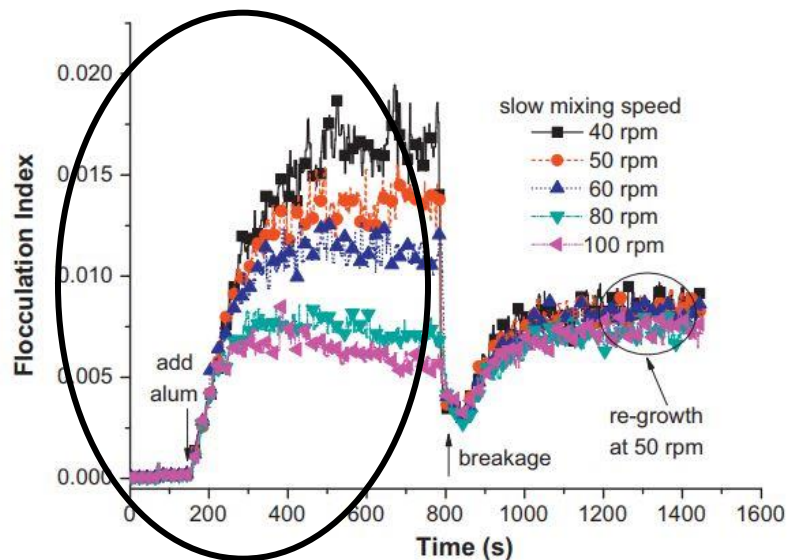


Figure 2.4. Effects of flocculation speed on floc growth with a constant rapid mix speed of 200 rpm for 60 s. (Yu et al., 2011).

Although floc size has an inverse relationship to mixing speed according to the data from Figure 2.4 (and particle size frequency curves); it was found that mixing speed and residual turbidity do not have the same relationship (Yu et al., 2011). Residual turbidity measurements decreased with rpm from 4 NTU to 2 NTU until 100 rpm of slow mixing, where the turbidity rose again to approximately 2.5 NTU.

2.2.3 Dosage Selection Criteria

Typical jar test procedures at a conventional water treatment facility use sedimentation as the solid-liquid separation mechanism (American Water Works Association, 2011). A sample is collected after a predetermined period of time that is meant to correlate to the full-scale sedimentation basin and turbidity removals are evaluated, with the dose that results in the lowest observed residual turbidity selected. Selecting the appropriate settling time is important due to the broadening of the perceived optimum dose window as sampling time increases (Reed & Robinson, 1984).

Bench-scale filtration with a membrane disc has been applied to low turbidity waters with good results as it is difficult to produce visible flocs under these conditions, which makes the application of settling a challenge. There has been research that suggests when applying membrane filtration to the jar test procedure specifically for low turbidity waters, that Whatman #40 filter paper be used (Wagner & Hudson, 1982). A jar test procedure that includes membrane filtration has also been shown to minimize random error that can occur using sedimentation techniques (Brink, Choi, AL-Ani, & Hendricks, 1988).

The application of sedimentation as the particulate removal mechanism in jar testing may not be reliable when predicting full-scale conventional plant performance due to issues with scaling-up (Hudson Jr., 1973). This is attributed to the large size of the scale-up. Findings show that when compared to both pilot and full-scale data, membrane filtration at the bench-scale displayed similar results to high turbidity waters (Brink et al., 1988). Additional findings indicate that scale is not an issue when using a filtration

apparatus to evaluate coagulation efficiency, as pilot-scale, dual-media filtration was used to evaluate effective coagulation in low turbidity waters (Mosher & Hendricks, 1986).

CHAPTER 3: METHODS AND PROCEDURES

3.1 Filter Apparatus and Jar Test instrument

A novel filter apparatus was used in conjunction with the standard jar test apparatus to analyze filterability as the primary particulate removal mechanism. Each individual filter was constructed from a 9" section of 2" diameter Schedule 40 clear PVC. The effluent of the filter pipe was fitted with a Schedule 40 PVC coupling National Pipe Thread (NPT) female \times socket connect. The socket end of the adapter was attached to the length of pipe. A Schedule 40 PVC, 2" NPT male \times 1/2" NPT female reducing hex bushing was threaded into the straight pipe adapter. Threaded into the female threads on the reducing bushing was a nylon tight-seal barbed tube fitting with the dimensions 1/4" tube inner diameter (ID) \times 1/2" NPT male. A 4.5" piece of 5/16" ID silicone rubber tubing (Tygon[®] R-3603) was affixed to the barb end of the tube fitting. A 1/4" ID \times 1/8" ID tube to tube straight reducer was inserted into the effluent end of the tube. The top of the filters were capped with #11 (2 3/16" \times 1 29/32") tapered, one hole, round, styrene-butadiene rubber (SBR) stoppers. The filters and the jars were connected using a 17" length of laboratory grade tubing (Tygon[®] R-3603) with an ID of 1/8". A 1/8" ID \times 1/8" ID tube to tube connector was at each end of the connecting tube. Figure 3.1 is a drawing of the previously described filter.

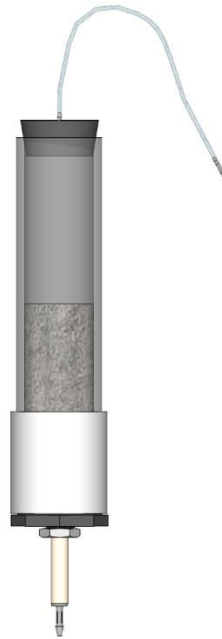


Figure 3.1. Filter drawing without filter stand or jar tester

Each filter was fitted with a 2” circular integrated media support caps (Leopold IMS[®]) to prevent filter media washout. The IMS cap was positioned flush with the bottom of the clear PVC pipe, before the coupling was attached. The filter media was Vitro Clean[®] crushed glass filtration media. The product number was “VF#25” and had an effective size of 0.45 mm with a uniformity coefficient of approximately 1.45. The media depth was 3 inches with 4 inches of head space. A filter stand was constructed that positioned the top of the filters at 24” above the ground.

The jar test apparatus used during experimentation was a Phipps & Bird PB-900[™] Programmable Jar Tester. The jar tester was programmable for continuous and sequential (i.e. tapered flocculation) mixing functions. The jar tester was designed with 6 stainless steel paddle stirrers that were 3” in length x 1” wide, allowing for 6 jars to be simultaneously coagulated, rapid mixed, flocculated, settled, and/or filtered. The jars used

for experimental analysis were square acrylic jar tester jars (Phipps & Bird B-KER²®). Each jar had a sample tap located 2” from the inside bottom surface of the jar. Figure 3.2 displays the jar tester with the filter apparatus attached.



Figure 3.2. Jar test instrument with filtration apparatus.

3.2 Filter Set-up and Maintenance

Prior to jar test analysis, each filter was filled with DI water. This was carried out by connecting the effluent end of the filter, at the tube hose barb on the reducing bushing, to the DI water tap in the lab. The water flow was continued at 40% bed expansion for 30 seconds before being reduced and prior to plugging the filter. The influent hose was

pinched and clamped closed before flow was completely terminated. This was to ensure that no air remained in the filter during the testing process.

Upon completion of each jar test, the filters were backwashed in the same manner by which they were filled. Backwash flow was carried out for a minimum of 30 seconds and was stopped once the backwash water was free of visible contaminants. After the completion of the backwash procedure, the filters were either refilled, if subsequent testing was to proceed, or allowed to air dry uncapped in the filter stand. It was necessary to monitor and refill the filter media when it dropped below the 3” mark on each filter.

3.3 Jar Testing Procedure

3.3.1 Initial Setup and Titration Procedures

The initial step in the jar testing procedure was to collect 2.2 L of raw water and add it to each jar. This volume was selected to allow for a sufficient volume to conduct a titration of a 200 mL sample and 2 L of water to be available for jar testing. The jar tester was turned on and set to continuously mix at 100 rpm. Kaolin was then dosed as a particle/turbidity source in each jar as the first step in creating a consistent and reproducible synthetic water. Kaolin was dosed in this manner for all experiments.

The coagulant used was Arcos Organics aluminum sulfate octadecahydrate (Alum, $\text{Al}_2(\text{SO}_4)_3 \cdot 18 \text{H}_2\text{O}$). The stock solution concentration was 10g/L and had a holding time of 30 days. Hydrochloric acid or sodium hydroxide was used at a concentration of 0.1 N to control the coagulated pH of each jar during testing.

Titration was necessary for each jar in order to determine the amount of pH controlling solution needed for a given coagulant dose. The pH range used during testing

was from 5.0 to 8.0 in increments of 0.5 units. Approximately 10 mL of water was wasted from the jar before a 200 mL sample was collected in a 250 mL glass beaker and placed on a stir plate (IKA® Color Squid Number One) with a magnetic stirring rod (1" x 3/8" octagonal). A pH meter (Fisher Scientific Accumet® Research AR15) was used with a pH probe (Accumet® Research 13-620-223A) to monitor pH. The meter was calibrated daily using 3-point calibration with buffer solutions of pH 4, 7, and 10; the previous day's calibrations being cleared prior. The pH of the sample was obtained and recorded as the raw water pH. The pH probe was then removed from the sample and the coagulant dose was added. The pH probe was replaced and the coagulated pH was recorded after the value had stabilized. Next, the necessary pH adjusting chemical was added to the coagulated sample with micropipettes (Eppendorf® Research plus, adjustable volume) in 0.01 to 1 mL increments until the target pH was obtained. The volume of pH adjusting chemical was recorded along with the final pH.

At this point, a 40-mL turbidity sample was collected from each jar in a round turbidity cell. Turbidity was measured using a turbidimeter (Hach 2100AN). Once the cells were placed in the turbidimeter, a timer was started and the reading was allowed to stabilize for 30 seconds. At the conclusion of this stabilization period, the lowest turbidity reading over the next 5 second was recorded as initial turbidity.

3.3.2 Coagulant Dose Preparation

The coagulant dose for each jar was loaded into a syringe (BD Leur-Lok™). Syringe volume with the respective coagulant dose ranges can be seen in Table 3.1. The first step in filling the syringe was to remove the plunger and attach a cap (BD Leur-Lok™)

to the tip to prevent the loss of coagulant. Coagulant was pipetted from the stock solution into the syringe. The plunger was replaced and the syringe was inverted. The cap was removed and the plunger was then depressed in order to push out the air from the syringe, ensuring not to dispense any of the coagulant. Each syringe was affixed above their corresponding jar with a strip of hook and loop fastener tape.

Table 3.1. Syringe volume with corresponding coagulant dosages.

Syringe Volume (mL)	Coagulant Volume (mL)
3	0 - ≤ 2
5	> 2 - ≤ 4
10	> 4 - ≤ 8
30	> 8 - 20

3.3.3 Jar Test Method and Particulate Removal Mechanisms

Table 3.2 provides a summary of the jar test procedures used in this research. The jar test procedure consisted of a 1-minute rapid mix period at 300 rpm ($G = 609 \text{ s}^{-1}$). Immediately after the initiation of the jar test program coagulant was dosed into each jar. Following the completion of the rapid mix stage a 200-mL sample was collected from each jar. The pH was measured and recorded as coagulated pH. It was the goal of the researcher to have this value be within 0.2 units of the target pH.

Table 3.2. Jar Test Procedure Summary with mixing intensities and duration.

Stage	Mixing Speed (rpm)	Duration (min)	Comments
Rapid Mix	300	1	
Flocculation Tapered	70/50/30	5/5/10	
Single-stage	120	10	
Particulate Removal Sedimentation	0	20	
Filtration	Same as final stage of flocculation	≈2*	800 mL of coagulated water flows to filter apparatus

*per filter

Following rapid mixing, there was a period of flocculation. Two flocculation methods were applied to bench top jar test to evaluate the effectiveness of single-stage flocculation when compared to tapered-flocculation. Single-stage flocculation consisted of 10 minutes of mixing at 120 rpm (174 s^{-1}). Low-intensity tapered flocculation (LITF) was carried in three stages for a total of 20 minutes (with mixing at 70 rpm (80 s^{-1}) for 5 minutes, 50 rpm (50 s^{-1}) for 5 minutes, and 30 rpm (24 s^{-1}) for 10 minutes). Flocculation will also be discussed later in this chapter as various approaches were analyzed for the purposes of this research. Following flocculation, there was a particulate removal stage, which included settling, filtering, and a combination of both.

Settling was carried out for a period of 20 minutes, whenever used. After the completion of the flocculation period, the paddles were carefully removed from the jars. This was to limit any outside interference on the settling process. At the completion of the settling period, an additional 10 mL was wasted from each jar and a turbidity sample was collected (following the same procedure as with the initial turbidity reading).

Filtration required the continuation of mixing, which was prolonged at the same intensity as at the end of the flocculation period. The filters were attached to the jars following the collection of the coagulated pH samples. The valves on the jars were opened in 15 second intervals beginning at the end of flocculation. This interval was to ensure that turbidity samples could be collected at the same point during the filtration process for each jar. The total volume of water that was allowed to flow through the filters was 800 mL, which is approximately 3.5 times the total volume of one filter (230 mL). Once the water level in the jars reached the 1 L mark in the jar, a filtered turbidity sample was collected and measured.

Particulate removal using a combination of settling and filtration followed the same procedure as with settling. After the completion of the settling period (20 minutes), 800 mL of settled water was allowed to flow through the filters with no mechanical mixing occurring. Turbidity samples were then collected and analyzed.

Once the final turbidity samples were collected and recorded, the final pH value and temperature were obtained. These values served as a means of quality control and allowed the researcher to monitor jar conditions to ensure consistency within a single test and as well as between trials.

3.4 Sample Waters

Six waters utilized during this study for the purposes of developing the novel filtered jar test procedure. The waters consisted of four synthetic waters and two natural waters. Water quality parameters for the experimental waters can be seen in Table 3.3. Not all waters were used in each stage of experimentation, and the water will be identified

through-out when necessary. Table 3.4 lists the descriptive names for each of the experimental waters.

Table 3.3. Water quality parameters of experimental waters.

	Turbidity (NTU)	pH	Temperature (°C)	Alkalinity (mg/L as CaCO ₃)	DOC (mg/L)	SUVA (L/mg·m)
Average (Minimum/Maximum)						
Natural Water #1	1.20 (0.91/1.30)	7.4 (7.2/7.7)	28.3 (27.8/28.6)	15.4 (15.0/17.0)	2.5*	-
Natural Water #2	3.38 (1.94/4.81)	7.34 (7.18/7.52)	22.3 (21.2/26.0)	40 (35/55)	3.53 (3.30/3.96)	2.39 (2.15/2.46)
Model Water #1	3.19 (2.85/3.44)	7.6 (7.5/7.9)	22.0 (21.4/22.6)	17**	2.5**	-
Model Water #2	42.2 (34.2/47.3)	8.08 (7.86/8.43)	21.5 (18.3/23.5)	38 (30/50)	3.23 (2.96/3.83)	4.23 (4.13/5.05)
Model Water #3	29.7 (27.6/34.9)	8.50 (8.32/8.75)	21.8 (21.0/22.6)	121 (90/155)	9.92 (9.00/11.1)	4.67 (4.30/4.98)
Model Water #4	1.66 (1.44/1.88)	8.29 (8.11/8.44)	21.0 (19.9/22.0)	69 (65/75)	5.71 (5.19/6.28)	3.15 (2.79/3.39)

* Measured value

** Target value

Table 3.4. Experimental waters and their respective descriptive names.

Water	Descriptive Name
Natural Model #1	Mt. Holly Water
Natural Model #2	Kannapolis Water
Model Water #1	Mt. Holly Model Water
Model Water #2	Moderate Turbidity/DOC/SUVA Water
Model Water #3	Moderate Turbidity – High DOC/SUVA Water
Model Water #4	Low Turbidity – Moderate DOC/SUVA Water

Model waters were developed and controlled for turbidity, alkalinity, TOC and SUVA by the addition of various products. Kaolin (Sigma-Aldrich) was added as the turbidity/particle source. The size of the kaolin particles was 0.1 – 4 µm. The stock solution concentration was 5 g/L. Alkalinity was added in the form of Sodium Bicarbonate (NaHCO₃, Fisher Scientific) to provide some buffering capacity to each water. Instant

coffee (Maxwell House, 8 g/L stock solution) and liquid fertilizer (Eco Lawn & Garden Super-Hume, 2% solution) were the surrogates used to control both TOC and SUVA. The liquid fertilizer is a humic and fulvic acid concentrate with a composition of 17% humic acid, 13% fulvic acid, and 4% humics obtained from Leonardite shale (Eco Lawn & Garden, 2013). Coffee solutions were made daily and all other solutions were limited to a holding time of one week. The Moderate turbidity/DOC/SUVA model water was initially made in 2.2 L batches in individual jars for benchtop testing, but a batch method (26.4 L) where only kaolin was dosed in the jars was later used. It will be noted when the water in question was synthesized individually or in a large batch. Model batch waters were always used for experiments within 24 hours.

The two natural waters utilized during this study were obtained from Mt. Holly Water Treatment Plant located in Mt. Holly, North Carolina and Kannapolis Water Treatment Plant located in Kannapolis, North Carolina. Water from the Mt. Holly Water Treatment Plant was collected from the raw water sample tap and all jar tests were conducted at the treatment facility. Water from the Kannapolis Water Treatment Plant was collected from the raw water tap in 7-gallon water jugs (Reliance Aqua-tainer[®]). The raw water collected from Kannapolis was stored at 4°C and used within 48 hours.

3.5 SUVA and Dissolved Organic Carbon

Raw water UV-254 absorption was measured with an UV-Vis spectrophotometer (Agilent Technologies Cary 60, Cary WinUV Version 5.0.0.999 software). The UV cell used was a standard quartz cuvette with a 1 cm light path. A raw water sample was collected in a glass 30 mL syringe (Micro-Mate[®] Interchangeable). The sample was

carefully filtered through a polycarbonate 0.4-micron membrane (GE, Model # K04CP02500). The filter membrane was placed in a 25-mm filter holder (Millipore Swinnex) with a pair of tweezers, ensuring the membrane was appropriately positioned without being compromised. The filter holder was attached to the syringe and the plunger was depressed with enough pressure to push the sample through the membrane. The water was filtered directly into an autoclaved, amber, 40 mL, round vial. After the sample filtration was complete, the membrane was inspected to certify there was no damage or complications during the process that could have affected the quality of the sample.

Prior to UV absorption analysis, the instrument was zeroed using ultrapure water. The UV cell was cleaned by blotting with a lint-free wipe, then wiped with a sheet of lens paper before zeroing and between each reading. The “Q” on the cell was always placed facing the lamp module. After zeroing, the cuvette was filled with raw water and placed back into the cell holder with the same orientation as when zeroed. Three measurements were taken for each sample and verified to be within the specifications of the instrument. The lowest of the three readings was recorded. The sample was disposed of, and the cell was rinsed using ultrapure water before running another sample. It was not verified that there was no sample contamination from the sample vials and filtration equipment used during TOC testing.

After UV analysis, DOC of the sample was measured. Dissolved organic carbon was measured using a total organic carbon analyzer (Shimadzu TOC-L, Shimadzu ASI-L Autosampler). The instrument follows Standard Method 5310B. TOC measurement software (Shimadzu Control L Version 1.00) was used for data recording. A calibration curve was created using the calibration curve wizard. Standards were produced using auto-

dilutions from a 10 mg DOC/L stock solution. Figure 3.3 is a graph of the calibration curve.

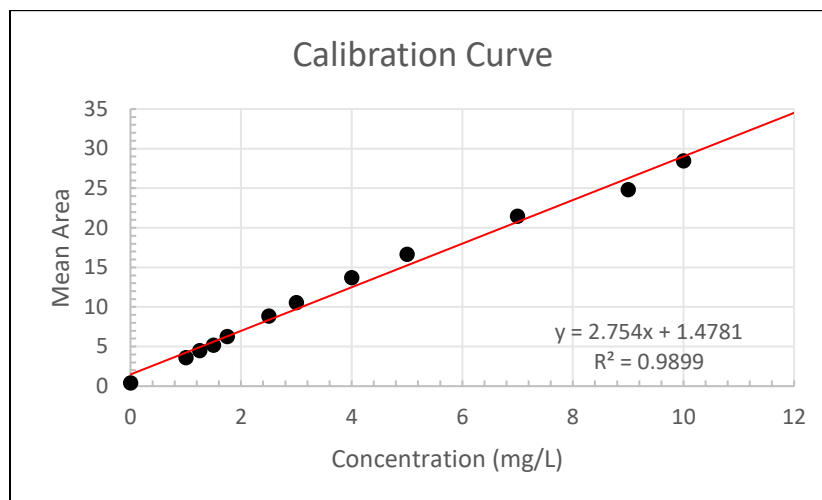


Figure 3.3. Shimadzu TOC-L calibration curve from TOC Control L software.

Raw sample DOC analysis was preceded by two runs with ultrapure water. After all raw water samples had been measured another wash cycle with ultrapure water was conducted. These were used to ensure the instrument was clear of contamination from previous measurements.

3.6 Flocculation Mixing Analysis

As previously mentioned, several different flocculation schemes were analyzed during this research. A photometric dispersion analyzer (PDA 2000, Rank Brothers, LTD, London, UK) was used to evaluate how changing flocculation procedures affected floc size. The mixing intensities used during analysis were 24, 36, 50, 80, 115, and 174 s^{-1} . These G values corresponded to flocculation at 30, 40, 50, 70, 90, and 120 rpm on the jar

test apparatus with 1.8 L of water at 20 °C. This temperature was assumed and used for calculation purposes only.

The PDA 2000 was used during flocculation analysis to monitor flocculation growth rates and peak floc size. The premise of PDA theory was previously discussed in other sections. Aggregation was monitored in a continuous flow-through cell as a beam of light from a high intensity LED was directed through the cell. The transmittance of light through the coagulated sample was measured by a photodiode, and the signal was converted to a voltage proportional to the intensity. The voltage signal's A.C. component was amplified, and signal fluctuations measured. The amplification allows for fluctuations of <1 mV in a 10 V signal to be examined. The RMS of the A.C. signal was found by the PDA 2000, and the ratio of RMS to D.C. voltage (FI) was the output used for flocculation monitoring. Particle aggregation causes the FI to increase. Throughout experimentation, the RMS gain was set at 0.80 and the D.C. gain was set to 5.00. The PDA's electronic filter was on during all monitoring. The filter used data averaging over an interval of 5 seconds, which allowed for a smoother output signal.

Mixing during PDA analysis was carried out using an overhead mixer (IKA[®]-Werke Eurostar Power Control-Visc S1) with a 3.4" hydrofoil impeller. LabView software was utilized to control mixing and record PDA data. Automation of the mixing program allowed for consistent transitions between the stages of the flocculation process. A USB data acquisition module (Cole-Parmer Instrument Company, Item # 18200-00) was used to carry out communications between the peripheral instruments and the LabView program.

Figure 3.4 is a schematic of the apparatus configuration used during PDA analysis. A support jack (BrandTech Scientific Inc.) was used to ensure that the hydraulic head during flocculation testing matched that of the bench jar test to provide similar filter loading rates. A jar (Phipps & Bird™ B-KER²®) sample tap was connected to an equal tee with 1/4" ID polyethylene opaque tubing. A sample valve was connected to the branch (3/8" polyethylene tubing with push-to-connect ball valve). Tubing (Masterflex® L/S® 15 A 60 F) was used from the tee to the PDA instrument with 1/8" ID tubing (Tygon® R-3603) at the flow cell and transitioned back to 3/16" ID silicone tubing (Masterflex® L/S® 15 A 60 F). Flow was circulated using a peristaltic pump with computerized drive (Cole-Parmer Instrument Company, Masterflex® L/S® Model 7550-10) and pump head (Masterflex® Easy Load, Model 7518-02).

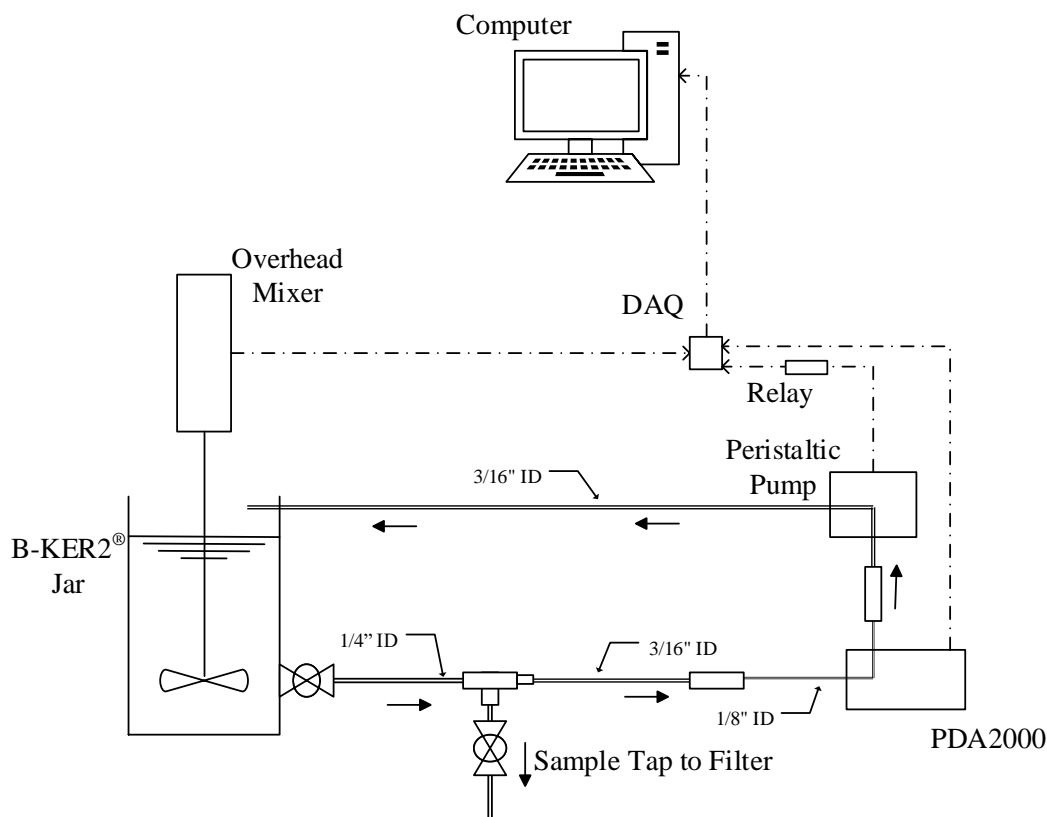


Figure 3.4. PDA Apparatus Schematic.

Each trial consisted of a one-minute rapid mix at an intensity of 609 s^{-1} (300 rpm, 2 L of water @ 20°C) and 10 minutes of single-stage flocculation. There were two tapered flocculation procedures evaluated. Tapered flocculation consisted of 3 stages at a duration of 5 minutes for the first 2 stages and 10 minutes for the final stage. Mixing intensities (RMS velocity gradients) were 80 s^{-1} for the first stage, 50 s^{-1} for the second, and 24 s^{-1} for the final stage during the first trial of staged flocculation experimentation. The second tapered-flocculation experiment consisted of mixing intensities of 174, 155, and 80 s^{-1} for the first, second, and third stages respectively. Single-stage mixing intensities of 174 and 24 s^{-1} were evaluated individually for particle removal efficiency using filtration in a manner similar to that applied to jar testing procedures. Filtration analysis was carried out

under 2 different treatment conditions. To mimic flocculation under the charge neutralization coagulation mechanism a coagulant dose of 5.0 mg/L as Alum was selected and the target coagulated pH was 5.0. Sweep flocculation conditions targeted a coagulated pH of 7.0 with a coagulant dose of 50 mg/L as Alum. After preliminary testing, 174 s⁻¹ single-stage and the first tapered-flocculation (80 s⁻¹ for the first stage, 50 s⁻¹ for the second, and 24 s⁻¹ for the final stage) procedure were evaluated using full jar testing procedures using the previously mentioned flocculation times. All flocculation analysis was carried out with the moderate turbidity/DOC/SUVA model water. Prior to beginning each flocculation trial, the jar was filled with 2.3 L of model water and kaolin was added to achieve the desired turbidity. During this process, the mixing speed was set at 160 rpm (120 s⁻¹) using the manual control on the LabView program. The main valve on the jar was then opened. Approximately 10 mL of water was wasted through the sample tap and a 200-mL sample was collected. Titration was performed in the same manner as with the bench top procedures to determine appropriate chemical dosing. The initial temperature was also measured. A 40-mL turbidity sample was collected, measured, and recorded. Before adding the predetermined volume of pH adjusting chemical, it was necessary to ensure that the water level was at the 2 L mark on the jar. After pH adjustment, the pump was primed. After priming the pump, the pump was started with the LabView program through a connection with a VFD relay. The flow rate was preset to 20 mL/min. The PDA instrument was turned on and the gain was set (RMS = 80, dc = 5.0). Coagulant dose was prepared and administered with a pipette (Fisherbrand® 2-10 mL Finnpiipette). The desired flocculation parameters were entered into the program, and the mixer was taken out of manual mode. Upon starting the flocculation program, rapid mix was initiated, and a 1-

minute baseline measurement was recorded without the addition of coagulant. After one minute, the coagulant was added. A 200-mL pH sample was collected at the end of rapid mix, and the coagulated pH was recorded. If filtration was required, then the filter was connected at this point. At the end of the desired time period, data collection and the mixer were stopped. Filtration required an additional 5 minutes of flocculation, but the additional data were omitted from analysis. Final pH and temperature data were collected after testing was completed.

3.7 Filter Loading Rate

3.7.1 Deep Filter Apparatus

Preliminary evaluation of the relationship between filter loading rates and filter turbidities was conducted on a deep bed lab-scale filter apparatus with 18” of Vitro Clean® filter media. The filter was constructed using 2”, clear, schedule 40 PVC. Flow through the apparatus was controlled with a 0.5 h.p. motor and pump head (Washguard SST®, Micropump Inc.) with an A/C inverter control drive (Lenze® AC Tech SMVerter NEMA 4X). Flow was monitored with an inline flow meter (Endress-Hauser® Promag 50) with manual verification using a graduated cylinder. A schematic of the apparatus can be seen in Figure 3.5.

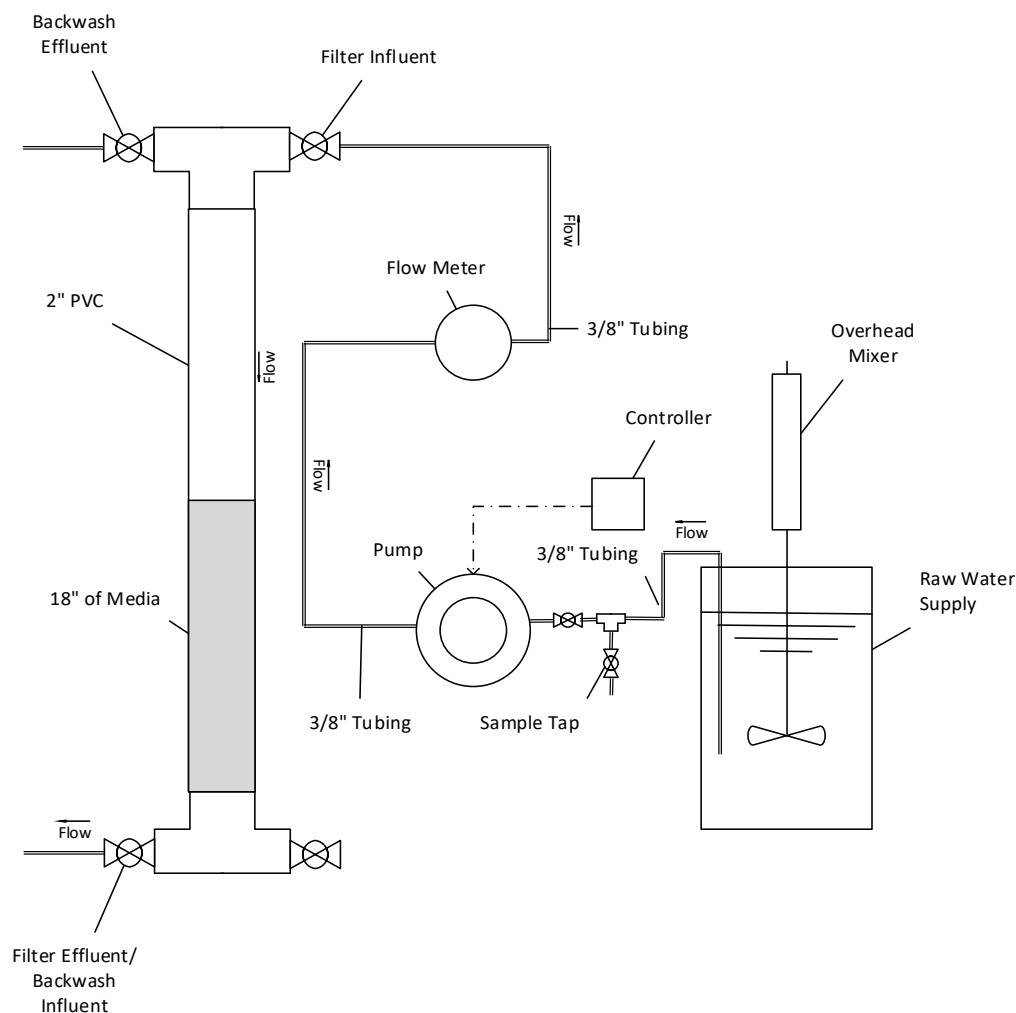


Figure 3.5. Schematic of deep filter apparatus.

Raw water was treated in 15L batches in a 5-gallon bucket. Mixing was carried out using an overhead blender (Caframo™ Stirrer BDC2002) with a 4.5” hydrofoil impeller. Mixing intensity modeled that from the jar tester apparatus. Rapid mix was at a G value of 609 s^{-1} (578 RPM) for 1 minute. Tapered flocculation was conducted with mixing at intensities of 80 (149 RPM), 50 (106 RPM), and 24 s^{-1} (RPM) for a duration of 5, 5, and 10 minutes, respectively. At the completion of the final stage of flocculation, mixing was continued and filtration began.

Filter loading rates evaluated were 4.67, 2.86, and 0.47 gpm/ft². A total of six treatment conditions were evaluated. Target coagulated pH values used were 5.5 and 6.5. The three alum doses were 0, 5, and 40 mg/L as Alum. Procedures followed those from Section 3.3.

3.7.2 Bench-Scale

Setup and experimentation for filter loading rate testing on the bench-scale followed jar test procedures from Section 3.2. A modified filter effluent tube was constructed with 5/16" ID tubing reduced to 1/8" ID tubing (Tygon[®] R-3603). These tubes were used on filters 2-6. Effluent tips were 2 tube-to-tube barb connectors (1/8" ID), 2 tube-to-tube reducers (1/8" ID × 1/16" ID), and a syringe tip (BD Leur-Lok[®]) with an 18-gauge needle (BD PrecisionGlide[®]). Flow from jars 2, 3, and 5 were reduced by using two-part epoxy to affix insulation sheathing from copper wire to the effluent tips. Jar 4 was an unaltered reducer and Jar 6 used the needle tip. Table 3.5 displays the flow rates with corresponding filter loading rates tested.

Table 3.5. Flow and loading rates used during flow rate analysis.

	Jar 1	Jar 2	Jar 3	Jar 4	Jar 5	Jar 6
Flow Rate (ml/min)	384	203	177	118	71	30
Loading Rate (gpm/ft ²)	4.65	2.46	2.14	1.43	0.86	0.36

CHAPTER 4: RESULTS AND DISCUSSION

4.1 Titration

Titration was an important step in the new jar test procedure. Alum is an acid and when treating with alum only the path of potential treatment conditions goes diagonally across a two-dimensional area. An example of this can be seen in Figure 4.1, where an alum only titration curve was graphed on the coagulation diagram from Figure 2.2. It is observed that increasing alum dose changes both coagulation variables (coagulation dose and coagulated pH) simultaneously. Operating with alum only limits treatment to an area of mostly sweep flocculation. It would be necessary to adjust coagulated pH to allow for the evaluation of treatment potential in other areas of the operational diagram. The primary difference between the new jar test procedure and the procedures that came before it is the recommendation to optimize both coagulation variables independently.

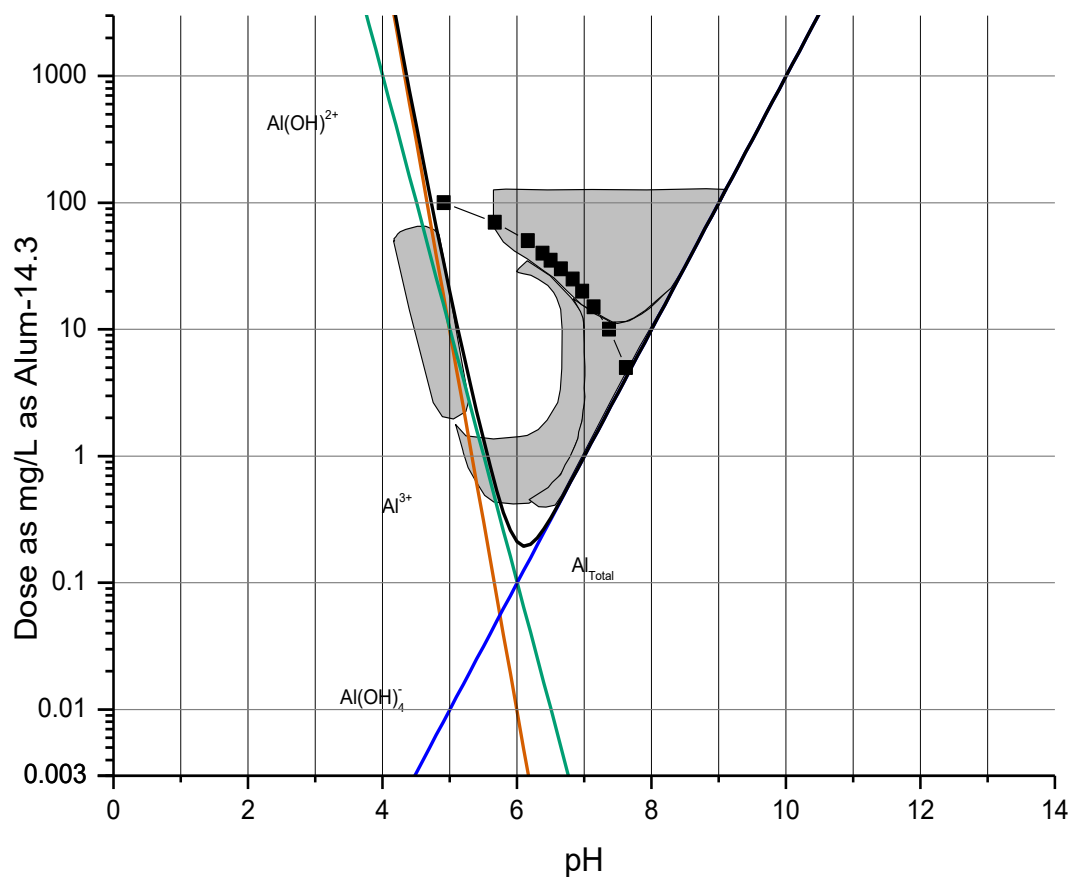


Figure 4.1. Operational coagulation diagram graphed with an alum-only titration curve from model water #2.

During jar testing, a titration was required for each jar to determine the amount of acid or base needed to achieve the target coagulated pH. Figure 4.2 displays data from an acid titration for model water #2. There was no coagulant dosed during this titration. The lowest target pH (5.5) required the greatest volume of acid (1.35 mL) to be added to the 200-mL water sample. Raw water pH was consistently between 8.0 and 8.5

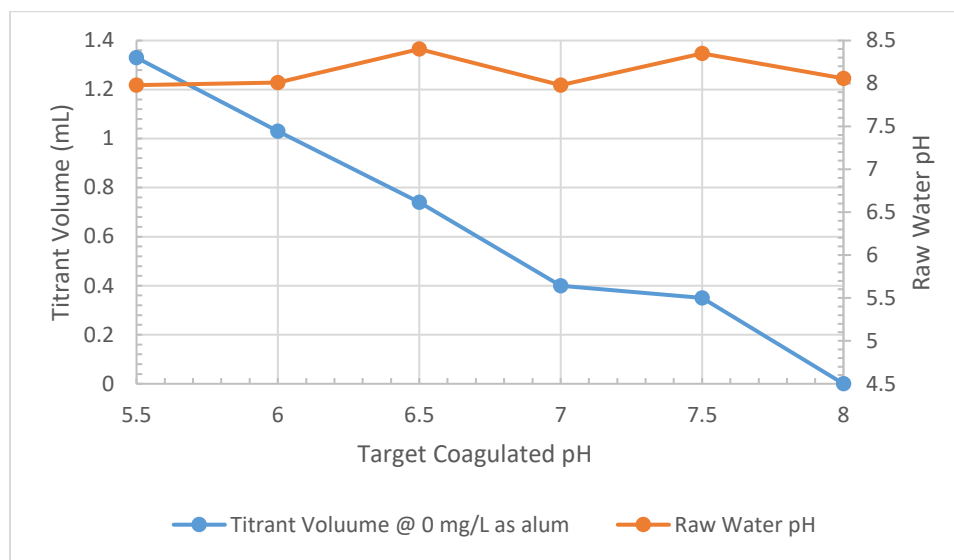


Figure 4.2. Acid titration curve without coagulant addition with raw water pH for model water #2.

Figure 4.3 displays a titration curve for model water #2 at an Alum dose of 30 mg/L. The coagulated pH after the addition of alum to the 200-mL beaker is also displayed. The average coagulated pH during titration for this particular data set was 6.65. For this set of titrations, it was necessary to add either acid or base depending on the target pH (i.e. acid was added when coagulated pH > target pH). This is indicated on the titration curve by a negative slope when acid (0.1 N HCl) was the titrant used and a positive slope when the sample was titrated with base (0.1 N NaOH). Acid was the titrant at the inflection point for this data set.

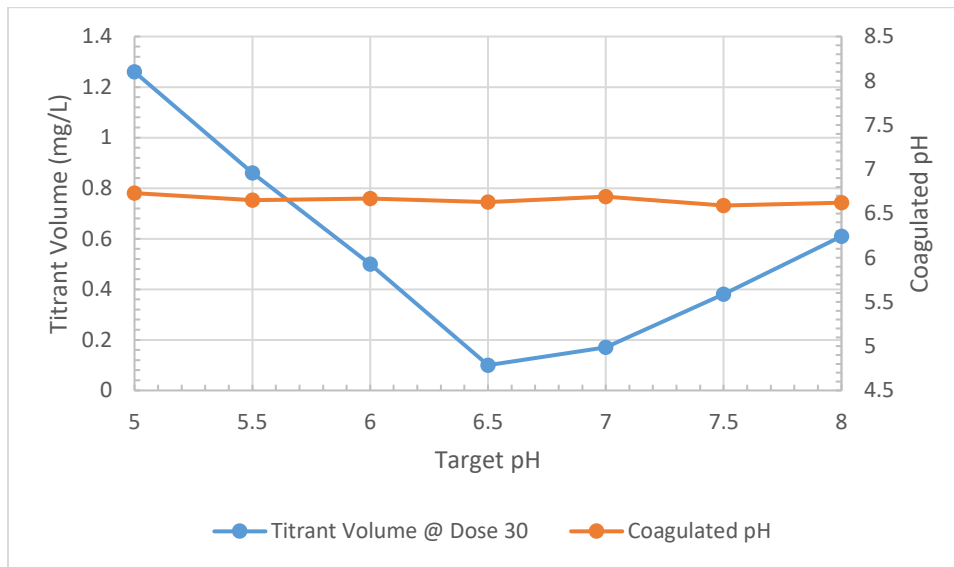


Figure 4.3. Titration curve at a coagulant dose of 30 mg/L as Alum with initial coagulated pH for model water #2.

A summary of the volume of titrant needed to reach the target pH for a series of jar tests for model water #2 can be seen in Figure 4.4. The data are from seven jar test experiments (42 individual jars) across an alum dose range from 0 to 25 mg/L as Alum.

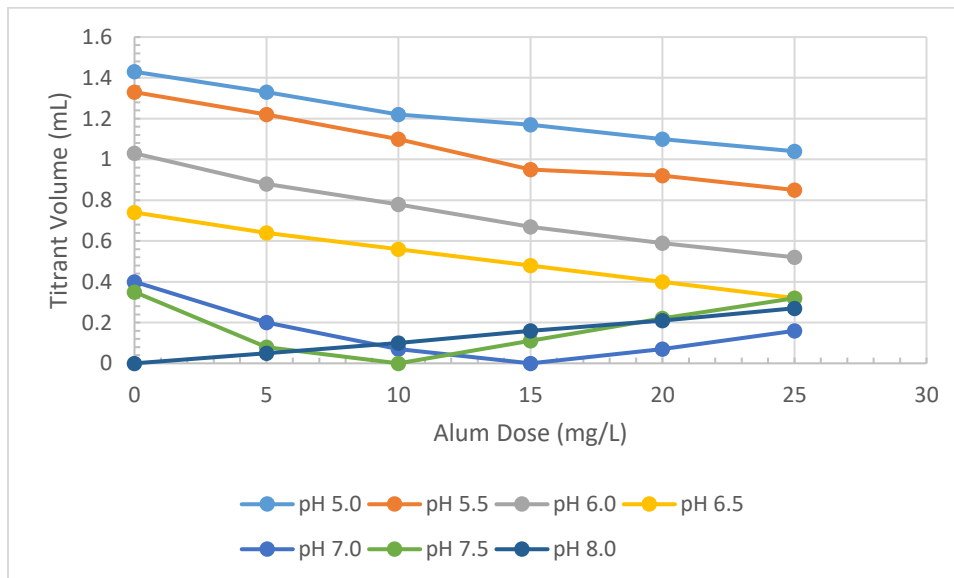


Figure 4.4. Summary of titrant volume addition for a series of seven jar test experiments (42 individual jars) using model water #2.

4.2. Filter Loading Rate Optimization

The objective of filter loading rate optimization was to evaluate the affects that filter loading rate had on filtered turbidity. An optimal filter loading rate would result in the identification of favorable coagulation conditions without falsely identifying suboptimum conditions as effective. Additional objectives were to determine the appropriate media depth and volume for the jar test filter apparatus.

4.2.1 Deep-Bed Filter Apparatus

Initial testing of the relationship between filter loading rate and treated water quality was analyzed on a filter apparatus that contained 18” of media. The media was the same as that from the bench-top filtration apparatus, described previously. The water used during experimentation was the model water #1 (Section 4.2.2). The filter loading rates tested were 4.76 gpm/ft², 2.86 gpm/ft², and 0.46 gpm/ft². Testing was conducted at a coagulated pH of 5.5 (Figure 4.5) and 6.5 (Figure 4.6).

In general, at a target coagulated pH of 5.5 (suboptimum in terms of turbidity removal), a reduction in filter loading rate resulted in lower filtered turbidities. At a target coagulated pH of 6.5, it was observed that filter loading rate had little effect on the filtered turbidities under more favorable coagulation conditions.

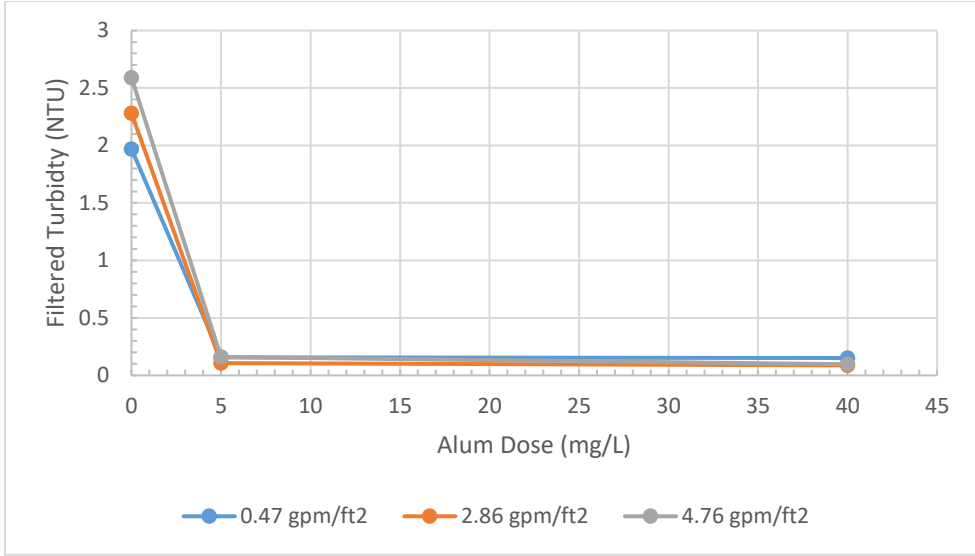


Figure 4.5. Flow rate comparisons with deep filter apparatus at a coagulated pH of 5.5 using model water #1.

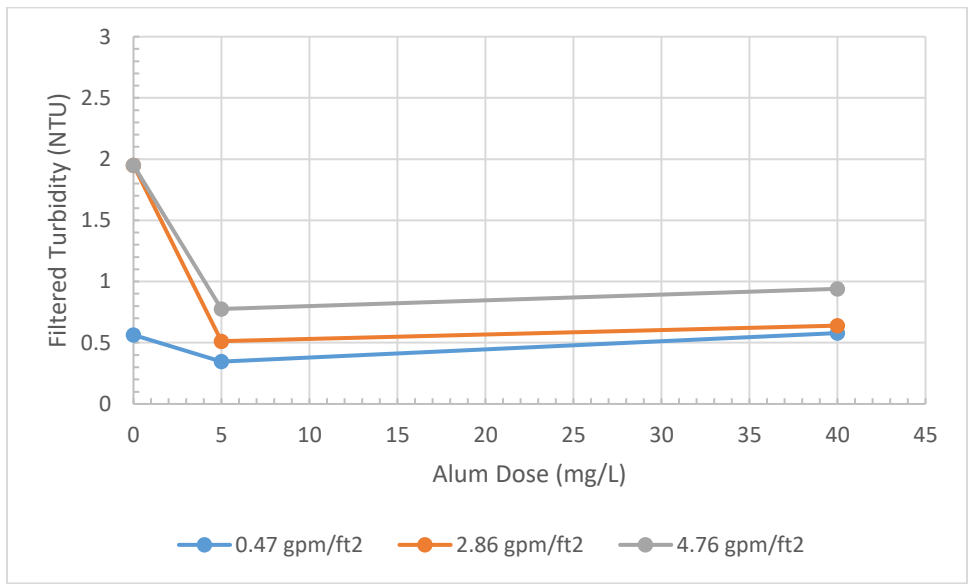


Figure 4.6. Flow rate comparisons with deep filter apparatus at a coagulated pH of 6.5 using model water #1.

4.2.2 Bench Scale Filtration Optimization

Following preliminary testing, filter loading rates were evaluated at the bench-scale with model water #1 on the jar test apparatus with 3” of filter media. This media depth

allowed for there to be enough filter volume available for backwashing and filter headspace without having to build a filter larger than the water volume available for filtration. The loading rates evaluated were 4.65 gpm/ft², 2.46 gpm/ft², 2.14 gpm/ft², 1.43 gpm/ft², 0.86 gpm/ft², and 0.36 gpm/ft². Testing was again conducted at a coagulated pH of 5.5 and 6.5. Results were reported as filtered turbidity and turbidity percent removal. It was observed that at a coagulated pH of 5.5 and a coagulant dose of 5 mg/L as Alum, a filter loading rate of 0.36 gpm/ft² resulted in a filtered turbidity of 0.98 NTU. At a coagulant dose of 5mg/L as alum, the filtered turbidities at all other flow rates ranged from 1.58 to 1.74 NTU. This was a decrease in turbidity removal of approximately 20 to 30%. The results for a target coagulated pH of 5.5 are shown in Figures 4.7 (filtered turbidity) and 4.8 (percent turbidity removal). There were no removals observed below a filtered turbidity of 0.98 NTU (70% removals).

Filter performance on the bench scale apparatus was less than what was observed with the deep filter apparatus (Figure 4.5) at a target coagulated pH of 5.5. Filtered turbidity increased when the filter depth was reduced from 18" of media to 3". This indicates that the filters could be designed in a manner that results in low filtered turbidities when coagulation conditions are poor. This is problematic when the goal of jar testing is to identify pH and coagulant combinations where coagulation conditions are optimal.

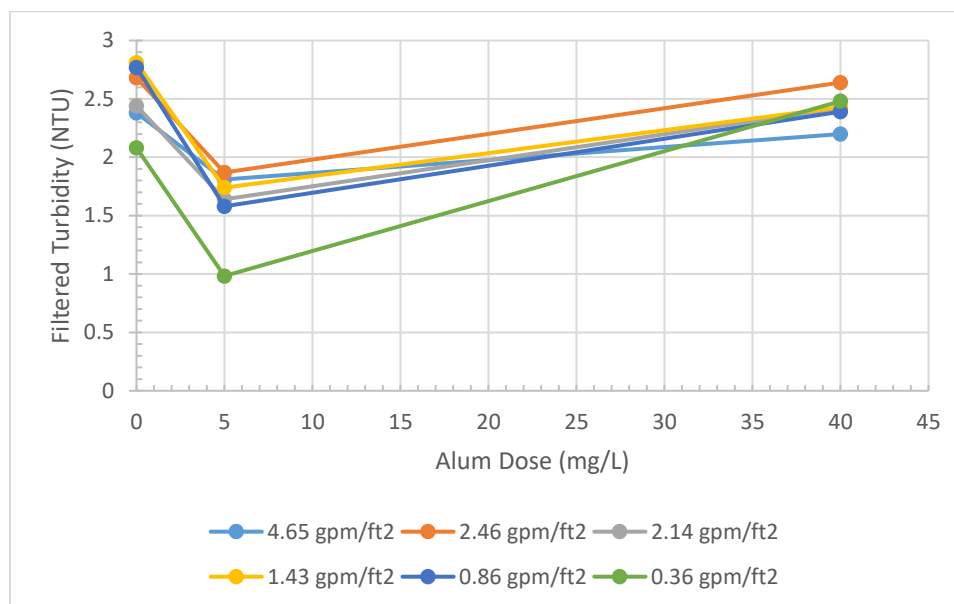


Figure 4.7. Flow rate testing on bench top filter apparatus reported as filtered turbidity at a coagulated pH of 5.5 using model water #1.

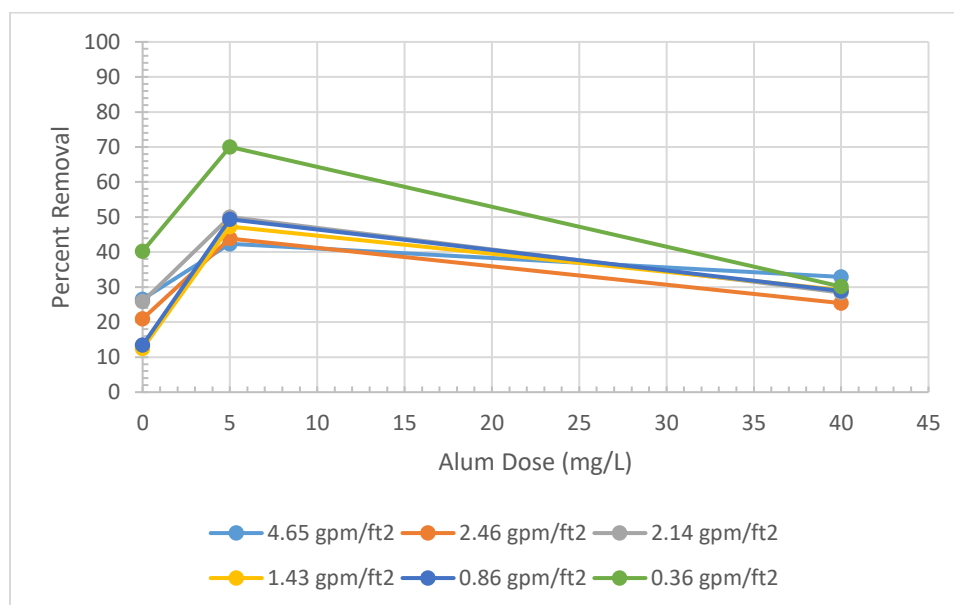


Figure 4.8. Flow rate testing on bench top filter apparatus reported as percent turbidity removal at a coagulated pH of 5.5 using model water #1.

The effects of filter loading rate on turbidity removals was also evaluated at a coagulated pH of 6.5. The results can be seen in Figures 4.9 (filtered turbidity) and 4.10 (percent turbidity removal). Changing filter loading rates had no significant effect on

treatment efficiency at a coagulated pH of 6.5 when compared to a coagulated pH of 5.5. This could be attributed to coagulation efficiency; since particle removal increases due to improved coagulation, the effects of filter loading rate on filtered turbidity are reduced. There was no significant difference between filter loading rates at a coagulated pH target of 6.5. Based on these results, a filter loading rating of 4.65 gpm/ft² was selected because it provides effective treatment through the jar test filtration apparatus in the shortest amount of time. Also, variations in loading rates between jars should have minimal effect on filtered results. This appears to be especially true when treatment is most efficient, which is precisely the conditions this method is intended to identify. Unlike in Figures 4.5 and 4.7, filter design does not appear to affect filtered turbidity when coagulation conditions are favorable.

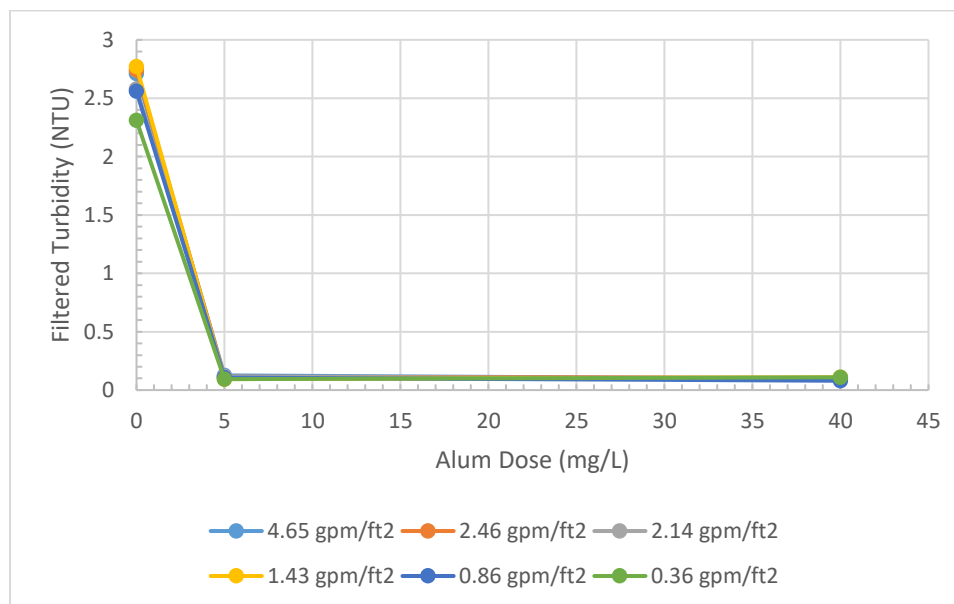


Figure 4.9. Flow rate testing on bench top filter apparatus reported as filtered turbidity at a coagulated pH of 6.5 using model water #1.

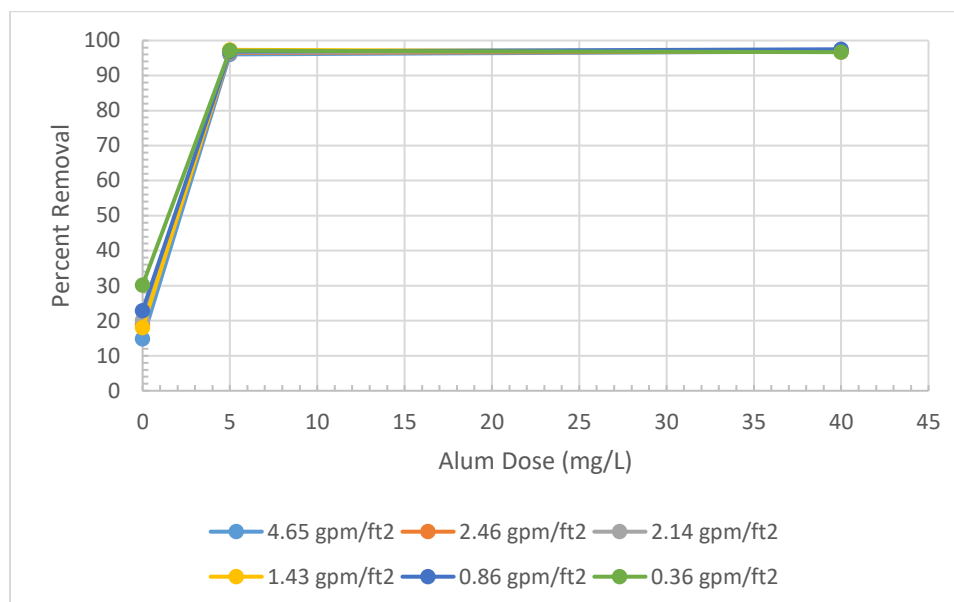


Figure 4.10. Flow rate testing on bench top filter apparatus reported as percent turbidity removal at a coagulated pH of 6.5 using model water #1.

4.3 Mt. Holly Water

4.3.1 Natural Water #1

Jar tests were conducted at the City of Mt. Holly's water treatment facility. Sedimentation results were compared to those from filtration. Triplicate testing was conducted for both sedimentation and filtration. Low-intensity tapered flocculation was used exclusively at Mt. Holly. Alum-only (no pH adjustment) was used during these jar tests because the Mt. Holly Water Treatment Plant does not have the ability to control coagulated pH with acid and does not utilize any pH adjustment with a base prior to the coagulation process. The results of jar testing are summarized in Figure 4.11 (final turbidity versus alum dose) and Figure 4.12 (percent turbidity removal versus alum dose). Percent turbidity removal results are provided throughout this paper to provide normalized results based on raw water turbidities. There will be scenarios where this result will be preferred to filtered turbidity, and it will be noted in the text.

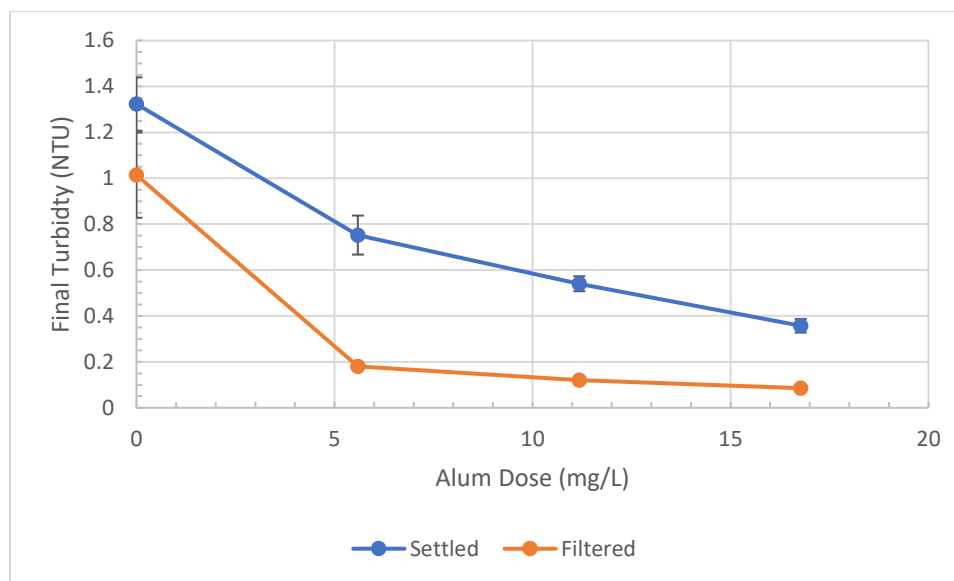


Figure 4.11. Final turbidity comparisons for settled and filtered jar tests at Mt. Holly Water Treatment Plant.

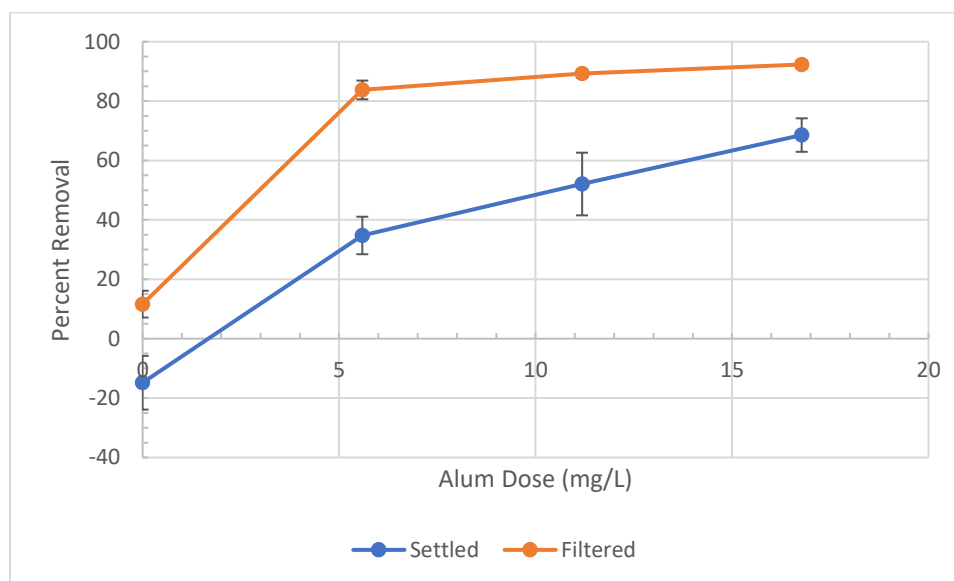


Figure 4.12. Percent turbidity removal comparisons for settled and filtered jar tests at Mt. Holly Water Treatment Plant.

Under all treatment conditions evaluated, filtration provided lower residual turbidities when compared to sedimentation. Filtration indicated an effective Alum dose of 5.6 mg/L based on final turbidity values (≤ 0.3 NTU), whereas sedimentation did not

indicate an effective treatment dose at any coagulant dose evaluated. During the time of these experiments, the plant was operating at a coagulated pH of 6.7 with an Alum dose of 13 mg/L. The filtered turbidity was 0.04 NTU.

Coagulated pH from jar testing at the Mt. Holly Water Treatment Plant can be seen in Figure 4.13. As previously mentioned, there was no pH control during experimentation. Values were similar during this series of testing.

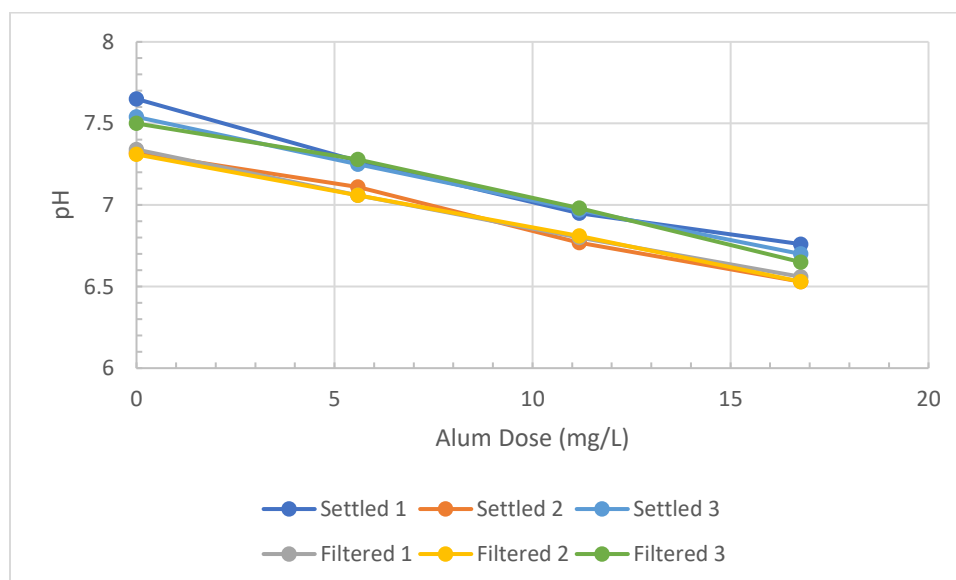


Figure 4.13. Coagulated pH for jar testing at the Mt. Holly Water Treatment Facility.

4.3.2 Model Water #1

A model water was made to mimic the raw water at the Mt. Holly Water Treatment Facility. A series of jar tests were conducted across a coagulant dose range from 0 to 35 mg/L as Alum. Coagulated pH was controlled. Filtration was applied as the particle removal mechanism. The results are summarized in Figure 4.14. Percent turbidity removals $\geq 95\%$ were observed at pH 6.5 with a coagulant dose of 8.0 mg/L as Alum. The same level of treatment was achieved with a coagulant dose of 10 mg/L as Alum at a

coagulated pH of 7.5. Similar turbidity removals were not observed at all other coagulated pH conditions tested.

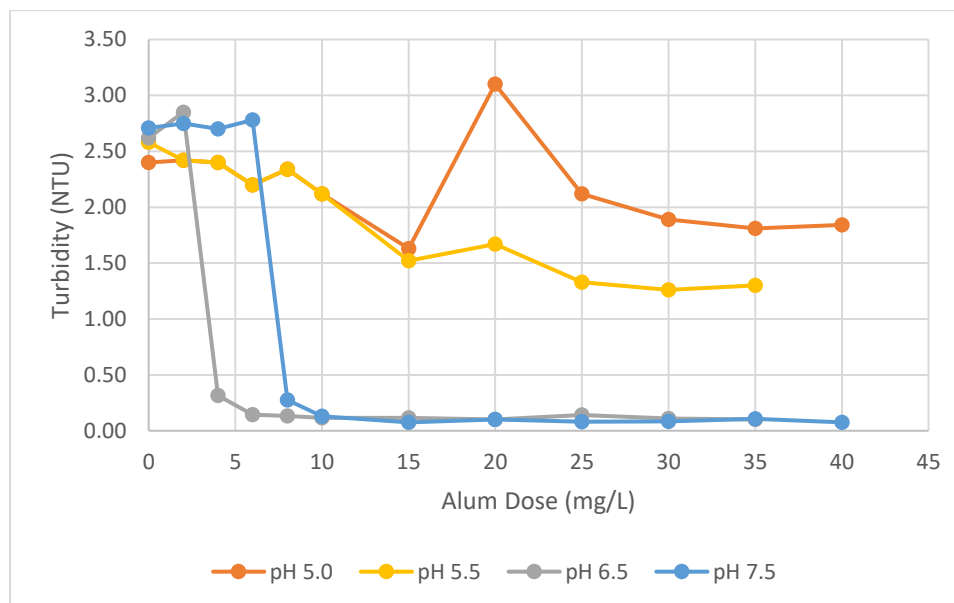


Figure 4.14. Model Water #1 filtered turbidity at a constant coagulated pH.

Filtered jar test results from the Natural water #1 was compared to the model water data from pH 6.5 and 7.5 in Figure 4.15. The natural water results and model water results from pH 6.5 show similar treatment effectiveness at a coagulant dose of approximately 6.0 mg/L as Alum and greater. An Alum dose ≥ 10 mg/L resulted in similar treatment effectiveness under all conditions. The plant was operating at a coagulated pH of 6.7 with an Alum dose of 13 mg/L. The filtered turbidity was 0.04 NTU, with an influent raw water turbidity near 1.00 NTU.

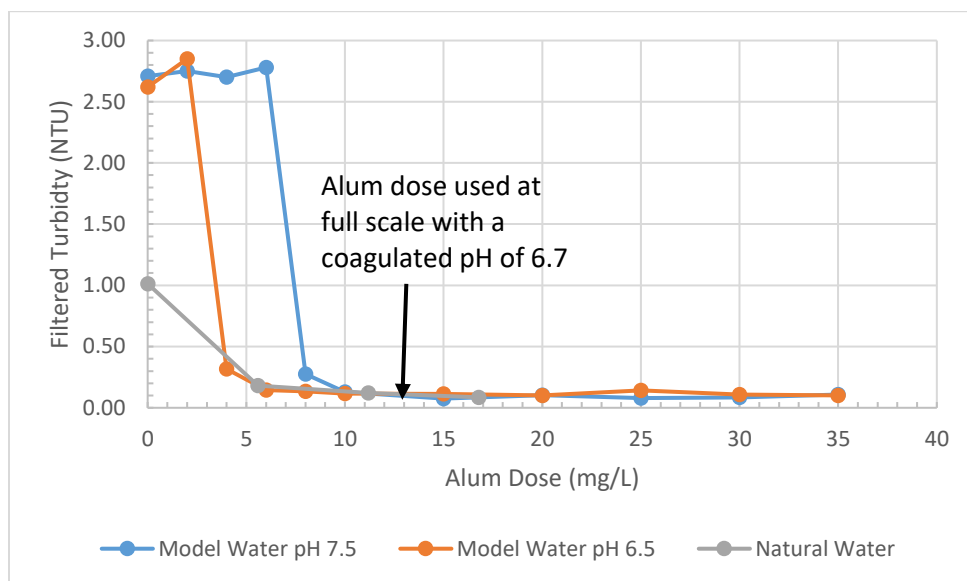


Figure 4.15. Comparison of filtered water turbidity for Mt. Holly natural and model water.

4.4 Natural Water #2

The City of Kannapolis set a goal for its water treatment plant to receive North Carolina's Area-Wide Optimization Program (AWOP) award, which requires combined filter effluent turbidities to remain below 0.1 NTU for 90% of the year. The staff expressed concerns about a problem of increasing combined filter effluent turbidity that occurred in conjunction with rising temperatures. The increased filtered turbidities that the plant was experiencing was not a compliance issue but blocked the aforementioned goal. The raw water at the treatment facility is classified as a low turbidity, low DOC/SUVA water. Low-intensity tapered flocculation with direct filtration was used to create a contour plot so treatment conditions at the plant could be analyzed.

Initially, LITF was applied with sedimentation at the request of the plant supervisor. Figure 4.16 is a graphical representation of the coagulated pH values from the series of jar tests used to create a contour plot for the natural water #2 using LITF with sedimentation

as the particulate removal mechanism. The purpose of this plot is to introduce the concept of how each of the subsequent contour plots were created and to provide a visual representation on where each data point would lie on the contour plot. Each point represents a single jar from a series of jar tests and has a percent turbidity removal associated with it. Plots are based on 14 jar tests with a total of 77 data points, not including the control dose.

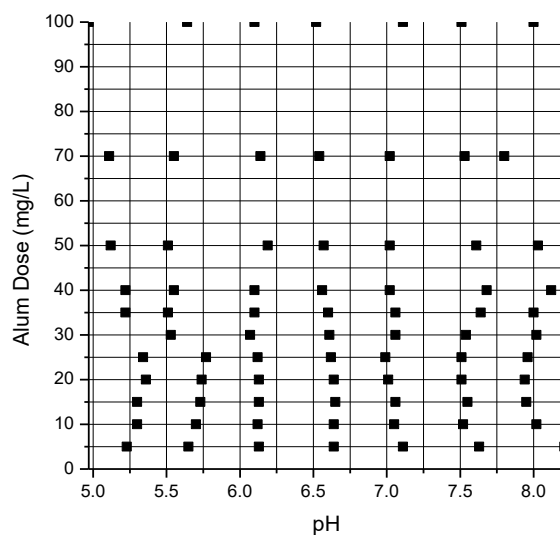


Figure 4.16. Coagulated pH values for natural water #2 contour plot using LITF with sedimentation. Each ■ represents a singular jar from a series of jar tests and has a filtered turbidity associated with it.

The contour plot created using LITF with sedimentation can be seen in Figure 4.17. Maximum treatment efficiency observed was 70 to 80% turbidity removals. The treatment facility is operating in an area of 60 to 70% turbidity removals. Operating conditions at the plant are indicated on the contour plot with a star. Under normal conditions at the treatment facility, filtered turbidities are below 0.1 NTU ($\geq 95\%$), although, according to

settled jar test results, treatment is not taking place in an area of maximum treatment efficiency.

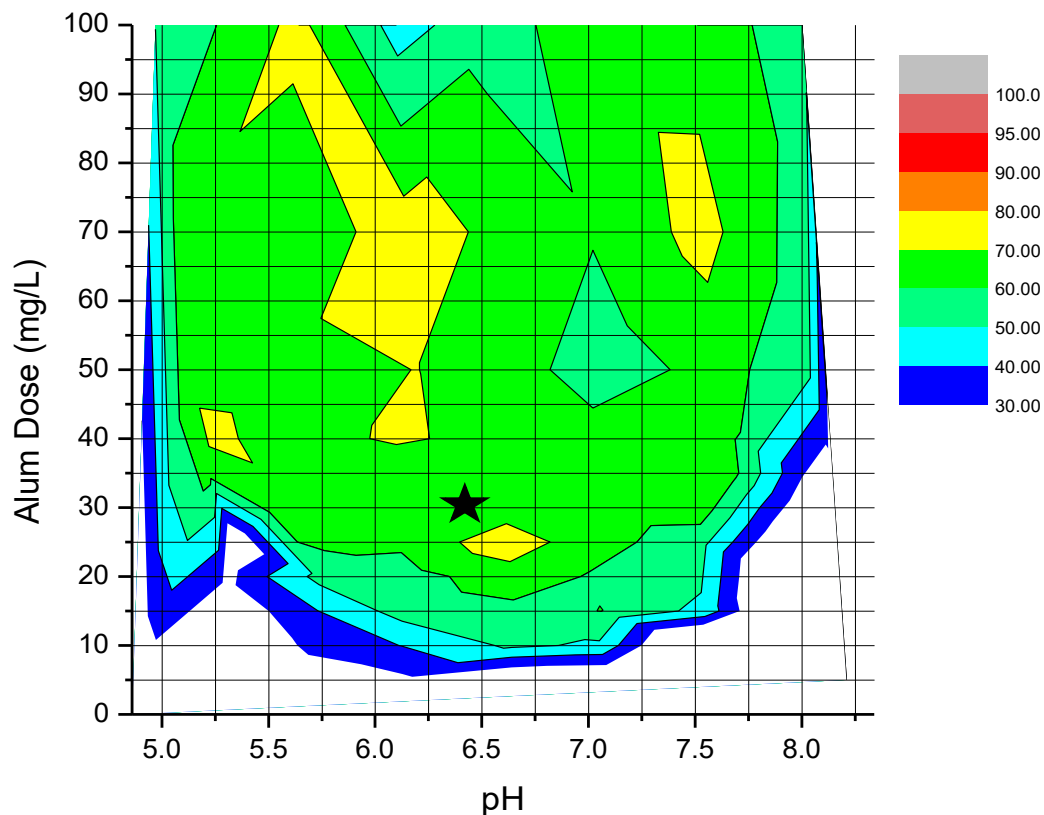


Figure 4.17. Contour plot of percent turbidity removal for natural water #2 using LITF with sedimentation. ★ represents Kannapolis Water Treatment Plant's typical operating conditions.

The contour plot created using LITF with sedimentation was graphed with an alum-only titration curve in Figure 4.18. The importance of the alum-only titration curve is to be able to determine if a water can be treated under optimum conditions using coagulant only without pH adjustment. Based on settled water jar test results, it was observed that the treatment facility can operate within the two zones of maximum observed turbidity

removals without any pH adjustment. The minimum coagulant dose to achieve this is approximately 23 mg/L as Alum.

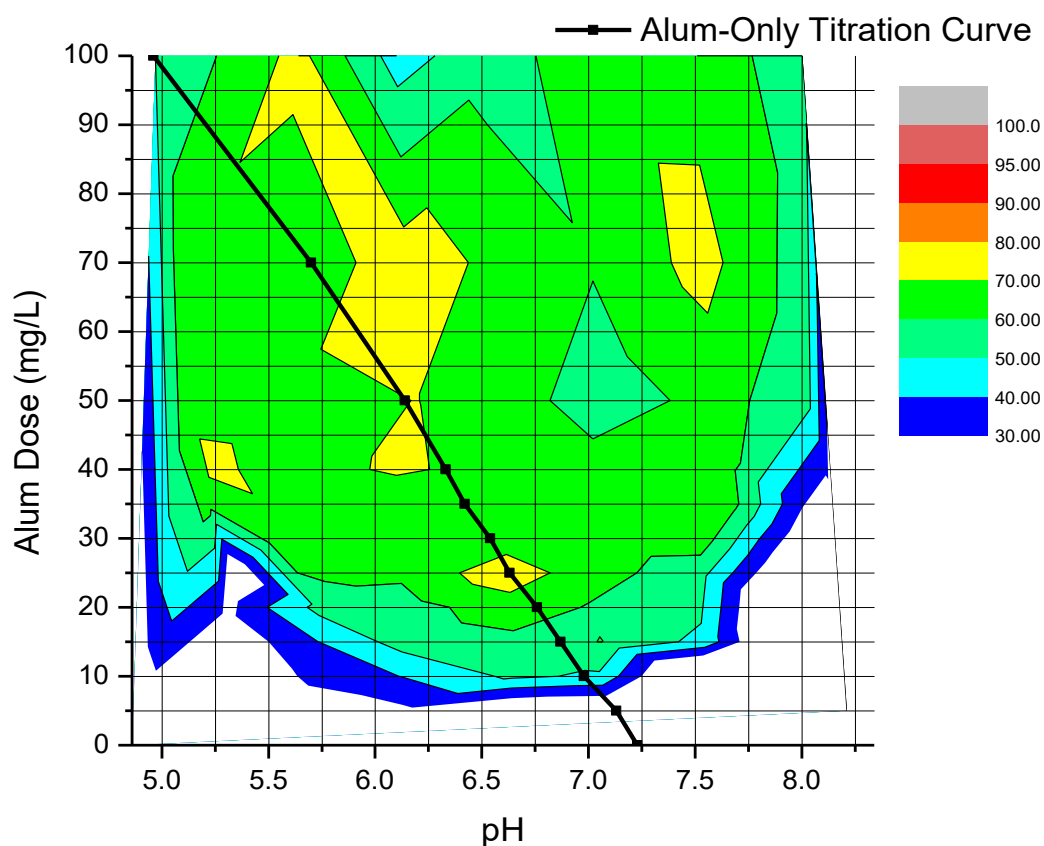


Figure 4.18. Contour plot of percent turbidity removal for natural water #2 using LITF with sedimentation graphed with an alum-only titration curve.

At the completion of sedimentation testing, the settled particles were resuspended over a 5-minute period at 10 rpm for 1 minute, 20 rpm for 1 minute and 30 rpm for 3 minutes before filtration was conducted while mixing was continued at 30 rpm. The resuspension process was verified by comparing direct filtration results to those from resuspension and filtration. Results can be seen in Figure 4.19. Coagulant was dosed at

30 mg/L as Alum at three target coagulated pH values (5.5, 6.5, and 7.5). One trial was run with direct filtration, while the second trial followed the resuspension procedure described above. The filtered turbidity results for each trial were not statistically different at all points evaluated. The p-values from a Poisson analysis between two values for the coagulated target pH values of 5.5, 6.5, and 7.5 were 0.96, 0.99, and 0.99, respectively.

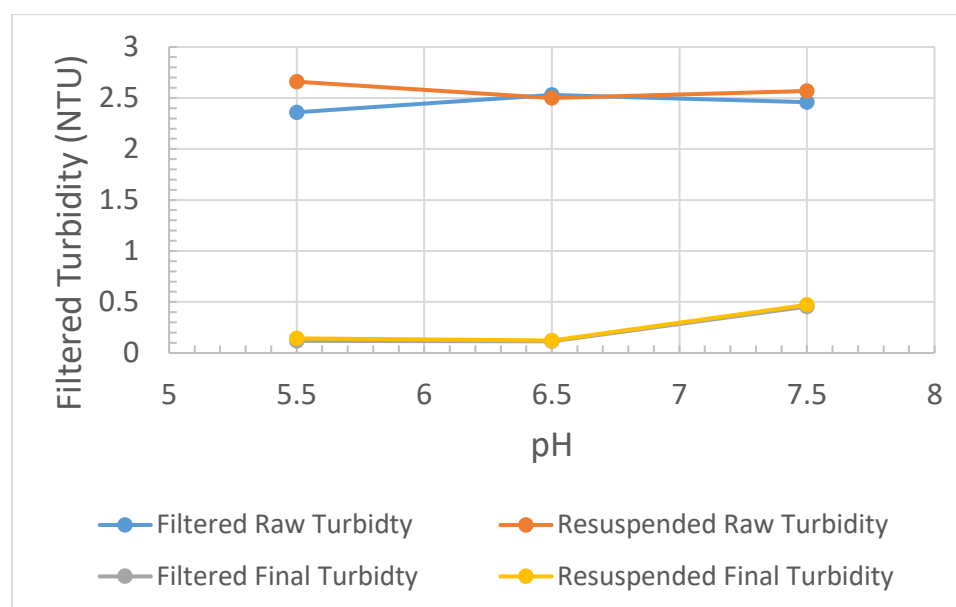


Figure 4.19. Comparison of direct filtration to filtration following settled particle resuspension for natural water #2.

Applying filtration (instead of sedimentation) to the jar test procedure revealed that the Kannapolis Water Treatment Facility is operating within a zone of treatment of at least 95% turbidity removals under typical treatment conditions, denoted by a star in Figure 4.20. Treatment conditions at the plant did not fall within a zone of maximum observed treatment efficiency when sedimentation was used. The filtered results show a single zone of maximum treatment efficiency ($\geq 95\%$) centered at pH of approximately 6.0 and a coagulant dose of 30 mg/L as Alum. The zone extends from a coagulated pH of approximately 5.25 to 6.75. The coagulant dose range is from 20 to 50 mg/L as Alum,

depending upon coagulated pH values. Treatment efficiency decreased as treatment conditions drifted from this centralized zone.

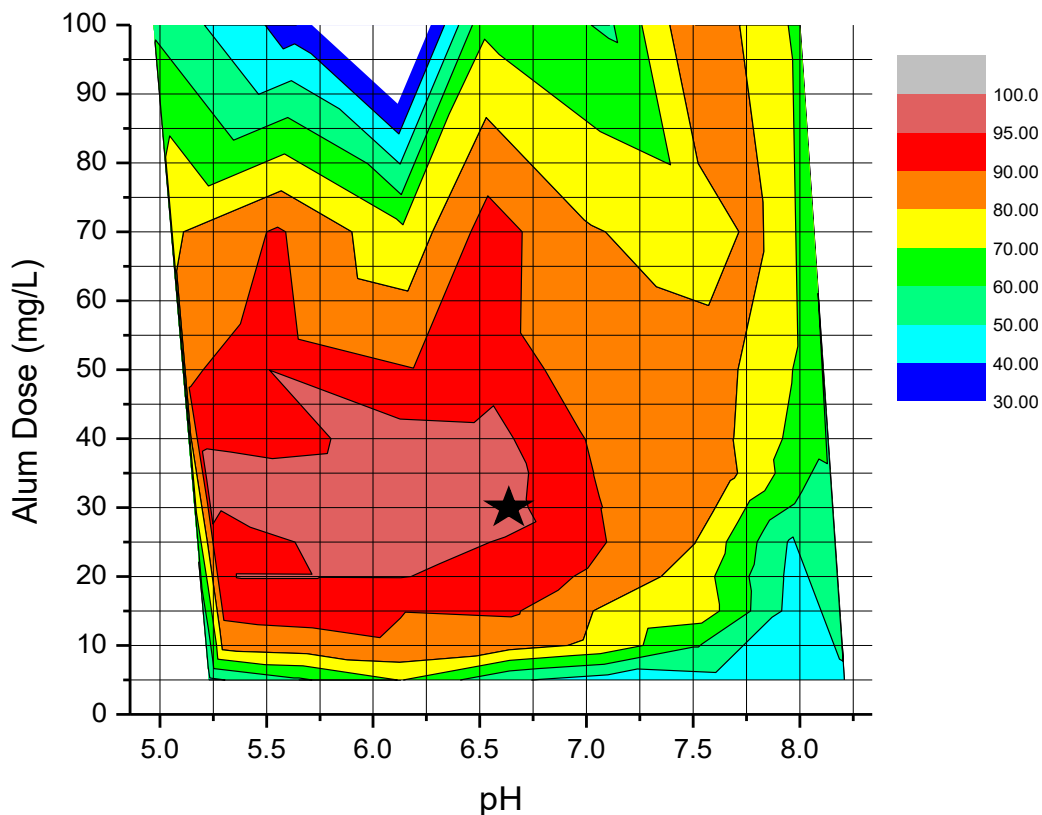


Figure 4.20. Contour plot of percent turbidity removal for natural water #2 using LITF with sedimentation. ★ represents Kannapolis Water Treatment Plant's typical operating conditions.

An alum-only titration curve was plotted over the contour plot from LITF with direct filtration in Figure 4.21. The minimum coagulant dose along this curve that was within the zone of maximum observed turbidity removal was at approximately 25 mg/L as Alum near a coagulated pH of 6.6. The most effective Alum dose range along the titration curve is from 25 mg/L (pH 6.6) to approximately 43 mg/L (pH 6.25).

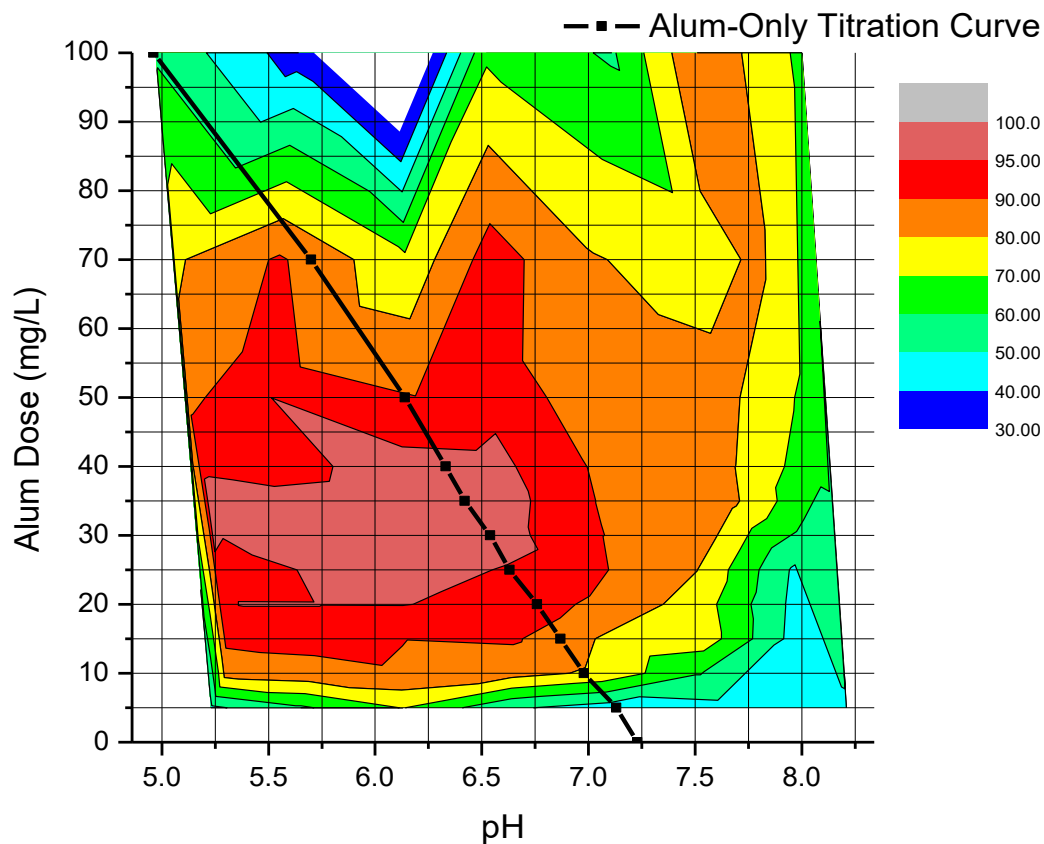


Figure 4.21. Contour plot of percent turbidity removal for natural water #2 using LITF with direct filtration graphed with an alum-only titration curve.

It was observed, when the 70% contour line from LITF with sedimentation was overlaid onto the contour plot from LITF with direct filtration (Figure 4.22), that there was minimal overlap between the zones of maximum turbidity removals from the two data sets. This indicates that using sedimentation as the particulate removal mechanism during jar testing failed to identify areas of maximum treatability. Also, as previously shown, the coagulated pH and alum dose combination being applied at the plant scale could not be determined from sedimentation results using a jar test method.

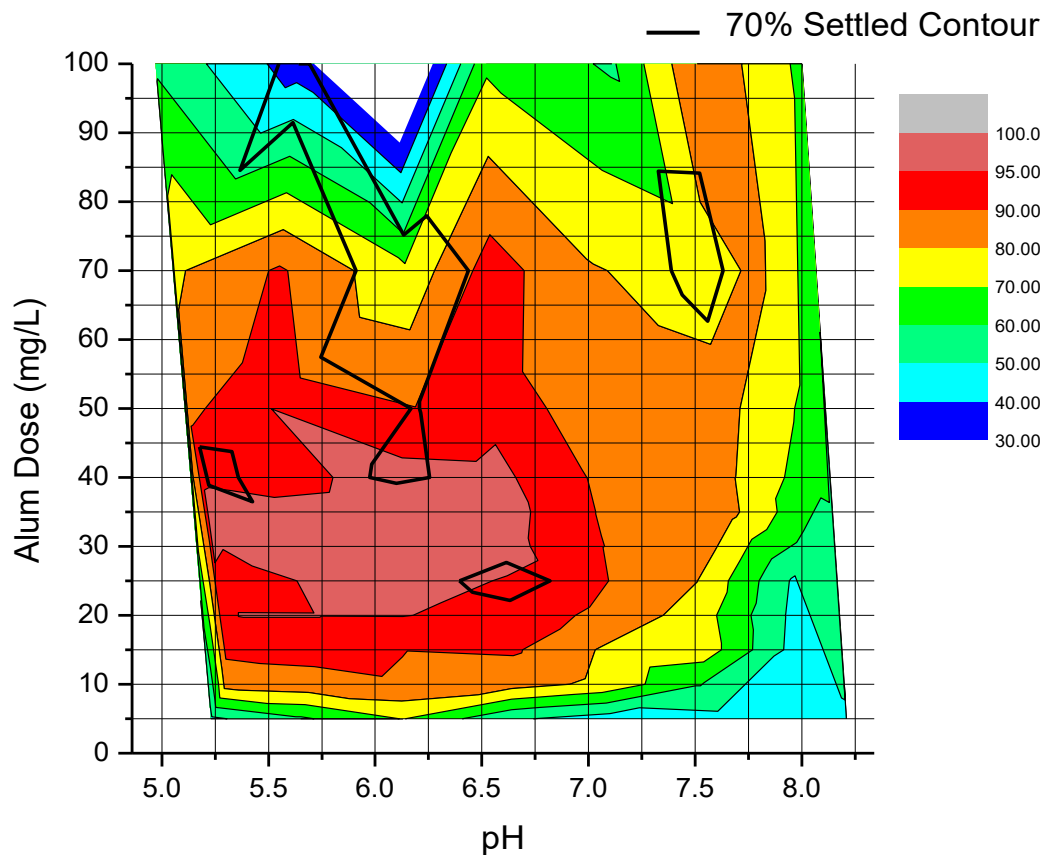


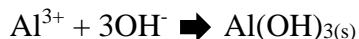
Figure 4.22. Contour plot of percent turbidity removal for natural water #2 using LITF with direct filtration and the 95% removal boundary from LITF with sedimentation.

Based on historical data and conversations with plant staff, it was hypothesized that the increasing water temperatures associated with late summer weather caused a shift in the treatment zone. This hypothesis was based on the relationship between temperature and the ionization constant of water (Au et al., 2011). Table 4.2 shows the relationship between pK_w ($-\log(K_w)$) and temperature.

Table 4.1. Temperature and pK_w.

Temp (°C)	pK _w
0	14.94
10	14.54
20	14.16
25	14.00
30	13.84
40	13.54

This is of importance due to the pK_w being the sum of the pH and pOH. A change in temperature causes a change in pK_w, which in turn causes the equilibrium pH to shift. A temperature correction is necessary because when alum is added to water, the dissociated aluminum ions react with the hydroxyl ions and not the hydrogen ions. The simplified form of this reaction is as follows, where Al(OH)₃ is the precipitate known as “floc”:



When alum is added to water with a pH of 7 at 25 °C, the concentration of hydroxyl ions available for the reaction is 10⁻⁷. When that same alum dose is added to water with a pH of 7 at a temperature of 30 °C, then the concentration of available hydroxyl ions is increased to 10^{-6.84}, a shift of 45%. Shifting the initial pH to 6.84 when the water temperature is 30 °C, ensures that similar alum reactions are occurring, as the initial hydroxyl ion concentration is held at a constant 10⁻⁷.

A theoretical temperature shift to 30 °C was applied to the filtered jar test data from Figure 4.21. A pK_w value of 14.08 was found for 22.3 °C through interpolation between known pK_w values at 20 °C and 25 °C. The contour plot was shifted down the pH scale 0.24 units lower. Results of this shift are plotted in Figure 4.23. It was observed that the

alum-only titration curve moved closer to the 95% contour boundary. The reduction in treatment efficiency along this boundary could be significant enough to be associated with the rising turbidities that are observed at the treatment facility. Increasing the alum dose along this titration curve does not alleviate the problem.

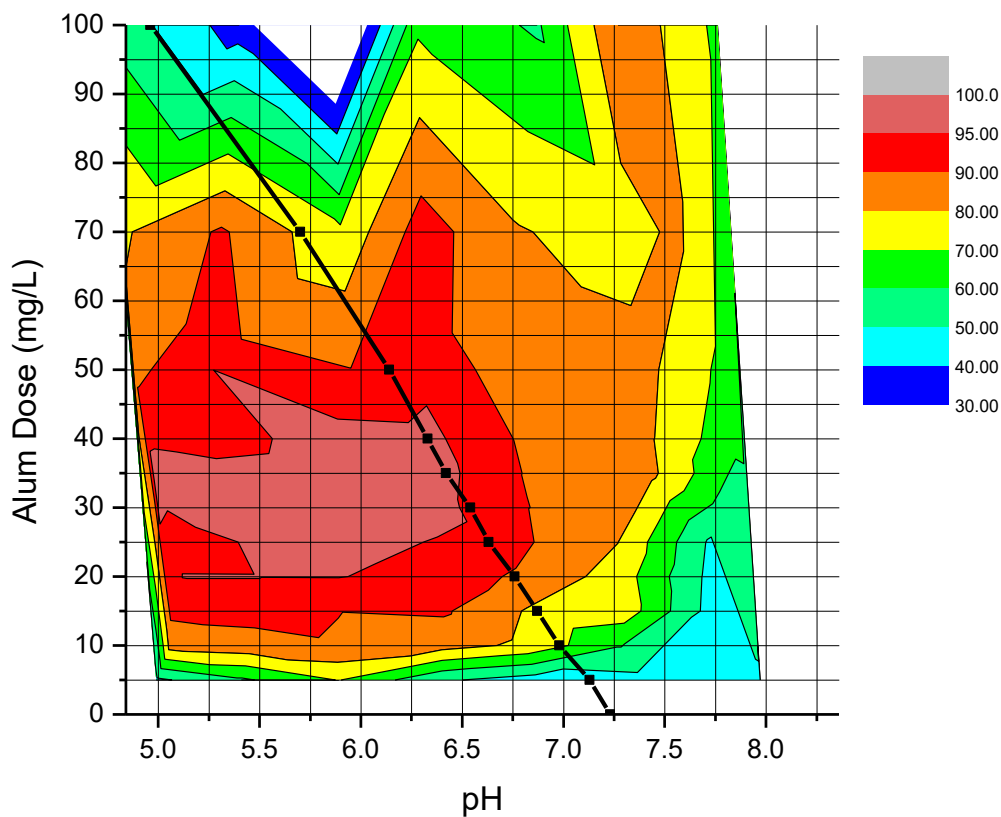


Figure 4.23. Contour plot of percent turbidity removal for natural water #2 using LITF with sedimentation with a theoretical temperature shift to 30 °C graphed with an alum-only titration curve.

It was determined that, instead of increasing the alum dose until the desired filtered turbidity removals were achieved, adjusting the pH with acid would allow for treatment conditions to remain in the zone of $\geq 95\%$ turbidity removals without having to increase

the dose. At this time, a trial of acid feed at the Kannapolis Water Treatment Facility has not been conducted.

4.5 Model Water #2

4.5.1 Flocculation Procedure Optimization

4.5.1.1 Photometric Dispersion Analysis

The application of filtration (instead of sedimentation) to the jar test procedure reduced the testing time by 20 minutes, to a total of 23 minutes. Optimizing the flocculation procedure could further reduce testing time without compromising the test's ability to identify optimal coagulation conditions.

Flocculation mixing intensities and their effects on floc formation were evaluated on model water #2 (moderate turbidity/DOC/SUVA). Figure 4.24 displays the results from single-stage flocculation over a 10-minute period. The coagulant dose (50 mg/L as Alum) and target coagulated pH of 7.0 were selected based on the theoretical sweep zone as indicated by the operational coagulation diagram in Figure 2.2. Prior to flocculation, a 1-minute baseline was collected without coagulant addition. Coagulant was added after the baseline was collected and rapid mixing was carried out at an intensity of 609 s^{-1} for 1 minute. This G-value is equivalent to mixing at 300 RPM on the jar test apparatus. Rapid floc growth began immediately following the completion of rapid mix for all flocculation mixing intensities. The mixing intensities evaluated were 24 (30 rpm), 36 (40 rpm), 50 (50 rpm), 80 (70 rpm), 115 (90 rpm), and 174 s^{-1} (120 rpm). The initial period of rapid growth was over a duration of approximately 60 to 120 seconds. The length of this growth period

decreased as flocculation mixing speeds increased. The floc growth rate during this period was also similar, regardless of mixing intensity.

After this initial period of rapid growth, a FI plateau was achieved. While mixing at lower intensities ($G = 24, 36, \text{ and } 50 \text{ s}^{-1}$) resulted in an FI plateau that either remained constant or had a slight increase over the duration of the flocculation period. Higher mixing intensities resulted in an FI plateau that decreased gradually following the end of the rapid growth phase. This corresponds with data and observations from previous researchers, that mixing intensity during flocculation has a direct effect on the size of the flocs formed (Yu et al., 2011).

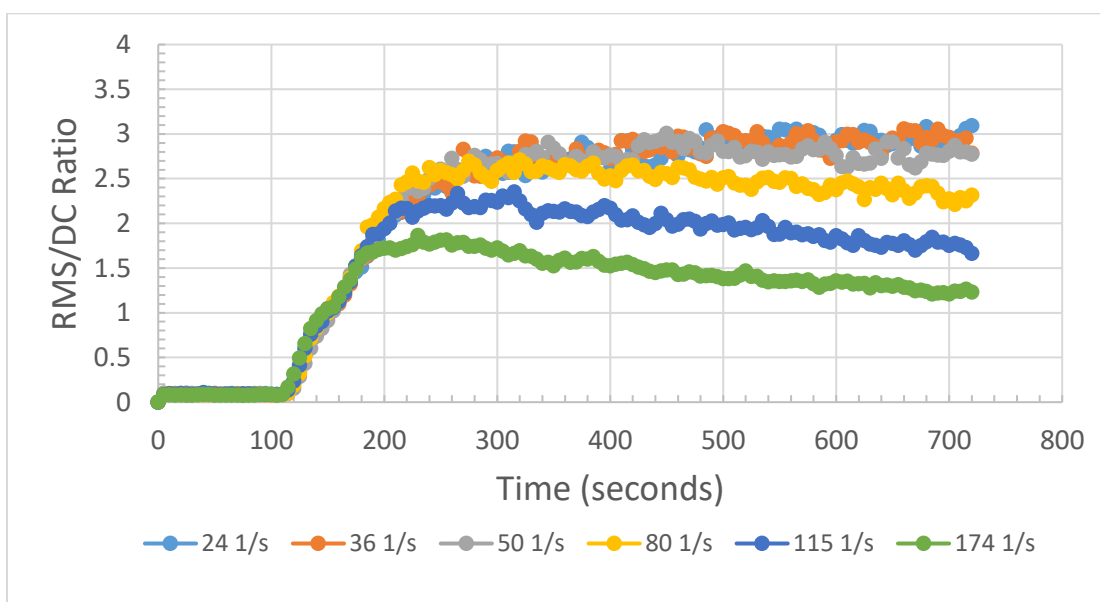


Figure 4.24. PDA analysis for moderate DOC/SUVA model water with single-stage flocculation. (Dose = 50 mg/L as Alum, pH = 7.0)

Under the same coagulation conditions, tapered flocculation was evaluated using PDA. The results of tapered flocculation analysis can be seen in Figure 4.25. Low-intensity tapered flocculation applied mixing intensities of 80, 50 and 24 s^{-1} (70, 50, and

30 rpm) for periods of 5, 5, and 10 minutes, respectively. This resulted in slightly higher FI plateau values than any observed during single-stage flocculation analysis. This could be attributed to either the applied flocculation technique or the extended duration of tapered flocculation, as the flocculation period was increased to 20 minutes for tapered flocculation. High-intensity tapered flocculation (HITF) with mixing intensities 174, 80, and 24 s^{-1} (120, 70, and 30 rpm) produced FI plateau values that were noticeably lower than those from LITF, even though mixing intensities in the final stage of flocculation were the same for each trial. This suggests that initial flocculation growth and floc size is a determining factor in final floc size, regardless of subsequent mixing intensities applied. This could potentially be attributed to the irreversibility of the floc break-up that would be expected at high mixing intensities as suggested by other researchers (Yu et al., 2011). A summary of the results of the PDA analysis for sweep conditions can be seen in Figure 4.26.

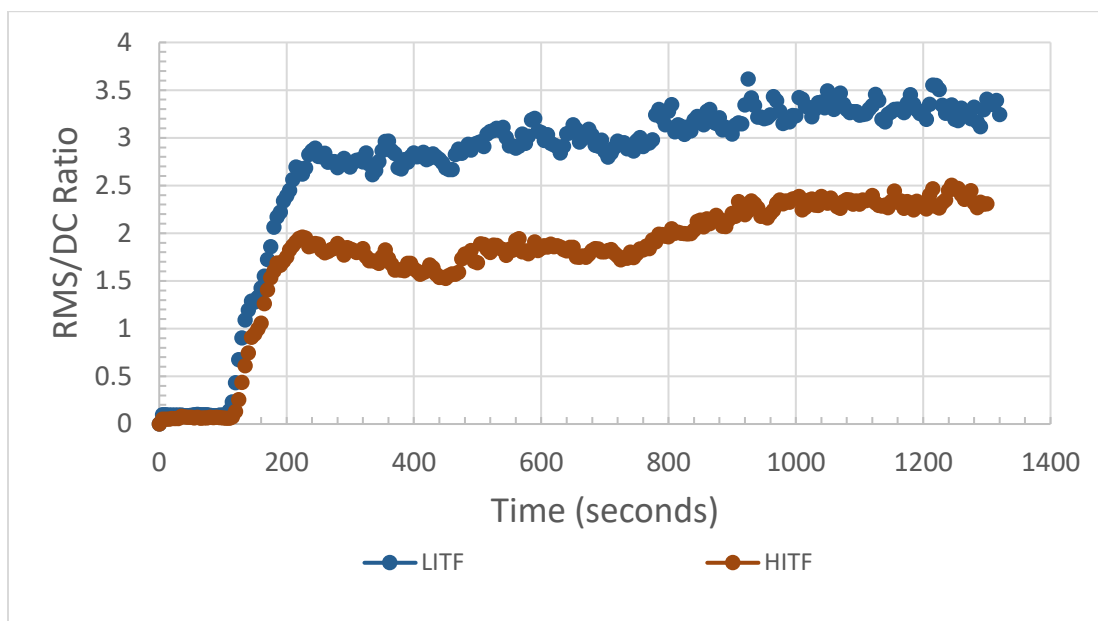


Figure 4.25. PDA analysis for model water #2 with tapered flocculation. (Dose = 50 mg/L as Alum, pH = 7.0)

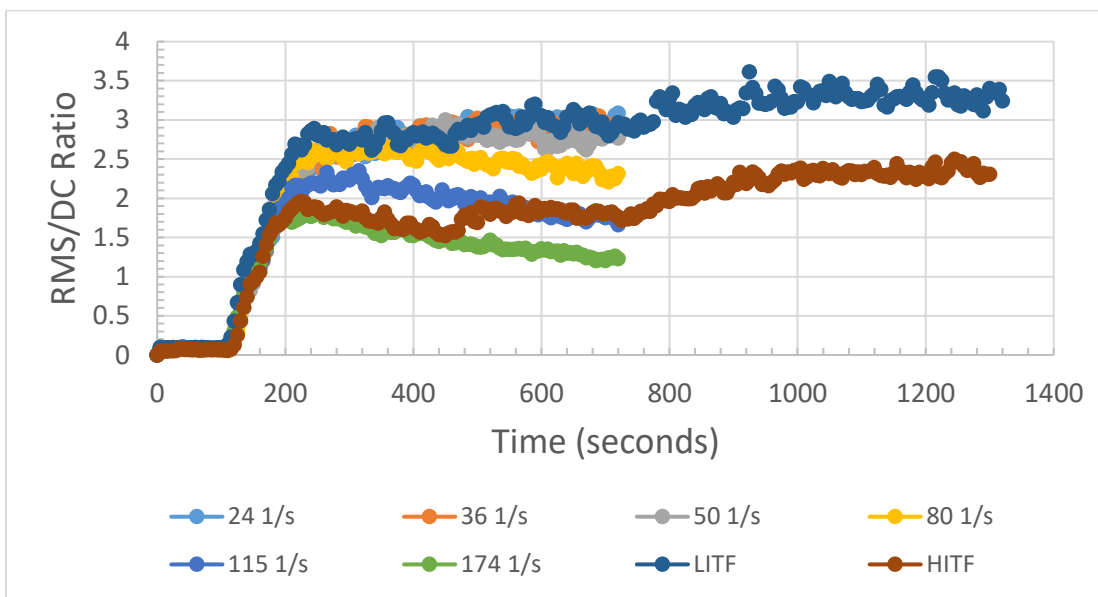


Figure 4.26. Summary of PDA analysis for model water #2. (Dose = 50 mg/L as Alum, pH = 7.0)

To evaluate the effect flocculation conditions would have on flocculation growth under charge neutralization conditions, LITF was used along with single-stage flocculation at mixing intensities of 24 and 174 s^{-1} . These mixing conditions were selected based on

the upper and lower extremes of single-stage flocculation and the procedure that resulted in the greatest FI value. Coagulation was carried out at a target coagulated pH of 5.0 with a coagulant dose of 5.0 mg/L as Alum. These coagulation conditions were not determined experimentally but were selected based on the coagulation operational diagram. Results of the PDA analysis can be seen in Figure 4.27. To indicate scale, the results for sweep flocculation analysis, under the same mixing conditions, are included.

When coagulation conditions mimicked that of the theoretical charge neutralization mechanism, flocculation growth followed similar trends regardless of applied mixing intensities. When compared to flocculation growth under sweep conditions, it can be seen that for all mixing conditions evaluated the floc growth rate was significantly less under charge neutralization. For charge neutralization, at the termination of each flocculation period the FI value had not plateaued (as it had when sweep flocculation was the coagulation mechanism). It is thought that this is caused by low floc concentrations under charge neutralization conditions, which does not lend itself to a high number of particle contact opportunities that would result in rapid growth as it would under sweep floc conditions (where there would be a higher concentration of precipitated floc particles).

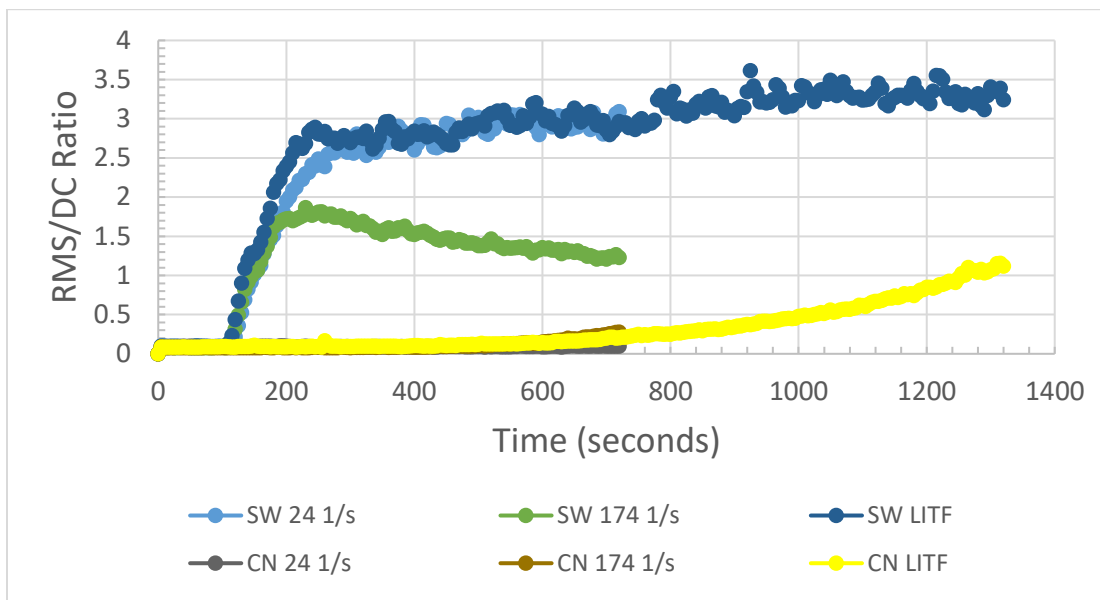


Figure 4.27. PDA analysis comparisons between sweep (Dose= 50 mg/L as Alum, pH = 7.0) and charge neutralization (Dose = 5.0 mg/L as Alum, pH = 5.0) mechanisms for model water #2.

4.5.1.2 Particulate Removal

With the insights gained in the previous section evaluation of the effect flocculation mixing intensity and time has on particle removal using filtration was carried out using single-stage flocculation at mixing intensities of 24 and 174 s^{-1} , and LITF. The goal of traditional jar test methods using settling as the particle removal mechanism is to produce a large, dense floc that is easily settled. When filtration is used in conjunction with the jar test apparatus, it may not be necessary to achieve those same floc characteristics to get similar results. For example, a smaller, tougher floc that is less prone to breaking could be ideal for filter comparisons while also being faster and simpler to produce. So, a filtration based jar test method would be more widely applicable.

Preliminary results were obtained when the coagulated water from the PDA analysis was filtered upon the completion of flocculation. A filter from the bench top

apparatus was used. The mixing and coagulation conditions were the same as those from Figure 4.28. The results from sweep flocculation are shown in Figure 4.28. A mixing intensity of 174 s^{-1} resulted in the lowest filtered turbidity (0.80 NTU) while LITF resulted in the worst removals of the conditions tested (7.62 NTU). This is inverse to the relationship mixing had on floc size.

The two single-stage flocculation procedures tested, resulted in similar filtered turbidities under charge neutralization ($\approx 27 \text{ NTU}$). LITF produced a filtered turbidity of 10.9 NTU. The filtered turbidities from these three flocculation procedures would be considered sub-optimal by a significant amount. Results are displayed in Figure 4.29. Based on preliminary results, applied mixing intensities during flocculation could have an effect on filtered turbidity. Preferred flocculation procedure could also potentially depend on the coagulation mechanism.

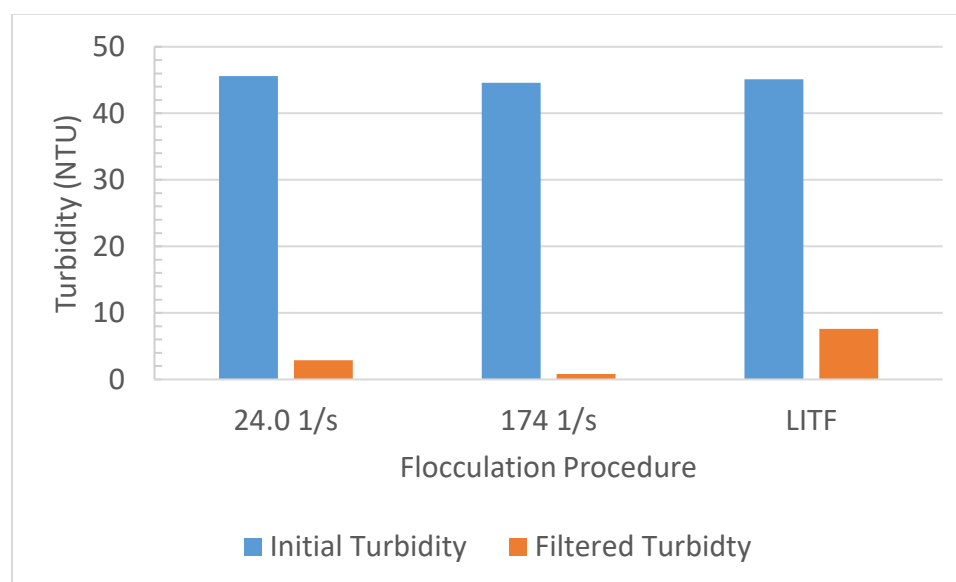


Figure 4.28. Effect of mixing intensities on filtered turbidity under sweep coagulation conditions using model water #2. (Dose = 50 mg/L as Alum, pH = 7.0)

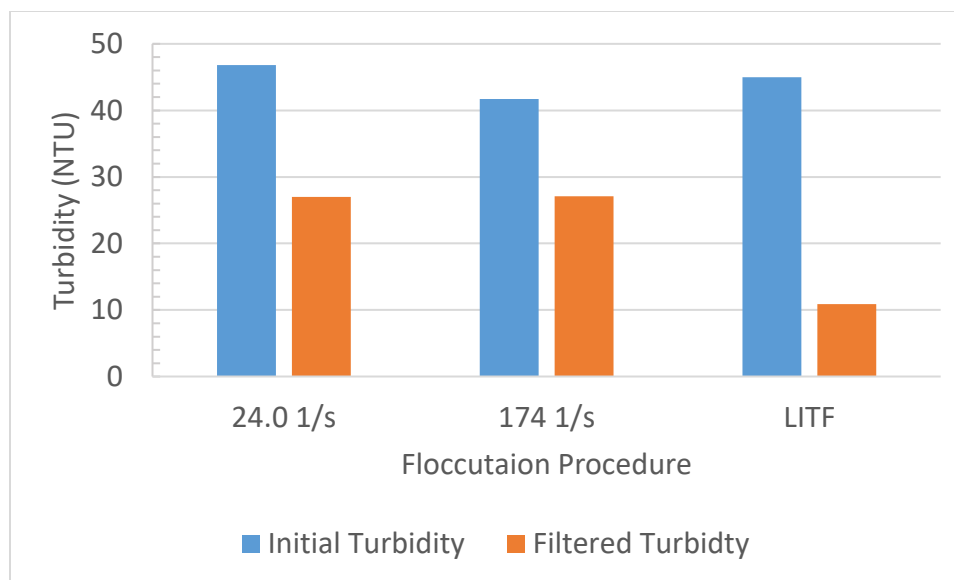


Figure 4.29. Effect of mixing intensities on filtered turbidity under charge neutralization conditions using model water #2 (Dose = 5.0 mg/L as Alum, pH = 5.0)

Additional experiments were conducted to evaluate the effect mixing conditions during flocculation have on filtered turbidity using the jar test apparatus. Coagulated pH was tested across a range of 5.0 to 7.5 in 0.5 increments. Alum doses tested were 0, 5, 10, 30, 50, 70, and 100 mg/L as Alum. Flocculation was carried out at either a G-value of 174 s^{-1} (120 RPM) or applying the LITF procedure, both followed by direct filtration. An additional set of experiments was conducted with using LITF with sedimentation and filtration. This method best mimics a full-scale water treatment plant and theoretically should provide a data set to compare the results from direct filtration. Also included in the results (for reference) is what has been defined as the upper pH limit (6.0) of charge neutralization in recent research (Edzwald, 2014). This limit is indicated by a yellow line at a coagulated pH of 6.0. Treatment on the left side of the line is considered charge neutralization and sweep flocculation is on the right.

Figure 4.30 is the results from the three jar test procedures investigated at 50 and 10 mg/L as alum. Figure 4.31 is the results from the three jar test procedures investigated at coagulated pH values of 6.5 and 5.5. It was observed that regardless of the procedure that turbidity removals were similar at a given coagulant dose and pH combination. The individual plots for each of the flocculation methods evaluated can be seen in Appendix A.

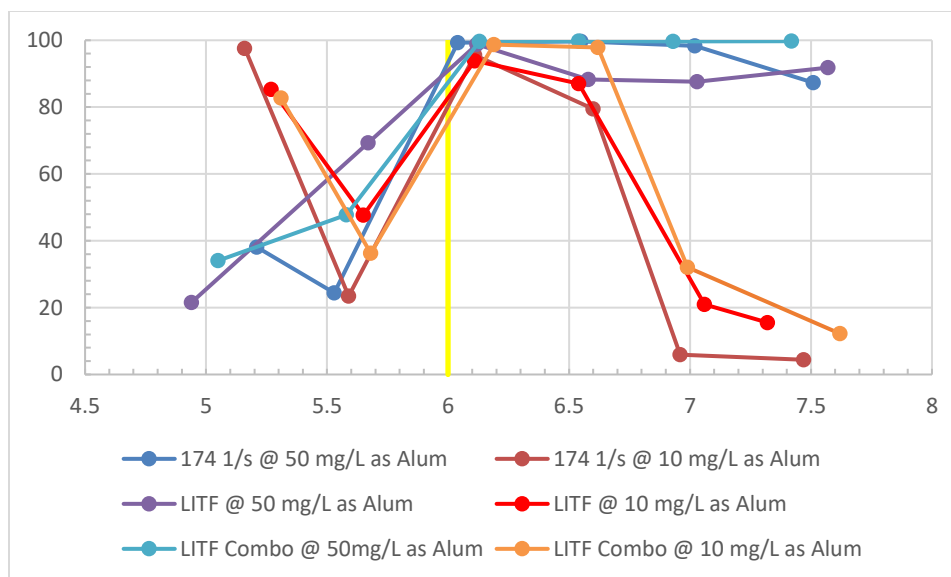


Figure 4.30. Summary of the results for the three jar test procedures evaluated at coagulant doses of 50 and 10 mg/L as Alum.

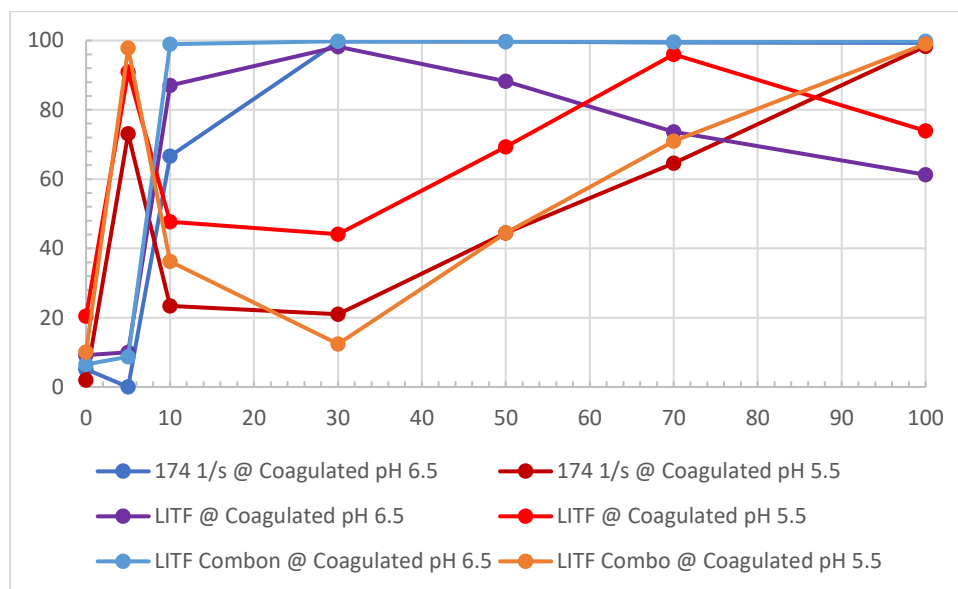


Figure 4.31. Summary of results for the three jar test procedures evaluated at coagulated pH values of 6.5 and 5.5.

After analysis of the results from Figures 4.30 and 4.31, it was determined that regardless of flocculation procedure similar conclusions could be drawn. This was particularly apparent when comparing the results from LITF with sedimentation and filtration to those from flocculation at an intensity of 174 s^{-1} . Overall, it appears that for model water #1, the largest zone of effective treatment exists between a coagulated pH of 6.0 and 6.5 and at a minimum coagulant dose of 10 to 30 mg/L as Alum (depending on coagulated pH). Additional jar testing was carried out to provide a more complete picture of potential treatment zones by use of contour plots. Treatment was analyzed across the same pH range as from previous contour plots, from 5.0 to 8.0 in target increments of 0.5 units. Alum was dosed from 0 to 100 mg/L as Alum at varying increments just as before, and the control was omitted.

The contour plot overlaid with an alum-only titration curve from experimentation with LITF with sedimentation only can be seen in Figure 4.32. It was observed that two

zones of treatment with a turbidity removal efficiency $\geq 95\%$ were present. The first zone was bound on the left and right by pH values of approximately 6.5 and 6.7 respectively. The approximate alum dose range was from 14 to 20 mg/L as Alum. The second zone of maximum observed treatment efficiency covered a wider pH range (6.5 to 7.0) from a coagulant dose of 29 to 35 mg/L as Alum. For comparison to filtration data, the 90% contour interval was used, as comparing 95% removals using filtration to 95% removals using sedimentation did not seem reasonable. All treatment condition observations will be based on turbidity removals of $\geq 90\%$. There is the potential for the water to be treated with 20 to 35 mg/L as Alum along the alum-only titration curve (without the aid of pH adjustment). According to the contour data, adjusting the coagulated pH could cut the effective coagulant dose to 10 mg/L as Alum.

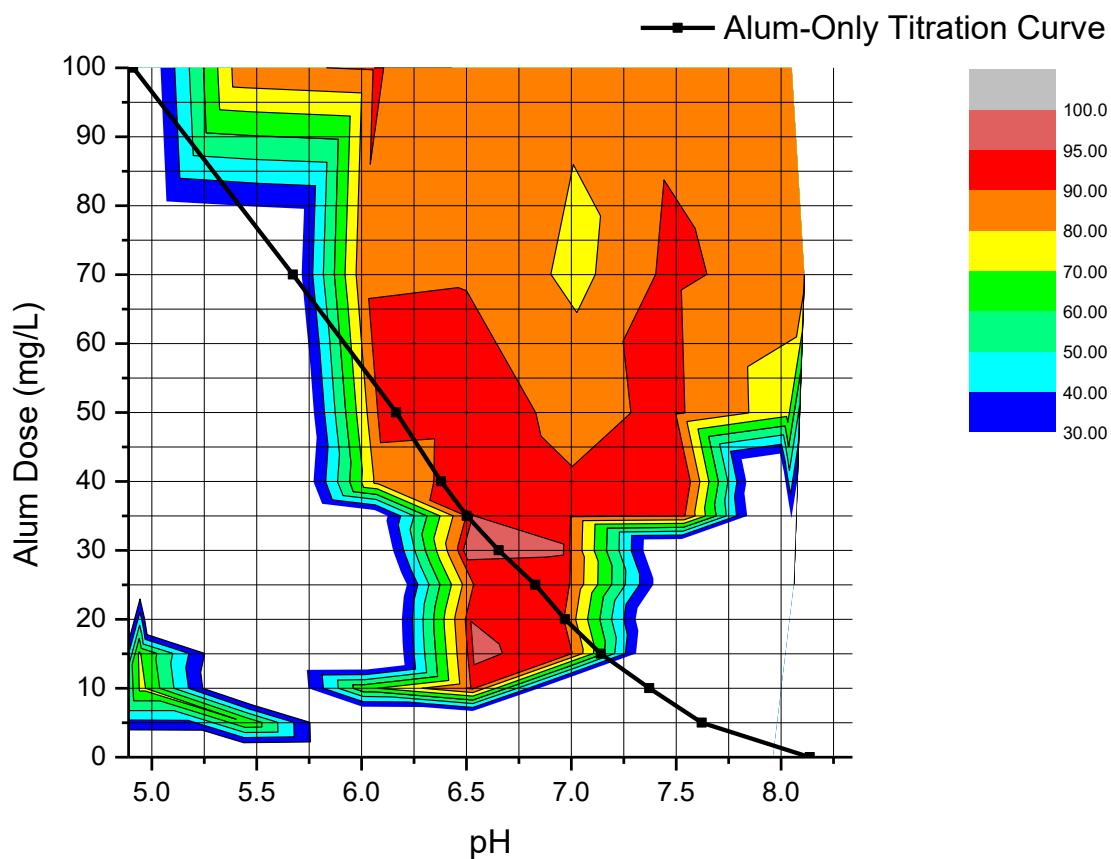


Figure 4.32. Contour plot of percent turbidity removal for model water #2 using LITF with sedimentation overlaid with an alum-only titration curve.

Next, LITF with direct filtration was used to create a contour plot for model water #2. Low-intensity tapered flocculation with direct filtration identified 3 zones where turbidity removals were $\geq 95\%$. The largest zone has a left boundary at a pH of approximately 6.1 across an Alum dose range from 12 to 58 mg/L. As coagulated pH proceeds up the pH scale, the zone tapers to a vertex at a coagulant dose of 30 mg/L as Alum and a pH value in the region of 7.2. The second zone begins at a similar pH (7.2) as the first ended, at an Alum dose of 25 mg/L and expands to a left boundary along pH 7.5 from 20 to 32 mg/L as Alum. The third zone appears to be a very small point at which

treatment is favorable. It is located at a coagulated pH of 5.7 and a coagulant dose of approximately 70 mg/L as Alum. Applying an alum-only titration curve to the contour plot shows that a broader range (25 – 55 mg/L as Alum) of alum-only treatment is identified when filtration is used in jar testing (in contrast to traditional sedimentation). The ability to control coagulated pH during treatment would allow for the minimum alum dose to achieve $\geq 95\%$ turbidity removals to be reduced to near 12 mg/L as Alum, compared to 25 mg/L as Alum when using coagulant only. The contour plot with an alum-only titration curve is shown in Figure 4.33.

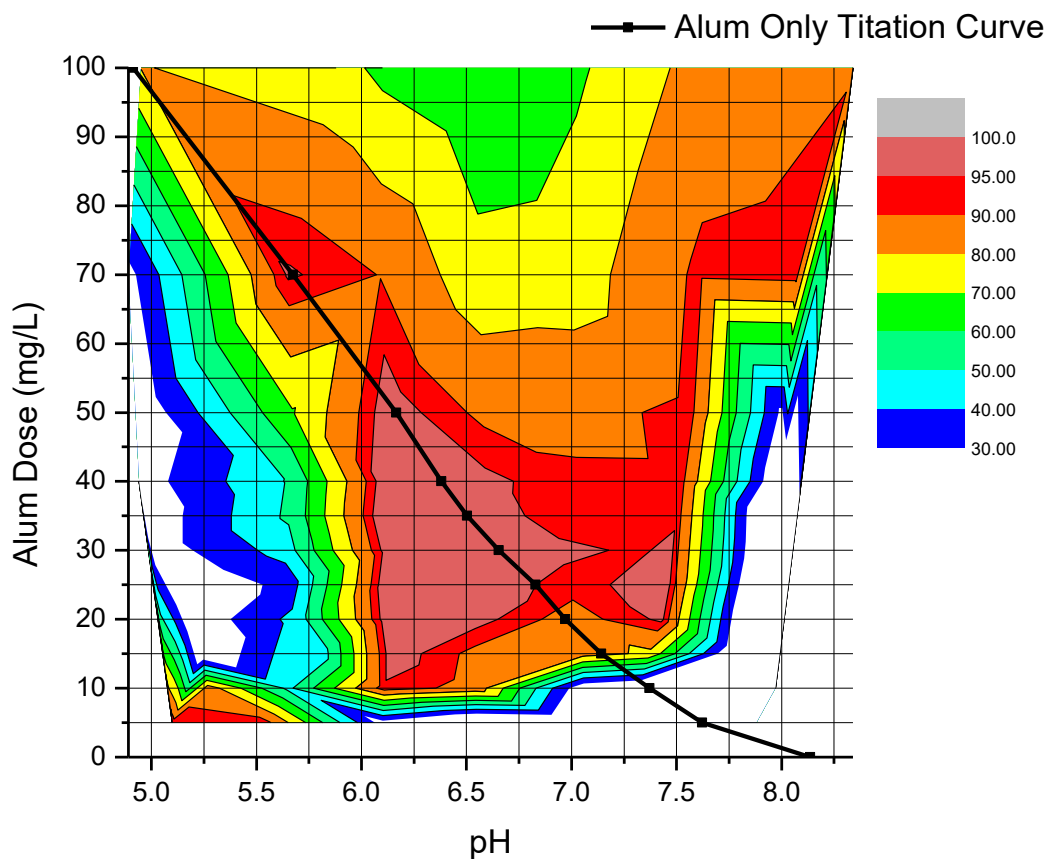


Figure 4.33. Contour plot of percent turbidity removal for model water #2 using LITF with direct filtration graphed with an alum-only titration curve.

The 90% turbidity removal boundary from the contour plot in Figure 4.32 was overlaid onto the contour plot from LITF with direct filtration. This can be seen in Figure 4.34. Sedimentation failed to identify two areas of maximum turbidity removals that were observed with direct filtration. The first is from near pH 6.0 to 6.5. The coagulant dose range for this area that was omitted extends from 10 mg/L as Alum to 45 mg/L. The second area of maximum treatment not identified by sedimentation is the of maximum observed turbidity removals between a pH of 7.2 and 7.5.

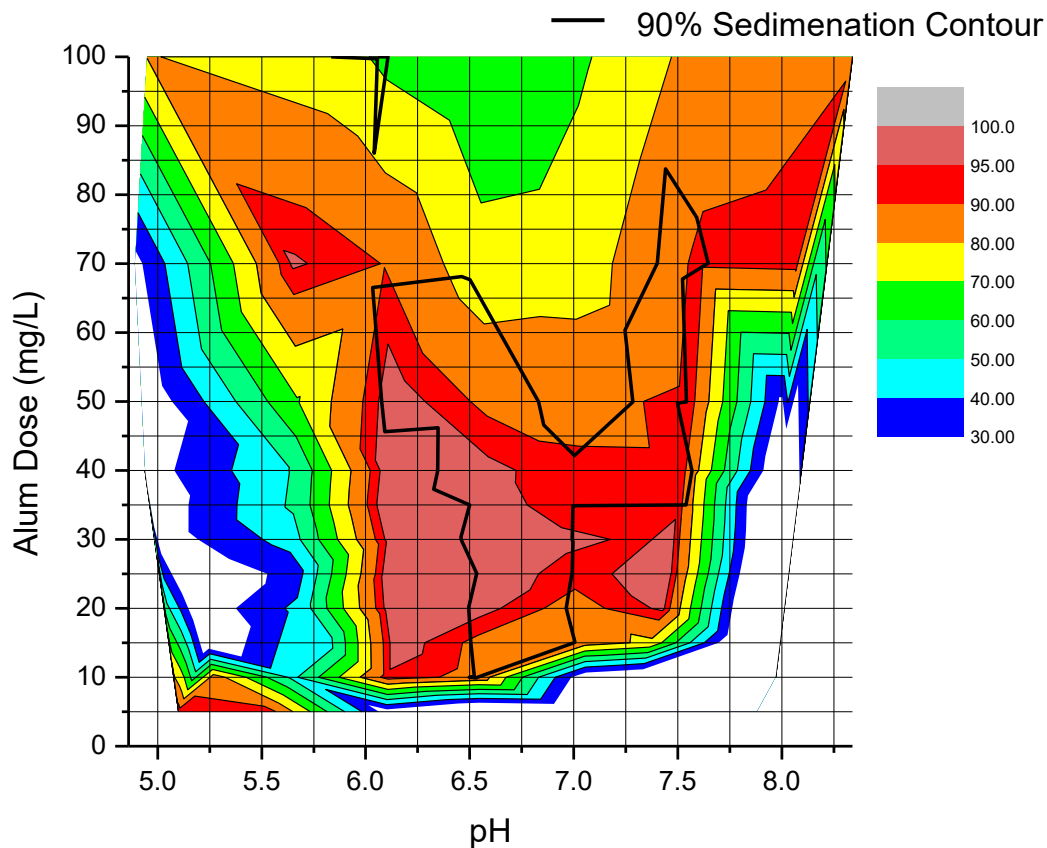


Figure 4.34. Contour plot of percent turbidity removal for model water #2 using LITF with direct filtration and the 90% removal boundary from LITF with sedimentation.

Figure 4.35 is the contour plot of the percent turbidity removals that resulted from single-stage flocculation at a mixing intensity of 174 s^{-1} with direct filtration as the particulate removal mechanism for model water #2. The figure also includes an alum-only titration curve. A single zone of treatment with turbidity removals of $\geq 95\%$ was observed. The zone is bound on the left by a pH of 6.1 and extends to a coagulated pH of approximately 7.5. The greatest coagulant dose range to achieve these removals occurs along the left boundary from 12 mg/L to 55 mg/L as Alum. The upper coagulant dose boundary drops to a dose of 45 mg/L at a pH of 6.5 and then increases, with pH to slightly

above 55 mg/L. The lower bound gradually increases from 12 mg/L to 25 mg/L as Alum with increasing pH. As treatment conditions radiate out from this centralized zone of treatment, there is a reduction in turbidity removals. Along the alum-only titration curve, treatment within the zone of maximum turbidity removals would be possible from 20 mg/L to 55 mg/L as Alum. The smallest effective coagulant dose along the alum-only titration curve is 5 mg/L lower than the 25 mg/L as Alum that was observed when using LITF with direct filtration. There appears to be the potential to reduce the minimum effective alum dose by approximately 8 mg/L (versus alum-only coagulation) by reducing the coagulated pH to near 6.1.

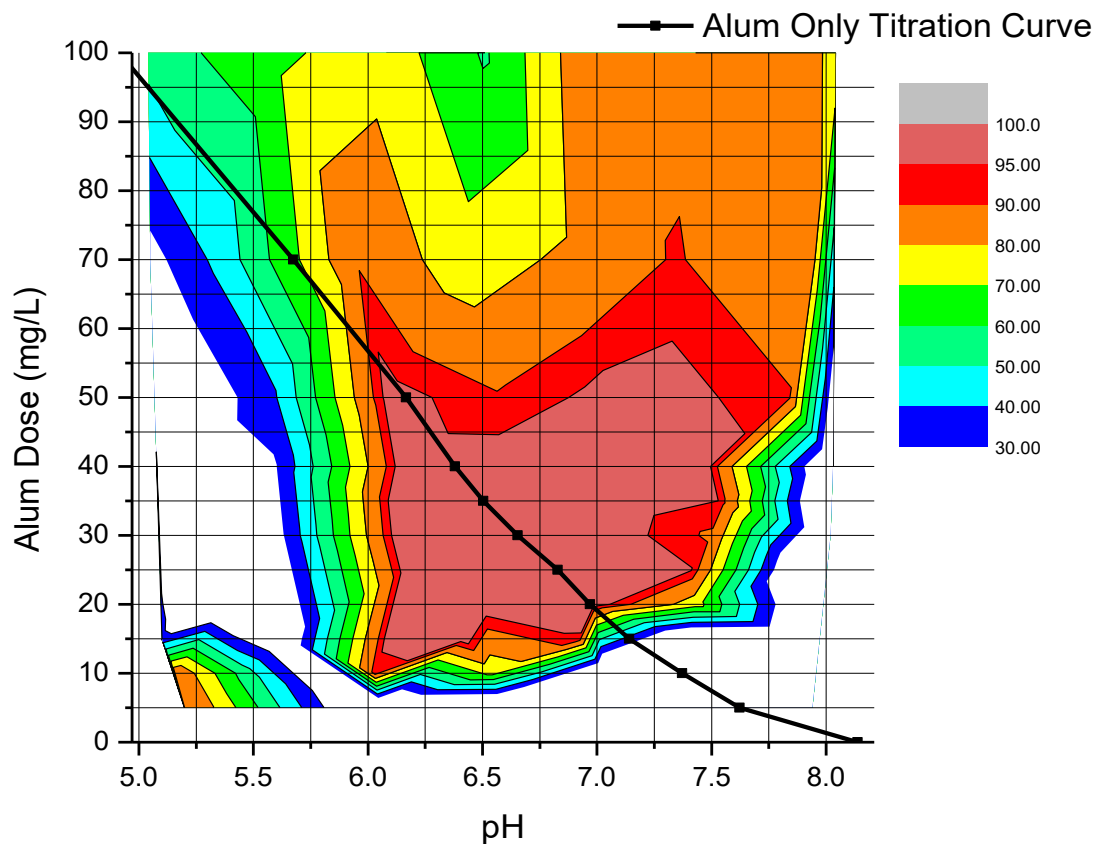


Figure 4.35. Contour plot of percent turbidity removal for model water #2 with flocculation at an intensity of 174 s⁻¹ and direct filtration graphed with an alum-only titration curve.

When the 95% removal contour boundary from LITF with direct filtration was plotted over the contour plot from single-stage flocculation, it was observed that the left boundary at pH 6.1 was similar. The zone of maximum filtered turbidity removal was significantly larger with the high intensity single-stage flocculation when compared to that from LITF. It was noted that the area of turbidity removals of at least 95% located at a pH of 5.7 and an Alum dose of 70 mg/L was not identified when flocculating at an intensity of 174 s⁻¹. Results are shown in Figure 4.36.

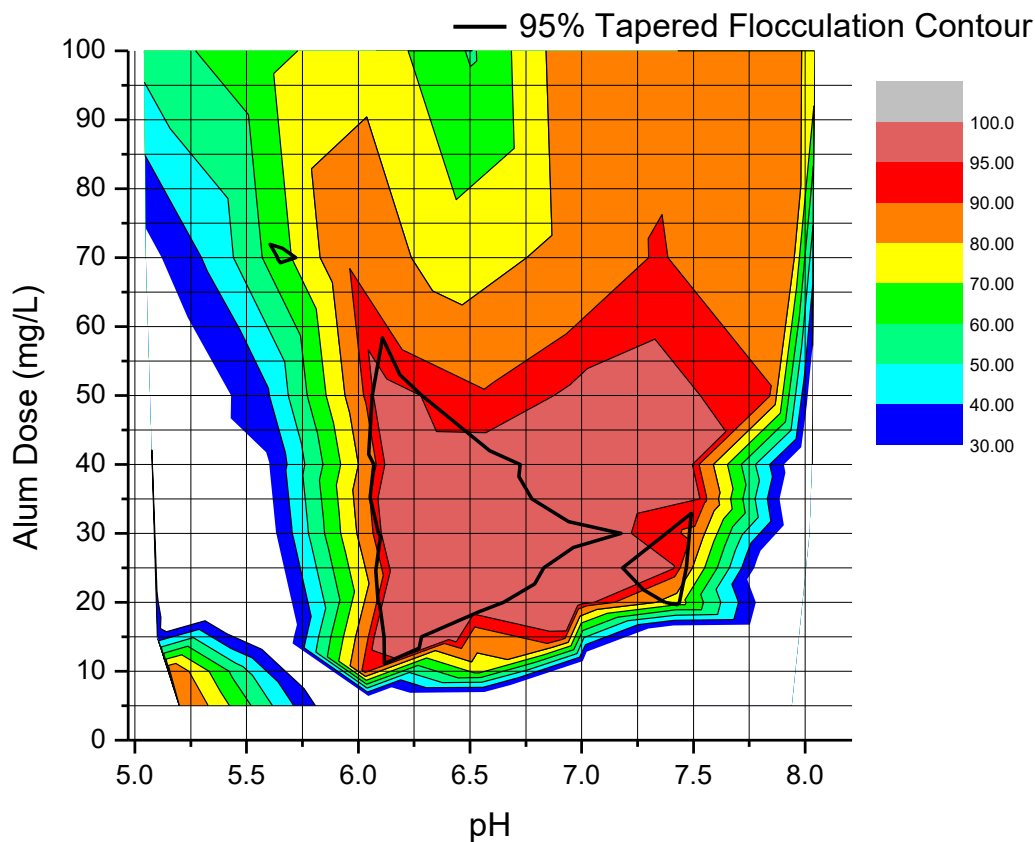


Figure 4.36. Contour plot of percent turbidity removal for model water #2 with flocculation at an intensity of 174 s^{-1} with direct filtration and the 95% removal boundary from LITF with direct filtration.

The fourth of four contour plots (with an alum-only titration curve was created for model water #2) using LITF with particulate removal being carried out through sedimentation prior to filtration. LITF with sedimentation and filtration resulted in a large zone of removals $\geq 95\%$ that extends from a coagulant dose of 10 to 100 mg/L as Alum. The left bound of the zone is a pH value of 6.0 and moves to below 5.75 at a coagulant dose of 70 mg/L as Alum. The right bound drifts from a pH of 6.5 to 8.0 until it reaches the upper pH limit of the contour plot. There is also a narrow zone of $\geq 95\%$ turbidity

removals that begins at slightly below pH 5.0 and extends to pH 5.5. It was observed that in this zone, significant turbidity removals were seen with an Alum dose of 5 mg/L. The minimum effective alum dose without pH adjustment was observed to be at 20 mg/L as Alum. This result is similar to what was seen when flocculation was carried out at an intensity of 174 s^{-1} with direct filtration. The contour plot for LITF with combination particulate removal can be seen in Figure 4.37.

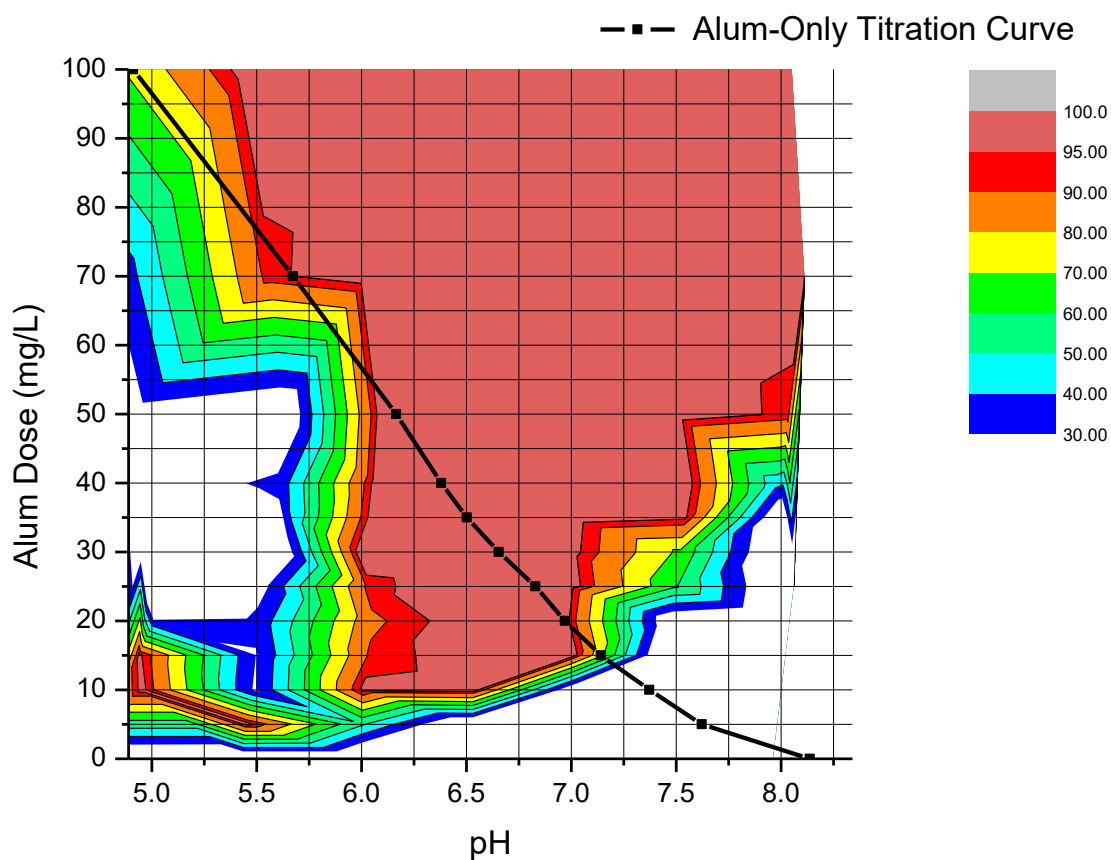


Figure 4.37. Contour plot of percent turbidity removal for model water #2 using LITF with a combination of sedimentation and filtration graphed with an alum-only titration curve.

Figure 4.38 shows the contour plot from LITF with sedimentation and filtration overlaid with the 95% contour line from LITF with direct filtration. Segments of similarity were observed on the left boundary. Above a coagulant dose of 55 mg/L as Alum, this similarity was not observed. Using sedimentation in conjunction with filtration may result in a marginally lower effective dose at a pH of approximately 6.0 when compared to direct filtration. Also, this method shows that 95% treatment is possible in the pH range of 5.0 to 5.5, where LITF with direct filtration did not identify this as a zone with that level of treatment, but 90% turbidity removals were observed. LITF with sedimentation and filtration failed to identify the zone of treatment located between pH 7.2 and pH 7.5.

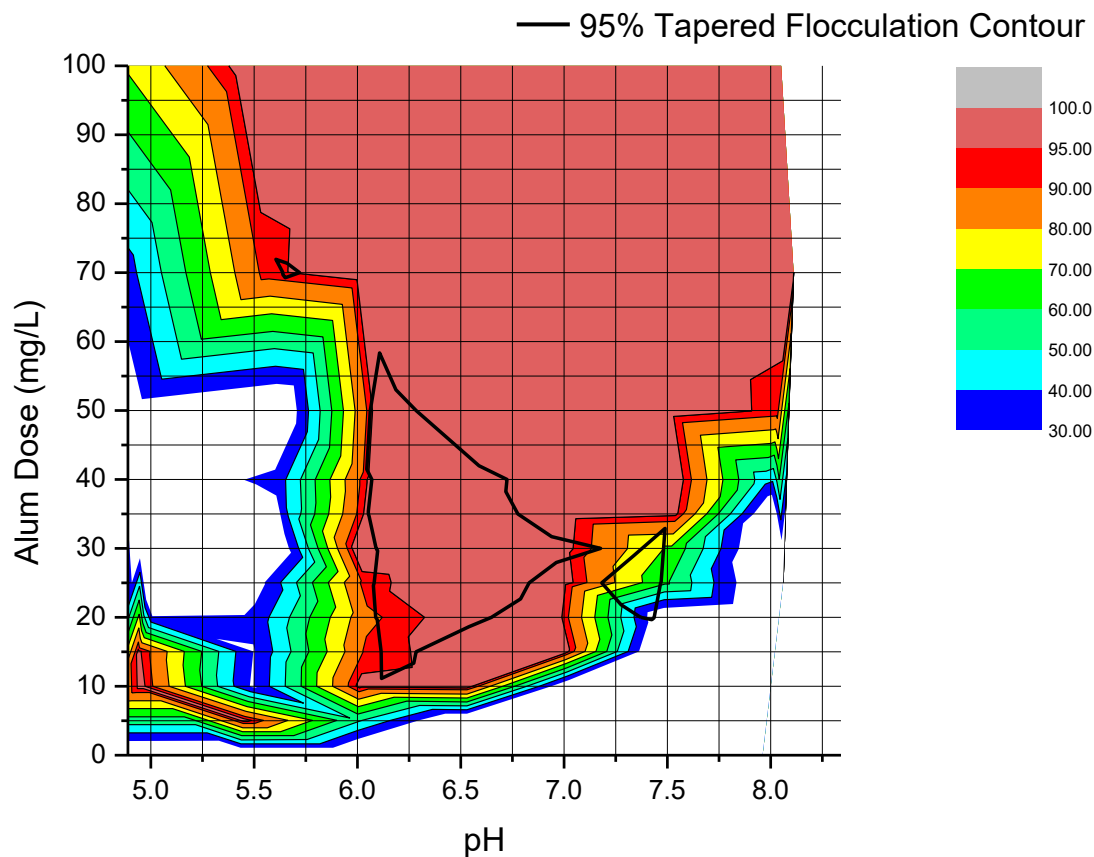


Figure 4.38. Contour plot of percent turbidity removal for model water #2 using LITF with a combination of sedimentation and filtration and the 95% removal boundary from LITF with direct filtration.

Figure 4.39 is a summary plot with the contour plot created using LITF with sedimentation and filtration overlaid contour boundaries from the previous plots. The 95% contour line from LITF and single-stage flocculation with direct filtration was used with the 90% contour line from LITF with sedimentation. The four contour plots are also compared individually in Figure 4.40. When sedimentation-only was using during jar testing, it failed to identify an area of maximum turbidity removals that was seen with direct filtration. This zone is from pH 6.0 to 6.5 and from a coagulant dose of 10 to 35mg/L as

Alum. Sedimentation also fails to identify a treatment zone located between pH 7.0 and 7.5. This zone extends from a coagulant dose of 15 mg/L to 35 mg/L as Alum. Both direct filtration procedures and the combination procedure identified a minimum coagulant dose of 10 mg/L as Alum at a pH near 6.0 where maximum turbidity removals were observed. When sedimentation and filtration are used in combination, a large zone of maximum observed turbidity removals was identified, where the other procedures failed to do so. Most of the zone is in an area above 50 mg/L as Alum, where coagulation conditions would not be considered due to lower effective coagulant doses being identified. Sedimentation prior to filtration may reduce the resolution needed to see what is occurring in all areas of the contour plot. These two considerations along with the additional time required to perform the jar test with sedimentation does not make it a desirable procedure. Low-intensity tapered flocculation failed to identify a significant portion of the zone of maximum observed turbidity removals that was seen when using single-stage flocculation. This portion of the zone has been highlighted in Figure 4.41, where the 95% contour lines for LITF and single-stage flocculation were plotted. It was observed that single-stage flocculation at an intensity of 174 s^{-1} (120 rpm) may have identified the more favorable treatment condition at a coagulated pH of 7.0 and an Alum dose of 15 mg/L. Low-intensity tapered flocculation indicates that a coagulated pH of 7.0 and an Alum dose of 15 mg/L is in an area where turbidity removals were less than the maximum turbidity removals observed. Sedimentation (either as a standalone particle removal mechanism or as a prerequisite to filtration) is not needed to determine effective coagulation conditions with the jar test apparatus. Both direct filtration procedures were evaluated on a third model water. Single-

stage flocculation at a mixing intensity of 174 s^{-1} (120 rpm) provided sufficient floc growth for coagulation optimization on the jar test apparatus with direct filtration.

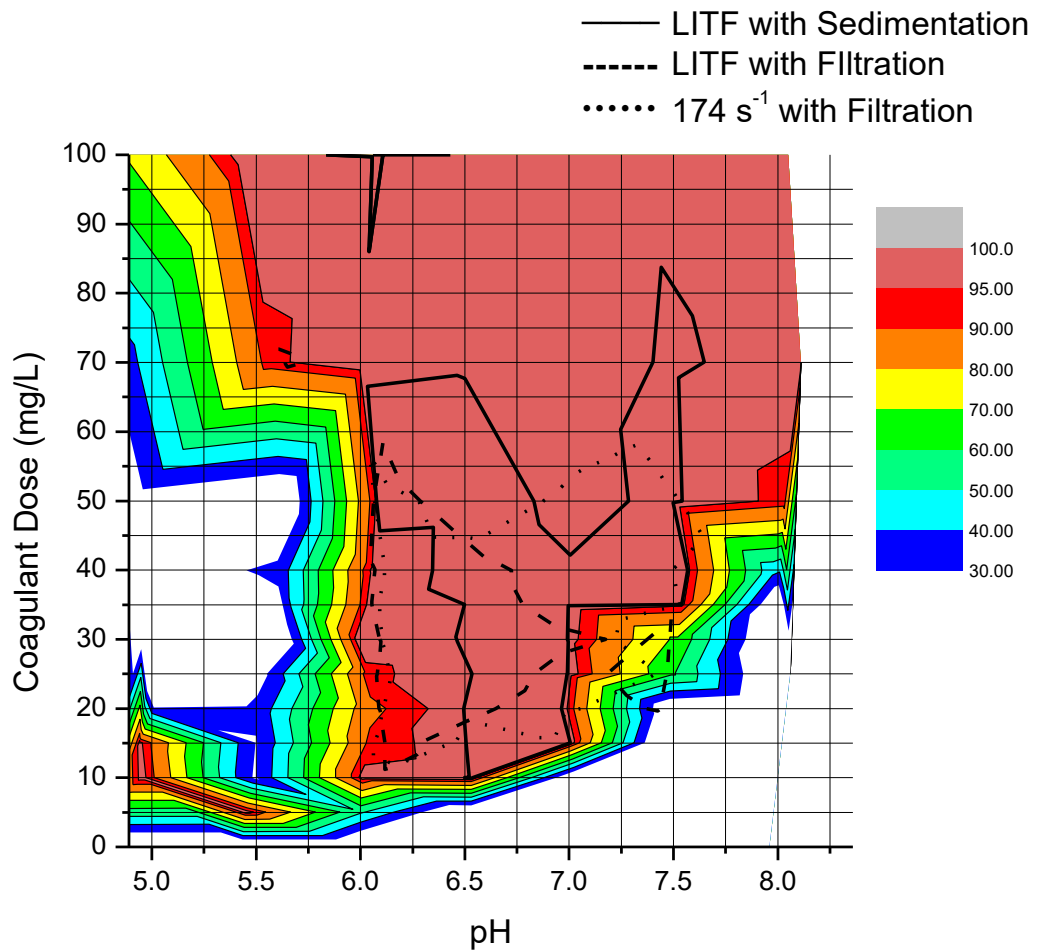


Figure 4.39. Contour plot of percent turbidity removal for model water #2 using LITF with a combination of sedimentation and filtration and the 95% removal boundary from LITF with direct filtration, LITF with sedimentation, and 174 s^{-1} with direct filtration.

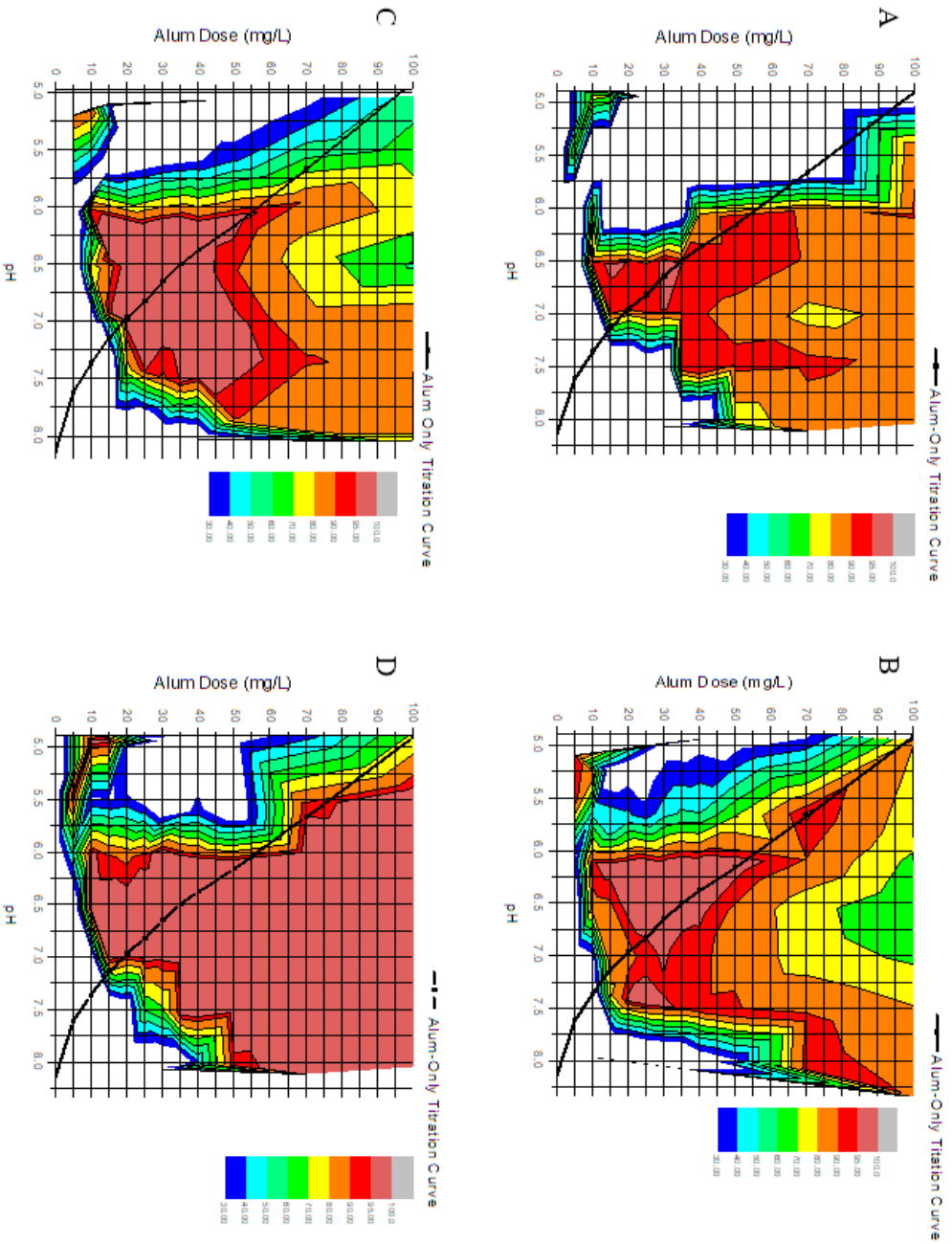


Figure 4.40. The four contour plots created from model water #2 using LITF with sedimentation (A), LITF with direct filtration (B), single-stage flocculation with direct filtration (C), and LITF with sedimentation and filtration (D).

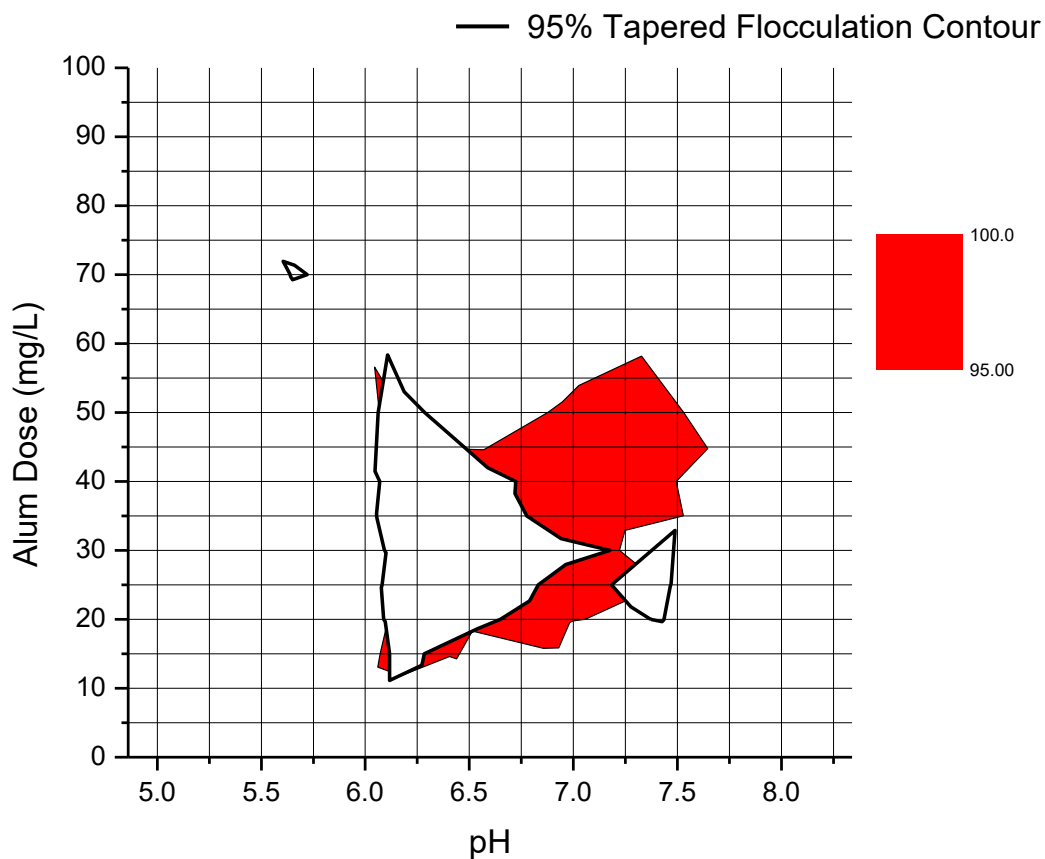


Figure 4.41. Maximum observed removals from LITF and single-stage flocculation with direct filtration. Areas of treatment not identified by LITF, but identified by single-stage flocculation are highlighted in red.

4.6 Model Water #3

Low-intensity tapered flocculation with direct filtration was applied to the model water #3 (moderate turbidity, high DOC/SUVA model water). A contour plot was created as in the previous section using the same alum doses and target coagulated pH values. Following the completion of this contour plot, in-lieu of recreating the contour plot in its entirety, flocculation at an intensity of 174 s^{-1} (120 RPM) with direct filtration was used to recreate the zone of maximum treatment efficiency.

The contour plot with an alum-only titration curve for model water #3 using LITF with direct filtration is shown in Figure 4.42. A single zone of treatment that resulted in turbidity removals of $\geq 95\%$ was observed. The zone is bound on the left by a pH value of approximately 5.75 and on the right at a pH of 6.0. The coagulant dose range is from 65 to 100 mg/L as Alum. There is the potential for this dose range to extend higher, as 100 mg/L as Alum was the highest dose applied during this research. It was observed that maximum effective treatment would not be possible using alum-only since the alum-only titration curve did not pass through a zone with 70% turbidity removals or greater. Treatment within the zone of most effective treatment would require pH adjustment with acid to reduce the coagulated pH. The lowest potential treatment dose with at least 95% turbidity removals was 65 mg/L as Alum, which could be achieved at a coagulated pH of approximately 5.75.

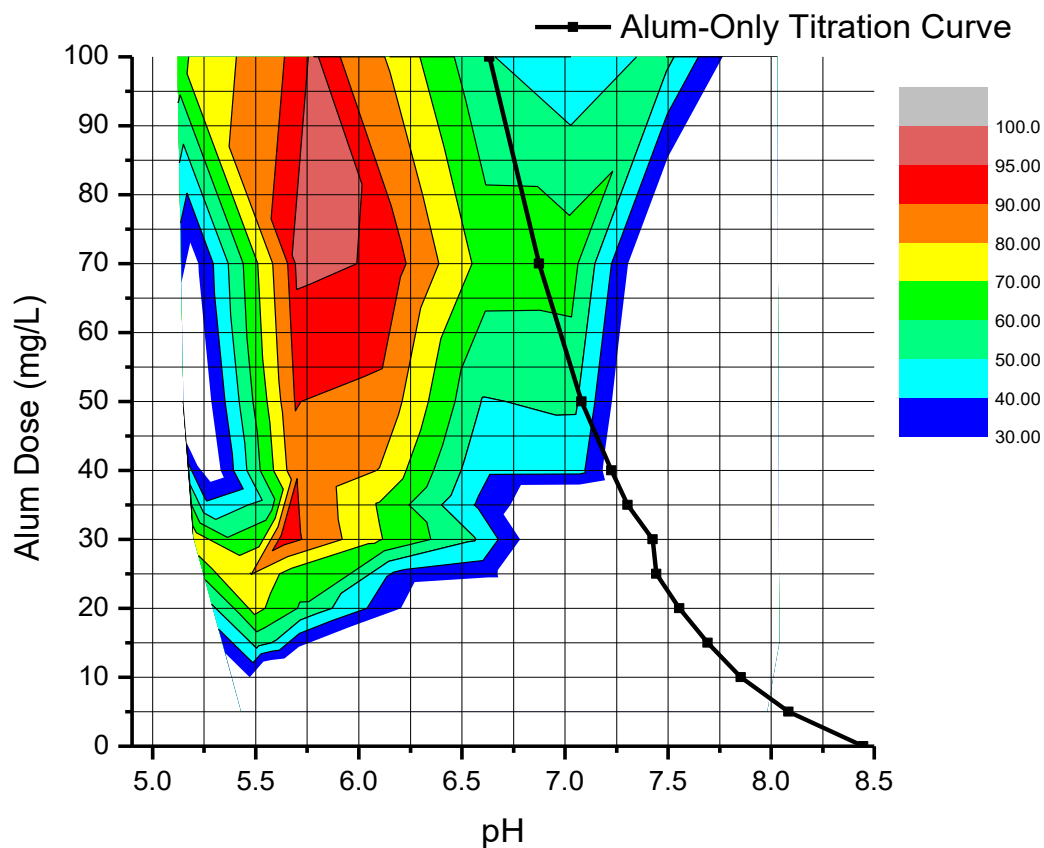


Figure 4.42. Contour plot of percent turbidity removal for model water #3 using LITF with direct filtration graphed with an alum-only titration curve.

Single-stage flocculation at an intensity of 174 s^{-1} with direct filtration at the zone of maximum observed turbidity removals can be seen in Figure 4.43. The 95% contour boundary from model water #3 using LITF with direct filtration was graphed over the contour plot from single-stage flocculation. There were two target coagulated pH values evaluated, 5.5 and 6.0, from 30 to 100 mg/L as Alum. The maximum observed turbidity removals were from 80 to 90%, located at a pH of 5.75 and a coagulant dose of 30 mg/L as Alum. The $\geq 95\%$ turbidity removal zone was not replicated with single-stage flocculation. In this area, 70 to 80% turbidity removals were the maximum observed with

treatment efficiency deteriorating as treatment conditions move away from a coagulated pH of 5.75 and out of the coagulant dose range between 65 to 75 mg/L as Alum. This is what was expected because of the high DOC and SUVA content of the water.

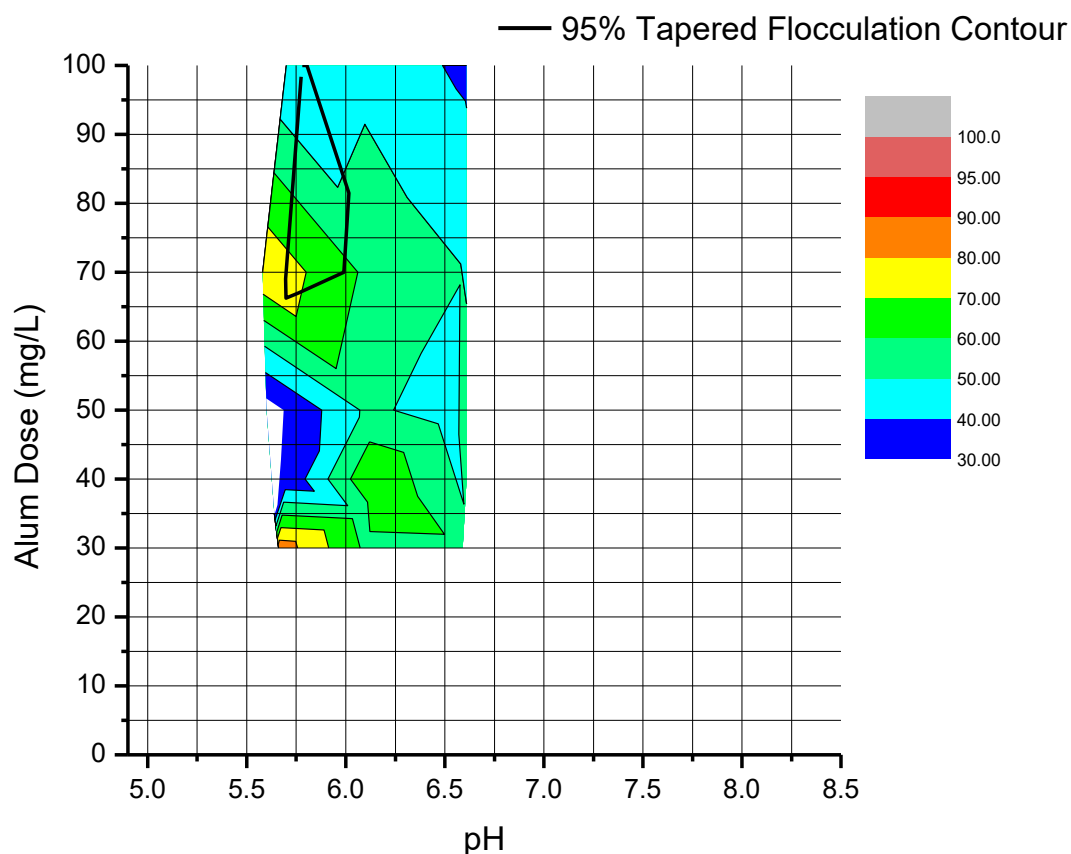


Figure 4.43. Contour plot of the zone of maximum treatment efficiency for model water #3 with flocculation at an intensity of 174 s^{-1} with direct filtration and 95% removal boundary from LITF with direct filtration.

The difference between these two plots led to the evaluation of the reproducibility of the data within this area with both flocculation procedures. Figure 4.44 is a plot of the original data set used to produce the contour plot using LITF with direct filtration at a target pH of 5.5. Also included in the graph is duplicate experiments of both LITF and single-

stage flocculation with direct filtration. Data are reported as average percent removals with standard deviation. The graphs of the new results for LITF and flocculation at an intensity of 174 s^{-1} had similar shapes when compared to that from the original data. Neither method of flocculation achieved the level of turbidity removals observed with the original data set with maximum observed removals being between 73 to 80% with the new data. There are two peaks in treatment efficiency that occurred at coagulant doses of 30 and 70 mg/L as Alum for both flocculation procedures in the new data set.

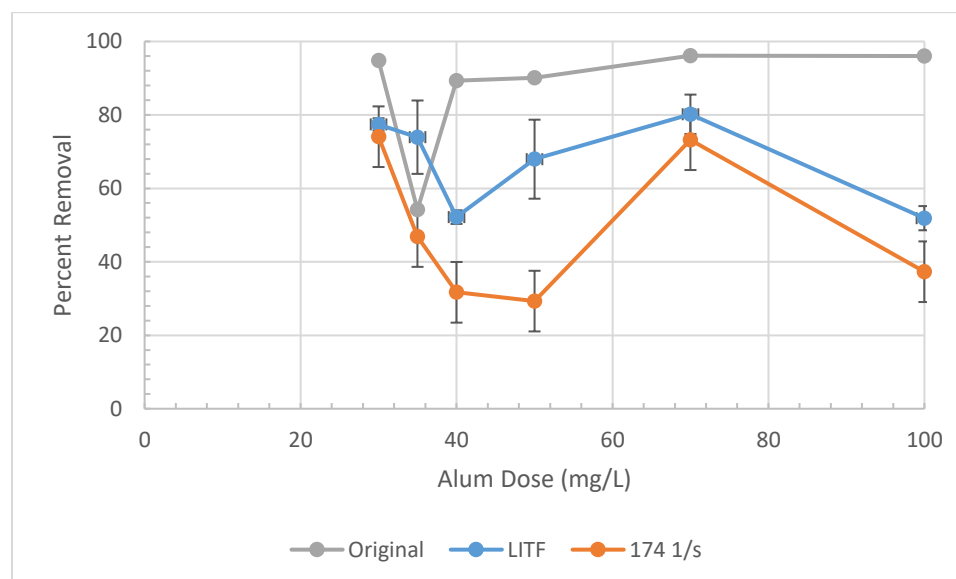


Figure 4.44. Original contour data for model water #3 using LITF with direct filtration at a target coagulated pH of 5.5 with duplicate results with standard deviation from LITF and single-stage flocculation with direct filtration.

Figure 4.45 is a graph of the coagulated pH values from the jar tests used to create Figure 4.44. It was observed that these values were similar at all data points and pH variation could not be attributed to the results shown in Figure 4.45. It is possible that during the creation of the contour plot that a coagulant-demanding substance could have been improperly dosed or accidentally omitted from the model water.

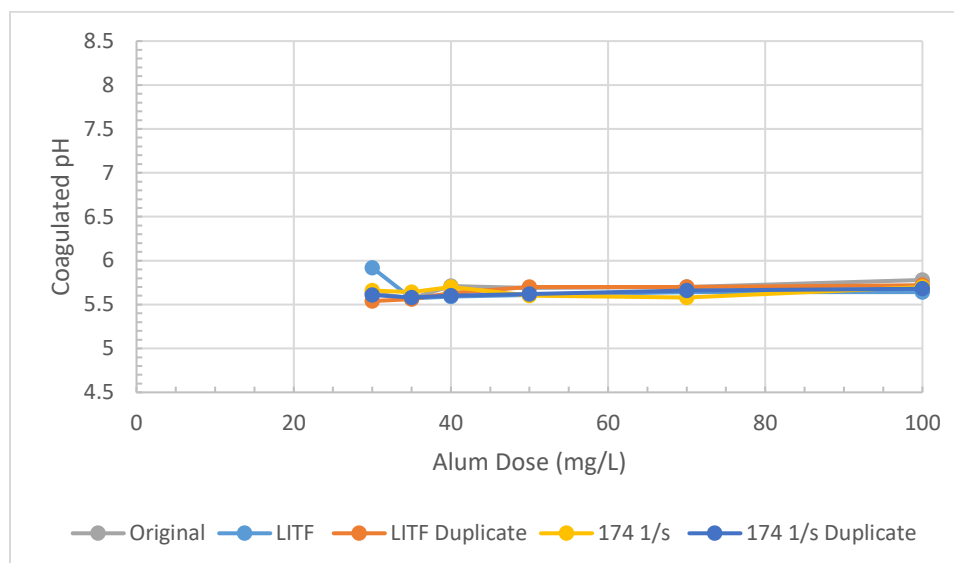


Figure 4.45. Coagulated pH values from jar test data for model water #3 from the original, LITF, and single-stage flocculation data sets.

Based on the results from this and the previous section, it was determined that both flocculation procedures would provide a treatment plant operator with the ability to identify coagulation conditions that resulted in effective treatment on the bench scale without tailoring the jar test procedure to match that of the treatment facility. Single-stage flocculation was the preferred method due to it being the most time-efficient procedure.

4.7 Coagulation Diagram Comparisons

4.7.1 Natural Water #2 Coagulation Diagram

The contour plots from natural water #2 in Figures 4.18 (sedimentation) and 4.21 (filtration) were overlaid on to the coagulation diagram from Figure 2.2. The coagulation diagram with the sedimentation contour plot can be seen in Figure 4.46. The yellow zones are regions of maximum observed turbidity removals. Also included in the figure is the pH

boundary for charge neutralization (green line) as defined by Edzwald where charge neutralization only occurs below a pH of 6.0.

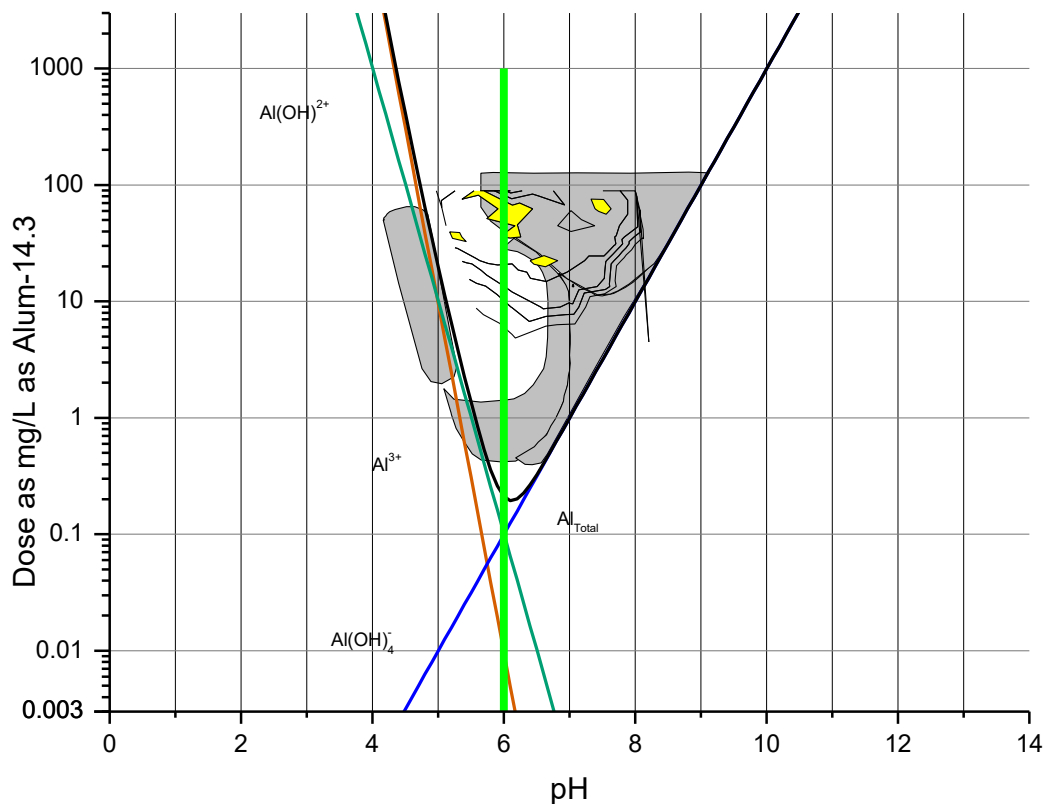


Figure 4.46. Operational diagram with the contour plot from natural water #2 with sedimentation as the particulate removal mechanism. Zone of observed turbidity removals $\geq 70\%$ is shaded yellow.

In Figure 4.47, the operational diagram is overlaid with the filtration contour plot from natural water #2. Filtration resulted in one zone of maximum observed turbidity removals shown in red. Also included in the figure is the pH boundary for charge neutralization (green line) as defined by Edzwald where charge neutralization only occurs below a pH of 6.0.

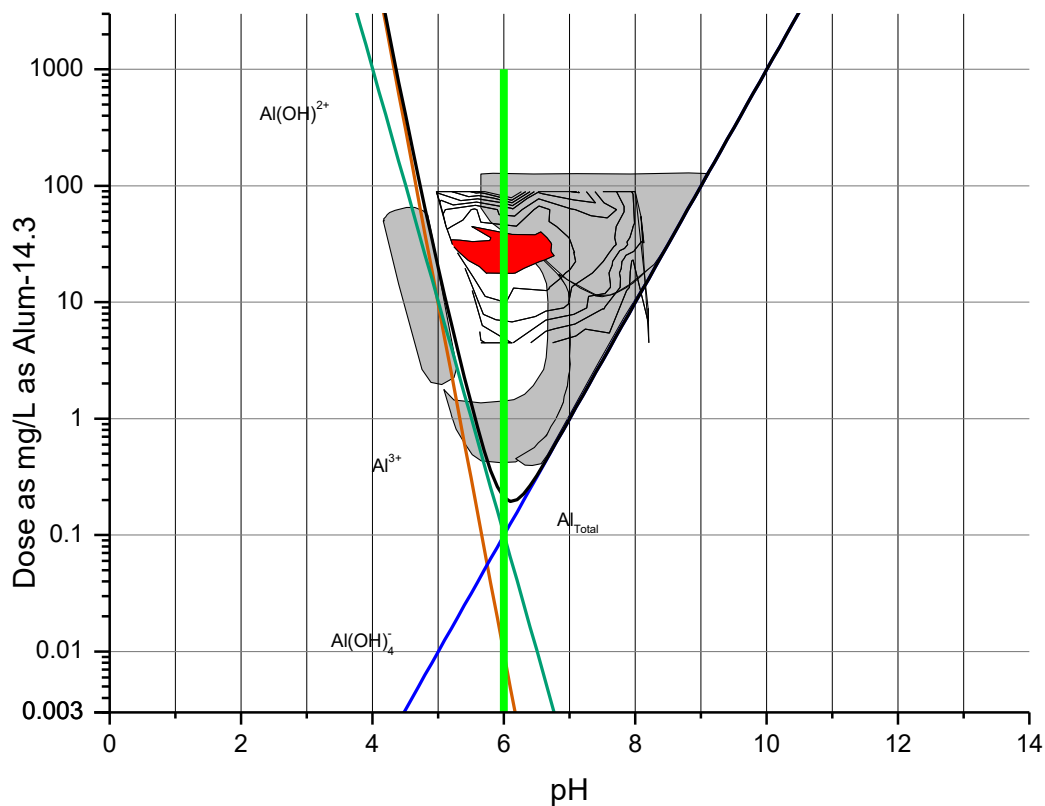


Figure 4.47. Operational diagram with the contour plot from natural water #2 with filtration as the particulate removal mechanism. Zone of maximum observed turbidity removals is shaded red.

4.7.2 Model Water #2 Coagulation Diagram

In the following figures the contour plots from Figures 4.32, 4.33, 4.35, and 4.37 were individually overlaid on to the coagulation diagram from Figure 2.2. The results of this comparison are shown in Figures 4.48 (LITF with sedimentation), 4.49 (LITF with direct filtration), 4.50 (Single-stage flocculation with direct filtration) and 4.51 (LITF with sedimentation and filtration). Also included in the figures is the pH boundary for charge neutralization (green line) as defined by Edzwald where charge neutralization only occurs below a pH of 6.0. It was observed that for all the contour plots, the majority of the

highlighted areas of treatment fell within the area of sweep flocculation as defined by both Edzwald and Amirtharajah.

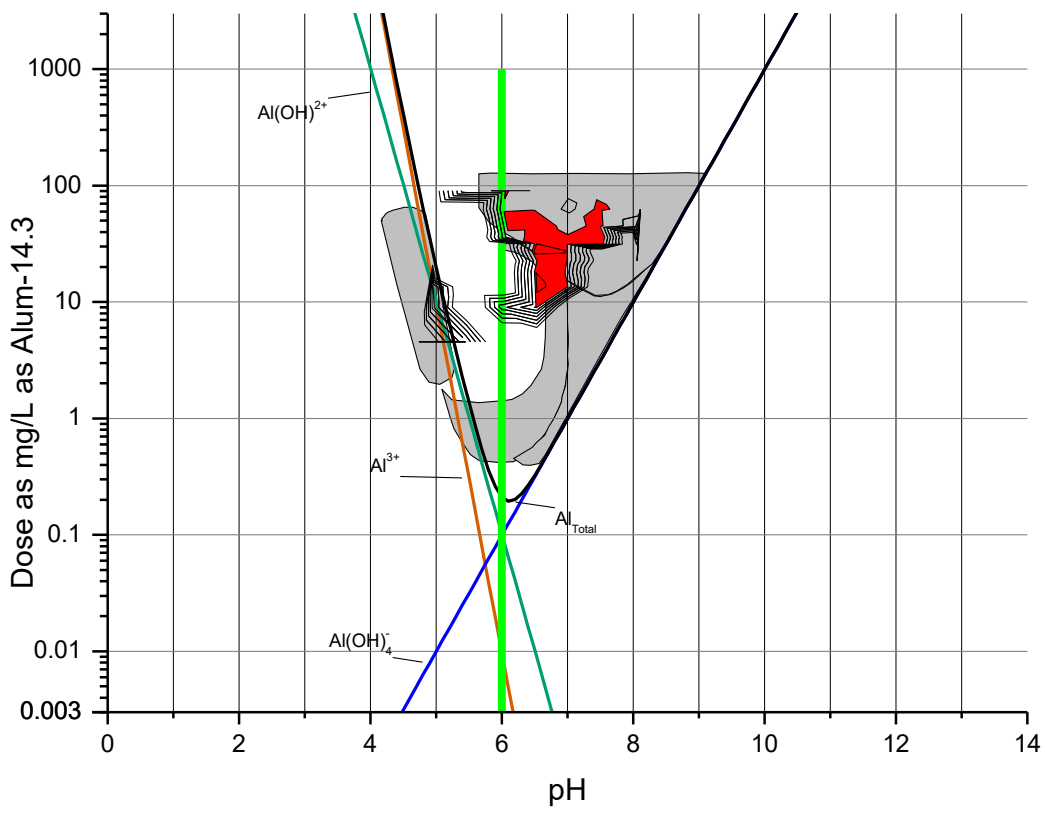


Figure 4.48. Operational coagulation diagram with the contour plot from LITF with sedimentation for model water #2. Zone of observed turbidity removals $\geq 90\%$ is shaded red.

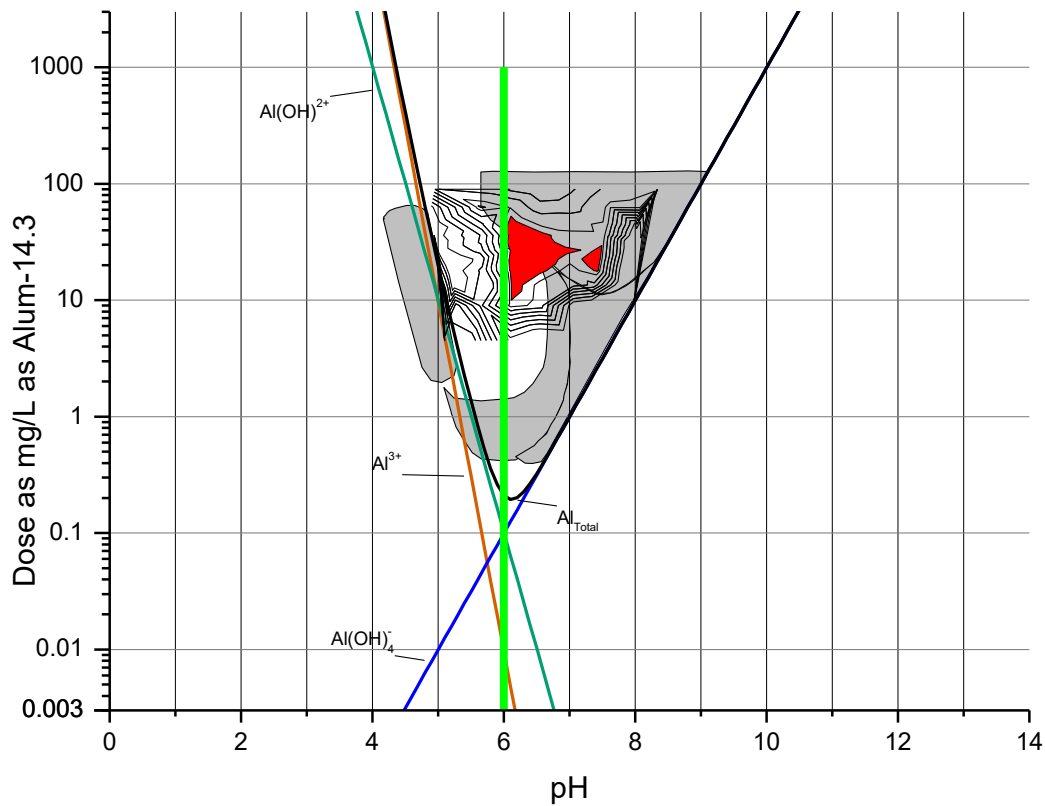


Figure 4.49. Operational coagulation diagram with the contour plot from LITF with direct filtration for model water #2. Zone of maximum observed turbidity removals is shaded red.

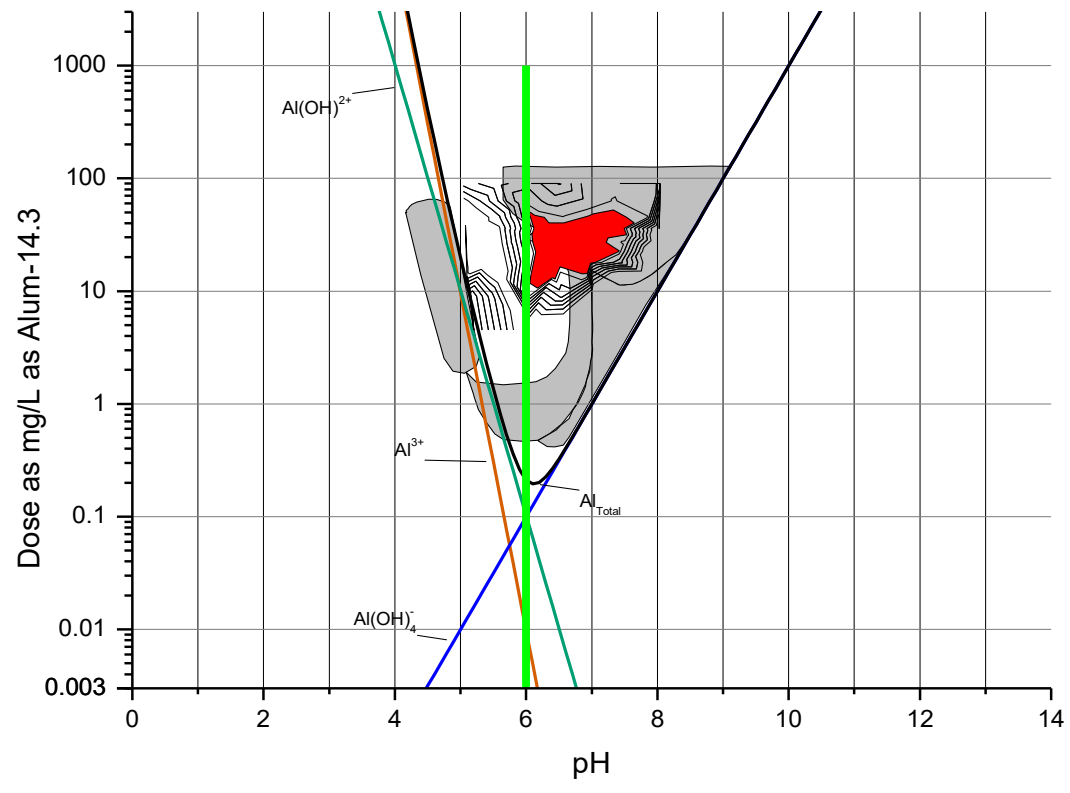


Figure 4.50. Operational coagulation diagram with the contour plot from single-stage flocculation at an intensity of 174 s-1 with direct filtration for model water #2. Zone of maximum observed turbidity removals is shaded red.

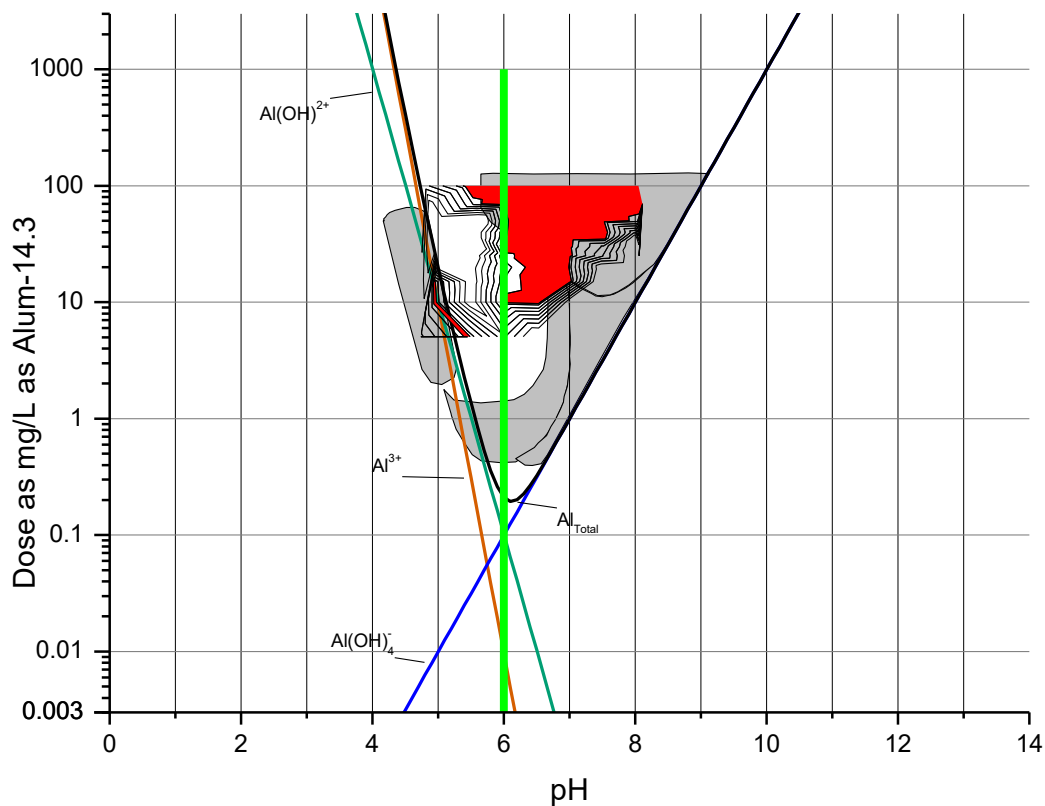


Figure 4.51. Operational coagulation diagram with the contour plot from LITF with sedimentation and filtration for model water #2. Zone of maximum observed turbidity removals is shaded red.

4.7.3 Model Water #3 Operational Diagram

In Figure 4.52, the operational diagram is overlaid with the LITF with direct filtration contour plot from model water #2. Filtration resulted in one zone of maximum observed turbidity removals shown in red. Also included in the figure is the pH boundary for charge neutralization (green line) as defined by Edzwald where charge neutralization only occurs below a pH of 6.0.

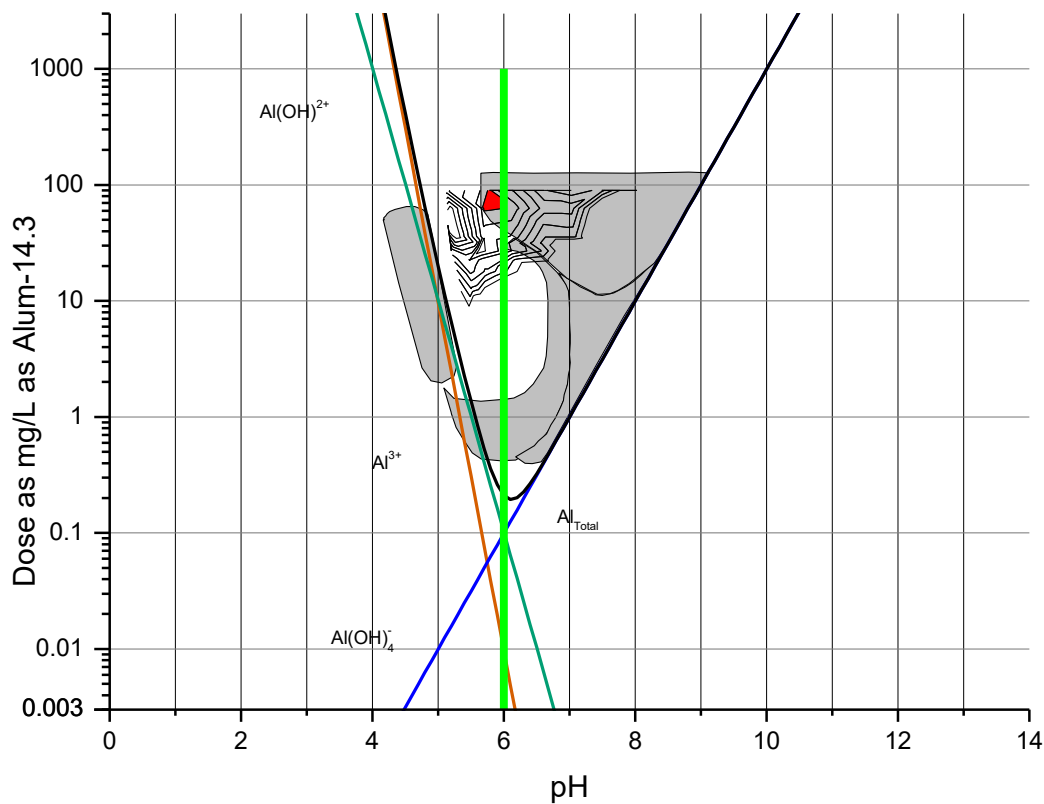


Figure 4.52. Operational coagulation diagram with the contour plot from LITF with direct filtration for model water #3. Zone of maximum observed turbidity removals is shaded red.

4.8 Alternating Single-Variable Optimization Method

Following the completion of contour mapping treatment zones of the three previous waters, an attempt was made to develop a procedure that identified coagulation conditions that provide effective treatment without the aid of a contour map. This was thought to be more practical, as most water treatment facilities are not going to have access to the mapping software. Secondly, treatment plant operators are not going to have the time to conduct the 14 jar tests needed to create a contour plot. The method optimizes each coagulation

variable independently. A final objective of this section was to make a recommendation to the initial coagulation conditions when beginning a series of optimization jar test.

4.8.1 Hypothetical Jar Test

Identification of treatment conditions with maximum treatment efficiency requires finding an effective coagulant dose and coagulated pH. The requirement to find effective coagulant dose and coagulated pH is true whether the most effective treatment conditions lie on the alum-only titration curve or not. A method was developed and evaluated using the previous contour plots. The contour plots created using single-stage flocculation and LITF with direct filtration from Sections 4.2, 4.3 and 4.4 were used. The goal of this assessment was to use a series of hypothetical jar tests and based on certain criteria have the series terminate in a zone of maximum treatment efficiency. A jar test series was terminated when the same coagulated pH and alum dose combination was selected on three consecutive occasions or a hypothetical jar test with the same coagulant doses and pH values was repeated. There were two assumptions followed during the hypothetical jar tests. The first was the target pH was achieved exactly in all cases. Secondly, the turbidity removals would be the same as what was previously seen in the creation of the contour plot.

The first step was to select an initial coagulated pH. There were three series of hypothetical jar tests applied to each contour plot. The initial coagulated pH values evaluated were 6.0, 6.5, and 7.0. At the start, these were evaluated across an alum dose range from 5 to 30 mg/L as Alum in 5 mg/L increments. The next step was to pick the lowest coagulant dose in the zone with the highest percent turbidity removals and evaluate

it across a range of pH values. If a point was on a zone boundary it was considered to be within the zone of higher turbidity removals. The range of pH values for the first pH optimization test was always 5.75 to 7.0 in 0.25 increments. The highest pH value, with highest percent turbidity removal, was selected. This pH and alum dose combination was then placed in the position of the fourth jar, and a third hypothetical jar test was evaluated with a constant pH and 6 alum doses in 5 mg/L increments. The preceding holds true unless the dose being evaluated during pH optimization is 15 mg/L or less, at which point the alum doses selected would be from 5 to 30 mg/L as Alum in 5 mg/L increments. An additional constant dose, variable pH test is conducted in the same manner as before with the previous selected pH and alum dose combination being placed in the third jar position. The positioning of the condition selected in the previous jar test in each hypothetical scenario was important as it prevented biasing the results to return the already known values. This alternating series of jar tests was continued until an alum dose/pH combination is selected on three consecutive occasions or a jar test is repeated, at this point the coagulated pH and alum dose selected would be considered the most effective based on that series of jar tests.

The results from the series of hypothetical jar tests for model water #2 using single-stage flocculation at a mixing intensity of 174 s^{-1} at an initial target coagulated pH of 6.0 can be seen in Figure 4.53. Each jar test in the series is numbered chronologically. The alum dose and coagulated pH value identified for this series of jar tests was 10 mg/L as Alum and 6.0 respectively. This point fell outside a zone of maximum observed treatment efficiency. A total of three jar tests were used to obtain these values.

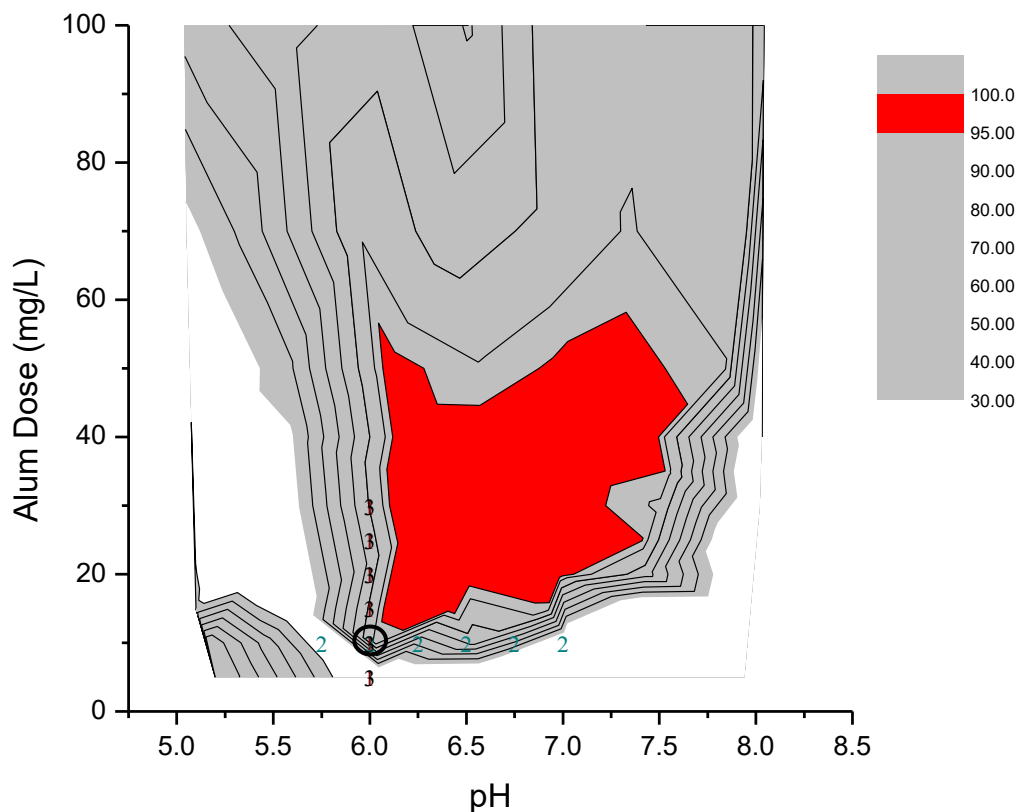


Figure 4.53. Hypothetical jar tests for model water #2 with flocculation at an intensity of 174 s^{-1} at an initial coagulated pH of 6.0. The selected alum dose and coagulated pH has been circled.

The results from the series of hypothetical jar tests for model water #2 using single-stage flocculation at a mixing intensity of 174 s^{-1} at an initial target coagulated pH of 6.5 can be seen in Figure 4.54. Each jar test in the series is numbered chronologically. The alum dose and coagulated pH value identified by this series of jar tests was 20 mg/L as Alum and 7.0 respectively. This point fell within a zone of maximum observed treatment efficiency. A total of four jar tests were used to obtain these values.

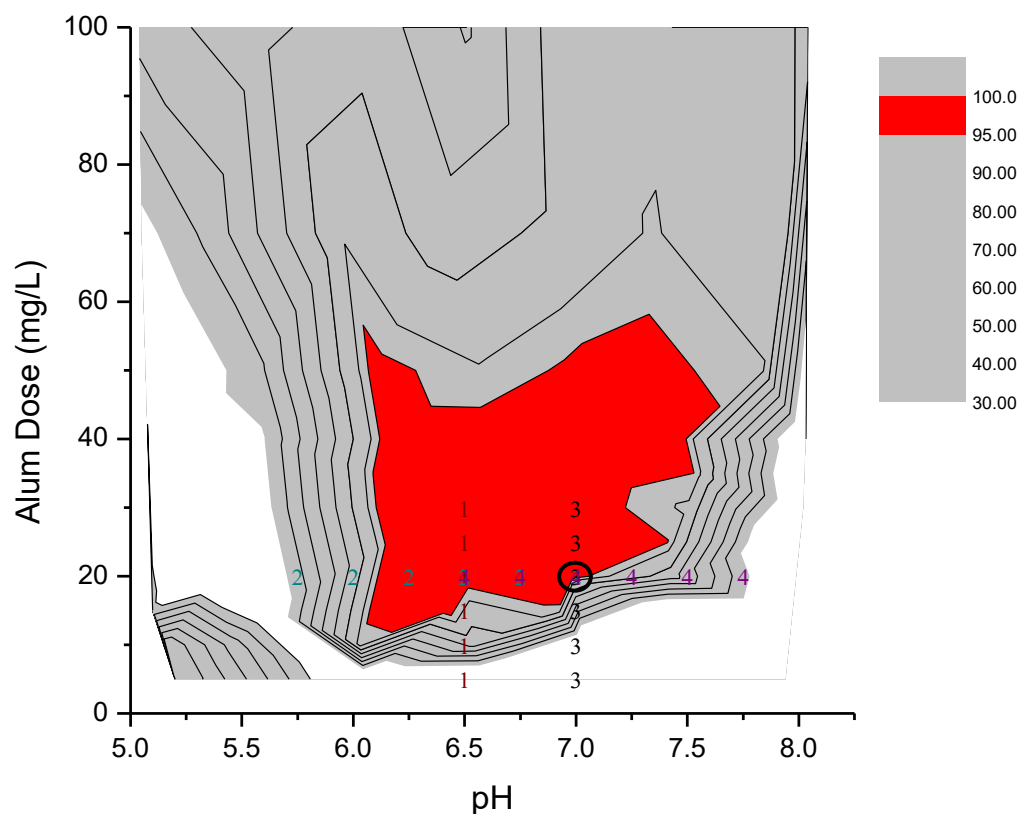


Figure 4.54. Hypothetical jar tests for model water #2 with flocculation at an intensity of 174 s^{-1} at an initial coagulated pH of 6.5. The selected alum dose and coagulated pH has been circled.

The results from the series of hypothetical jar tests for model water #2 using single-stage flocculation at a mixing intensity of 174 s^{-1} at an initial target coagulated pH of 7.0 can be seen in Figure 4.55. Each jar test in the series is numbered chronologically. The alum dose and coagulated pH value identified by this series of jar tests was 20 mg/L as Alum and 7.0 respectively. This point fell within a zone of maximum observed treatment efficiency. A total of four jar tests were used to obtain these values.

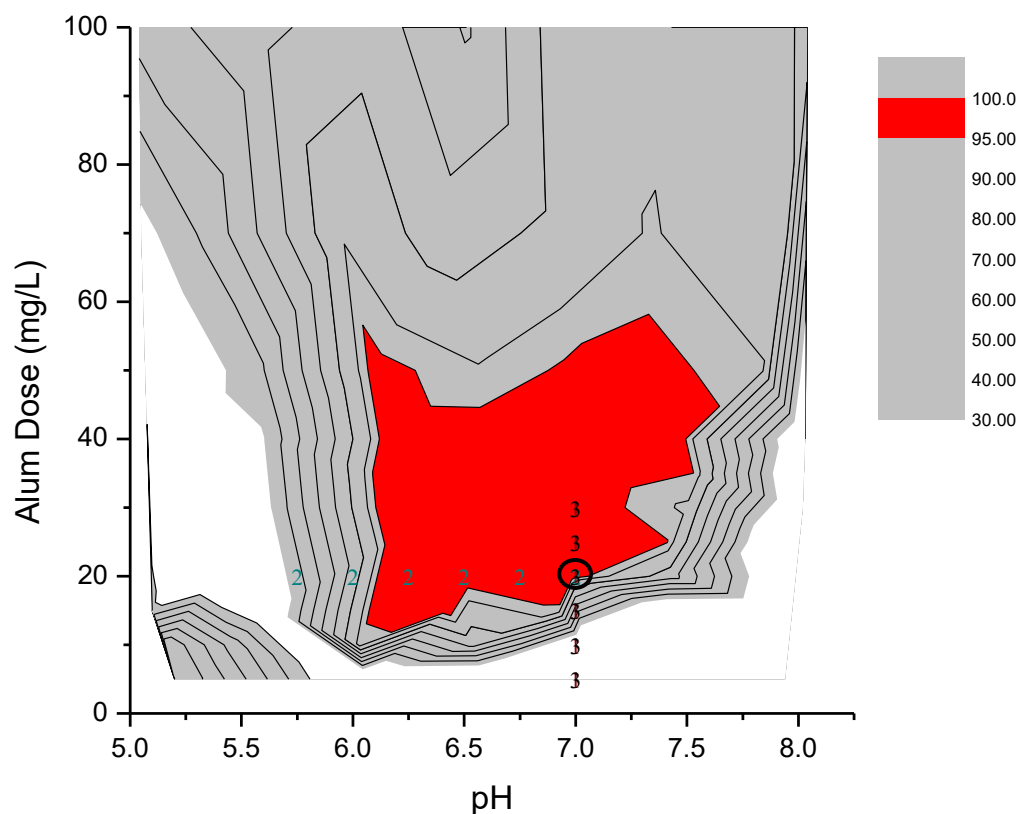


Figure 4.55. Hypothetical jar tests for model water #2 with flocculation at an intensity of 174 s-1 at an initial coagulated pH of 7.0. The selected alum dose and coagulated pH has been circled.

The results from the series of hypothetical jar tests for model water #2 using LITF at an initial target coagulated pH of 6.0 can be seen in Figure 4.56. Each jar test in the series is numbered chronologically. The alum dose and coagulated pH value identified by this series of jar tests was 15 mg/L as Alum and 6.25 respectively. This point fell within a zone of maximum observed treatment efficiency. A total of four jar tests were used to obtain these values.

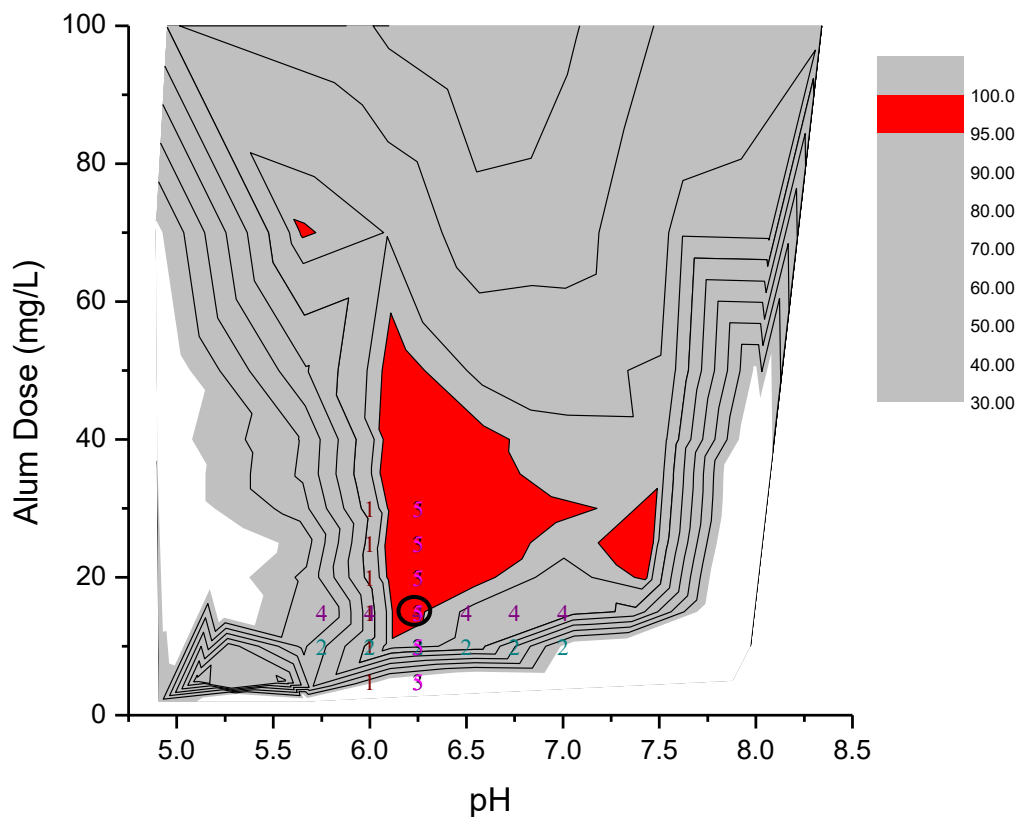


Figure 4.56. Hypothetical jar tests for model water #2 using LITF at an initial coagulated pH of 6.0. The selected alum dose and coagulated pH has been circled.

The results from the series of hypothetical jar tests for model water #2 using LITF at an initial target coagulated pH of 6.5 can be seen in Figure 4.57. Each jar test in the series is numbered chronologically. The alum dose and coagulated pH value identified by this series of jar tests was 20 mg/L as Alum and 6.5 respectively. This point fell within a zone of maximum observed treatment efficiency. A total of three jar tests were used to obtain these values.

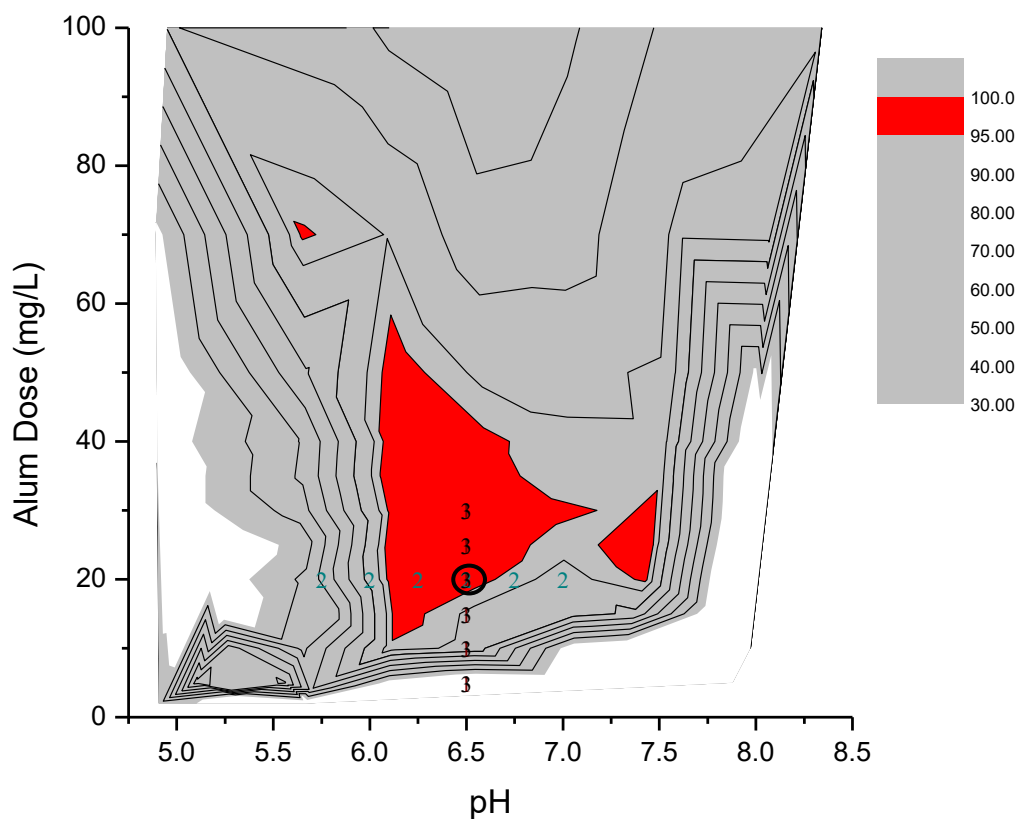


Figure 4.57. Hypothetical jar tests for model water #2 at an initial coagulated pH of 6.5. The selected alum dose and coagulated pH has been circled.

The results from the series of hypothetical jar tests for model water #2 using LITF at an initial target coagulated pH of 7.0 can be seen in Figure 4.58. Each jar test in the series is numbered chronologically. The alum dose and coagulated pH value identified by this series of jar tests was 30 mg/L as Alum and 7.0 respectively. This point fell within the zone of maximum observed treatment efficiency. A total of three jar tests were used to obtain these values.

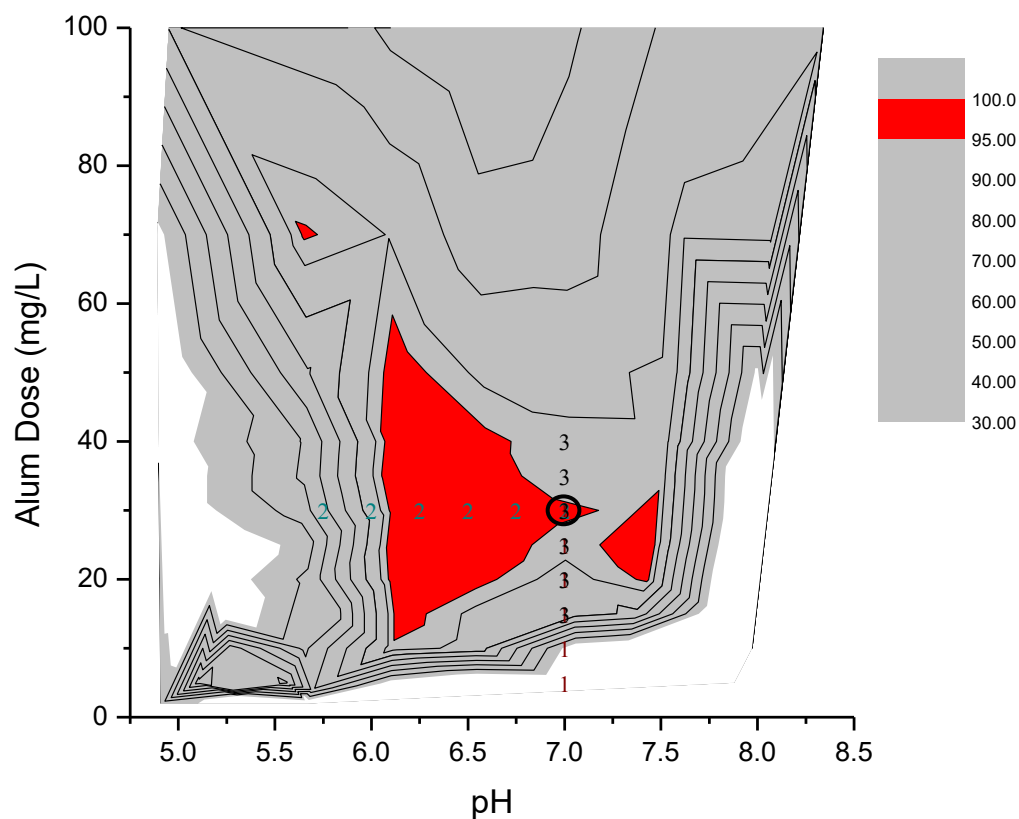


Figure 4.58. Hypothetical jar tests for model water #2 using LITF at an initial coagulated pH of 7.0. The selected alum dose and coagulated pH has been circled.

The results from the series of hypothetical jar tests for model water #3 using LITF at an initial target coagulated pH of 6.0 can be seen in Figure 4.59. Each jar test in the series is numbered chronologically. The alum dose and coagulated pH value identified by this series of jar tests was 30 mg/L as Alum and 5.75 respectively. This point fell outside a zone of maximum observed treatment efficiency. A total of four jar tests were used to obtain these values.

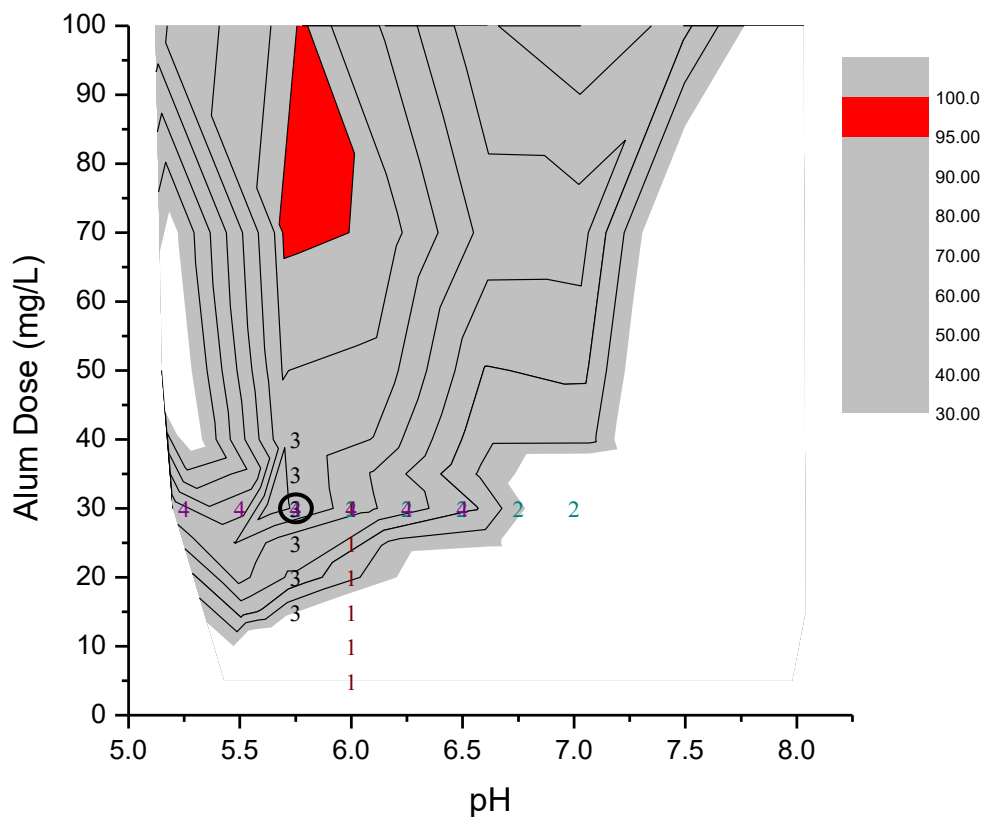


Figure 4.59. Hypothetical jar tests for model water #3 using LITF at an initial coagulated pH of 6.0. The selected alum dose and coagulated pH has been circled.

The results from the series of hypothetical jar tests for model water #3 using LITF at an initial target coagulated pH of 6.5 can be seen in Figure 4.60. Each jar test in the series is numbered chronologically. The alum dose and coagulated pH value identified by this series of jar tests was 30 mg/L as Alum and 5.75 respectively. This point fell outside a zone of maximum observed treatment efficiency. A total of four jar tests were used to obtain these values.

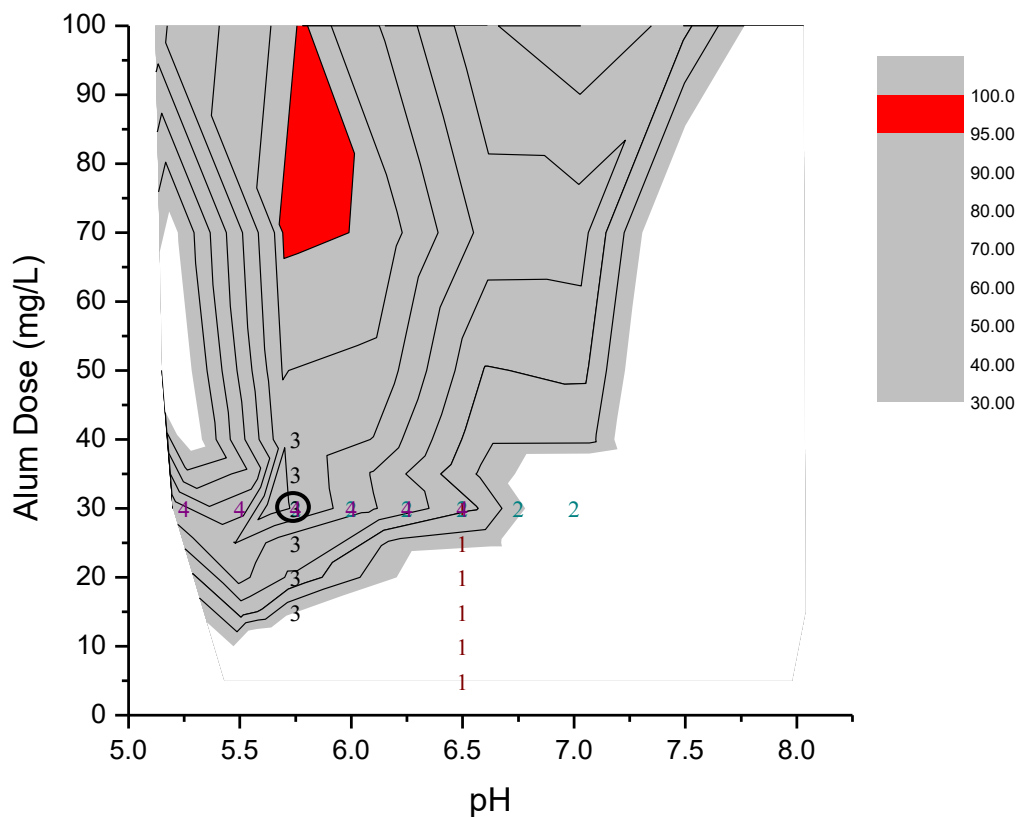


Figure 4.60. Hypothetical jar tests for model water #3 at an initial coagulated pH of 6.5. The selected alum dose and coagulated pH has been circled.

The results from the series of hypothetical jar tests for model water #3 using LITF at an initial target coagulated pH of 7.0 can be seen in Figure 4.61. Each jar test in the series is numbered chronologically. The alum dose and coagulated pH value identified by this series of jar tests was 30 mg/L as Alum and 5.75 respectively. This point fell outside a zone of maximum observed treatment efficiency. A total of four jar tests were used to obtain these values.

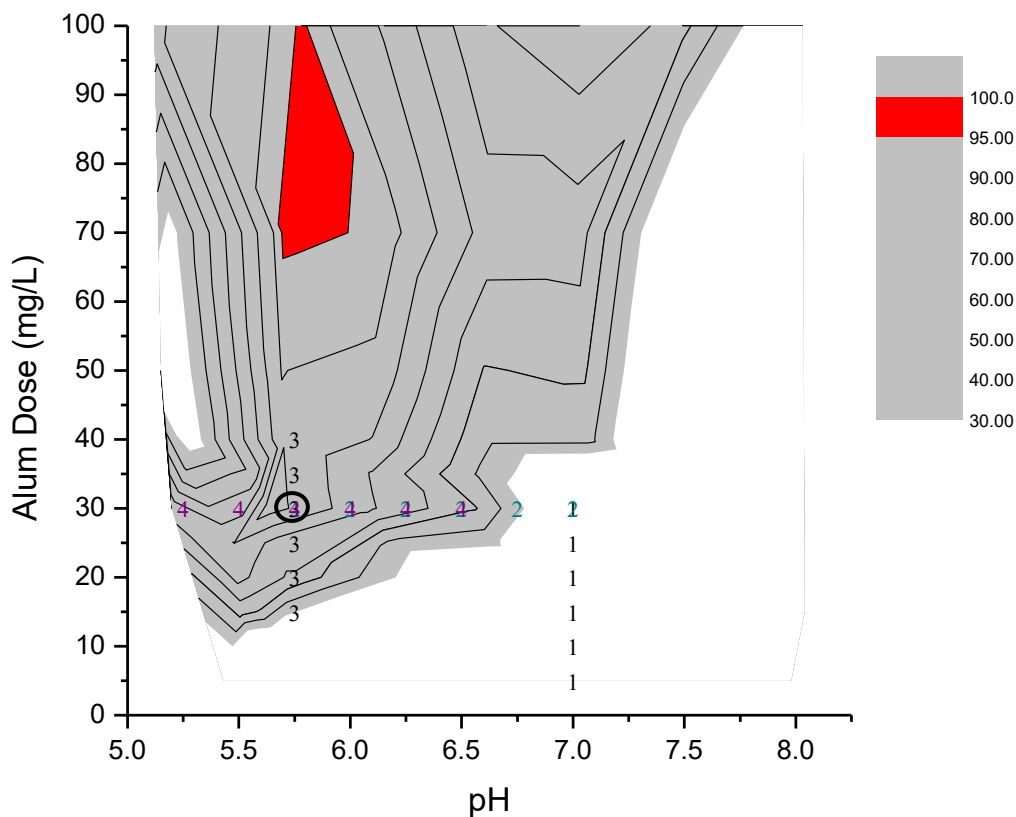


Figure 4.61. Hypothetical jar tests for model water #3 using LITF at an initial coagulated pH of 7.0. The selected alum dose and coagulated pH has been circled.

The results from the series of hypothetical jar tests for the Kannapolis model water using LITF at an initial target coagulated pH of 6.0 can be seen in Figure 4.62. Each jar test in the series is numbered chronologically. The alum dose and coagulated pH value identified by this series of jar tests was 20 mg/L as Alum and 6.0 respectively. This point fell within a zone of maximum observed treatment efficiency. A total of three jar tests were used to obtain these values.

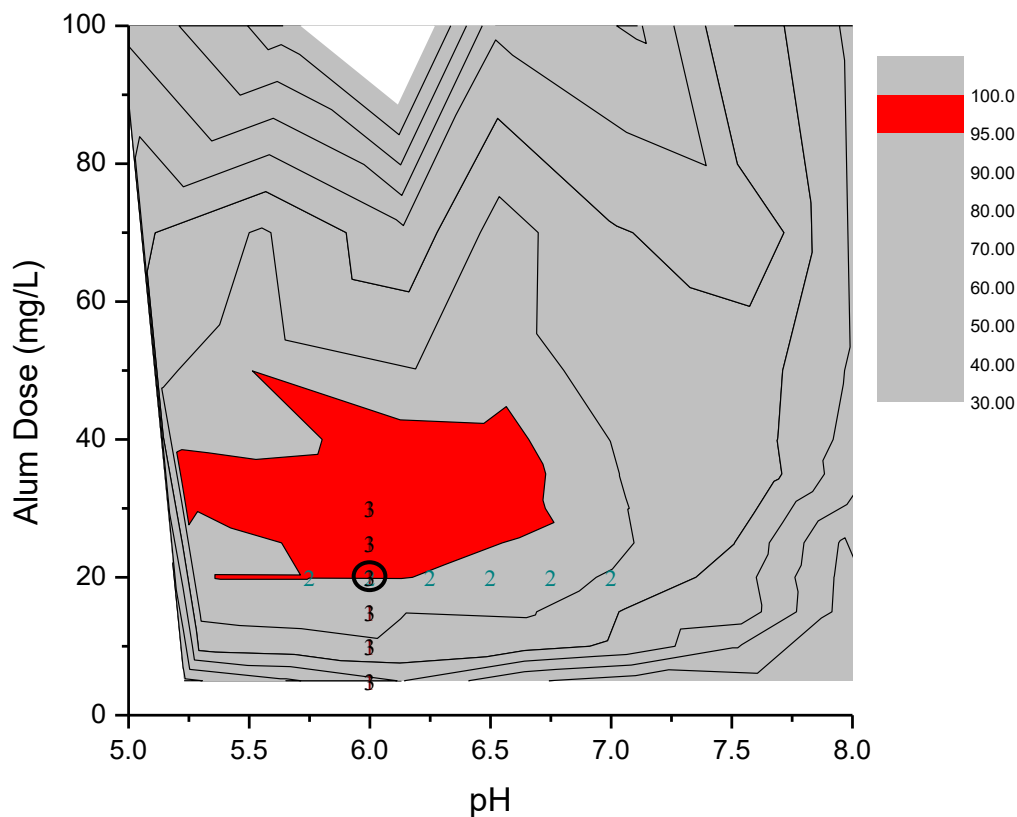


Figure 4.62. Hypothetical jar tests for natural water #2 using LITF at an initial coagulated pH of 6.0. The point of optimum alum dose and coagulated pH has been circled.

The results from the series of hypothetical jar tests for natural water #2 using LITF at an initial target coagulated pH of 6.5 can be seen in Figure 4.63. Each jar test in the series is numbered chronologically. The alum dose and coagulated pH value identified by this series of jar tests was 25 mg/L as Alum and 6.5 respectively. This point fell within a zone of maximum observed treatment efficiency. A total of three jar tests were used to obtain these values.

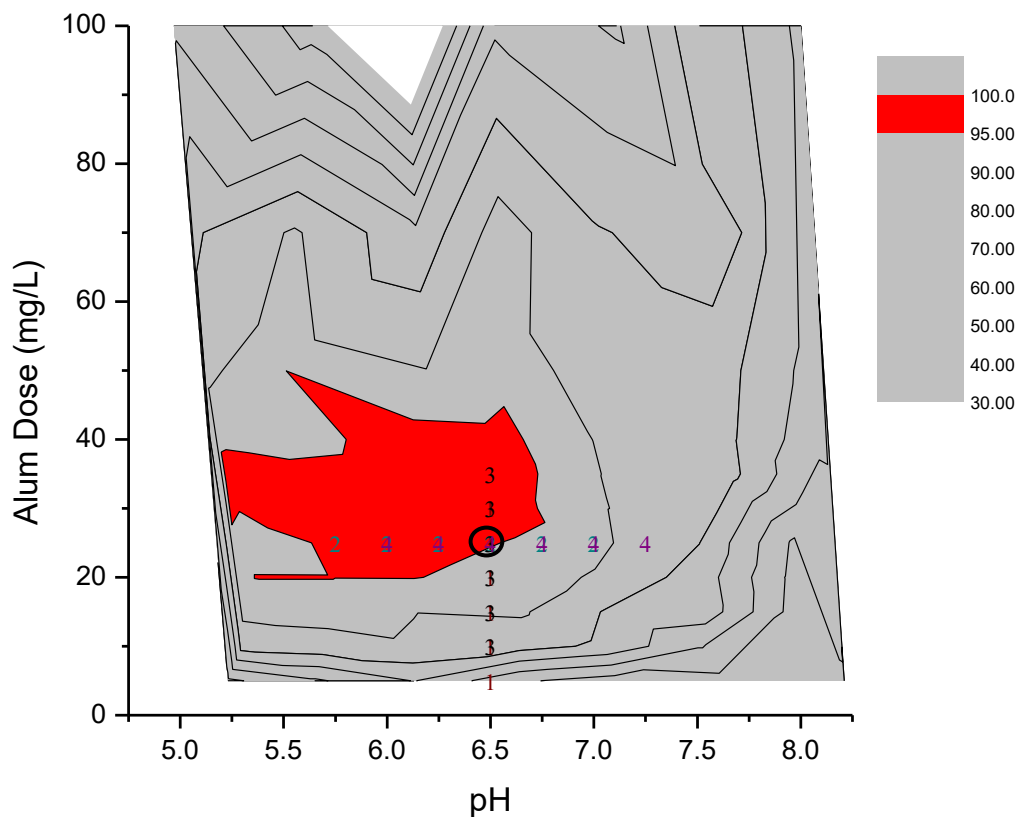


Figure 4.63. Hypothetical jar tests for natural water #2 using LITF at an initial coagulated pH of 6.5. The selected alum dose and coagulated pH has been circled.

The results from the series of hypothetical jar tests for natural water #2 using LITF at an initial target coagulated pH of 7.0 can be seen in Figure 4.64. Each jar test in the series is numbered chronologically. The alum dose and coagulated pH value identified by this series of jar tests was 25 mg/L as Alum and 6.0 respectively. This point fell within a zone of maximum observed treatment efficiency. A total of four jar tests were used to obtain these values.

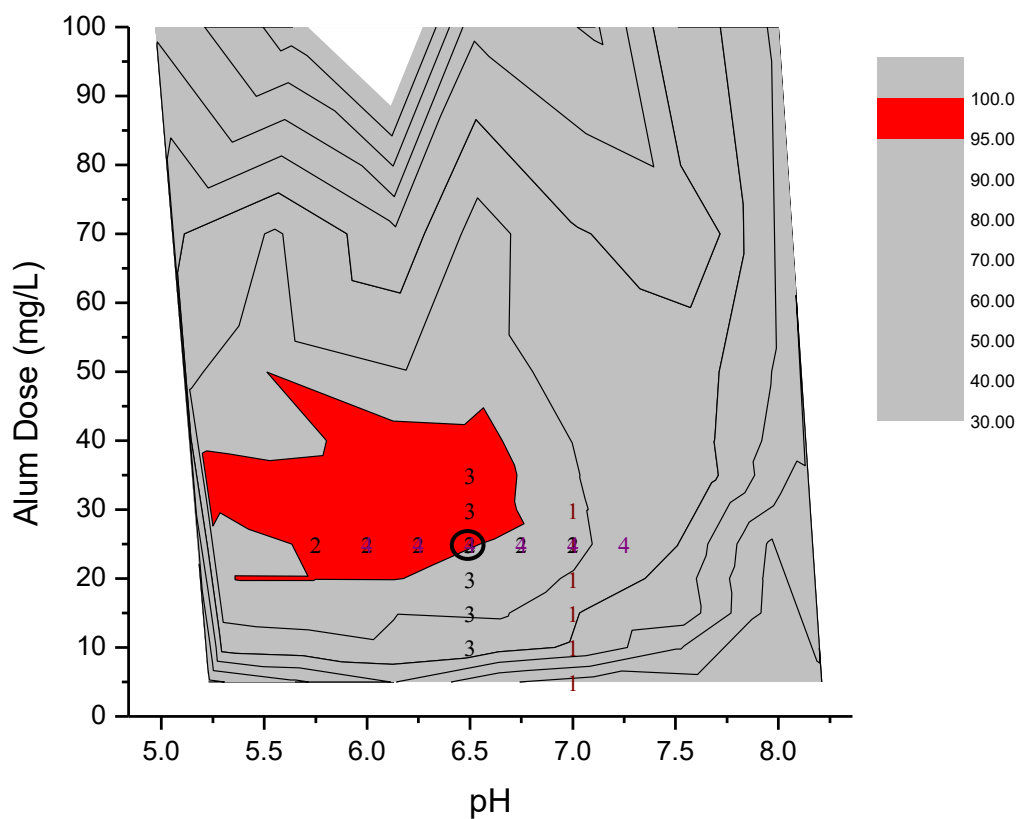


Figure 4.64. Hypothetical jar tests for natural water #2 at an initial coagulated pH of 7.0. The selected alum dose and coagulated pH has been circled.

A summary of the above results can be seen in Table 4.2. It was observed that hypothetical jar testing conducted at an initial coagulated pH of 6.5 or 7.0 resulted in a coagulant dose and coagulated pH combination that fell within a zone of maximum observed turbidity removals for all waters evaluated except for model water #3. For this model water all three hypothetical jar tests resulted in the same coagulant dose (30 mg/L as Alum) and coagulated pH (6.25) combination and this point fell outside of the zone of maximum observed turbidity removals.

Table 4.2. Summary of the results from the series of hypothetical jar tests with results that fell within a zone of maximum observed treatment efficiency highlighted.

Water	Selected Conditions					
	6.0		6.5		7.0	
	Alum Dose (mg/L)	pH	Alum Dose (mg/L)	pH	Alum Dose (mg/L)	pH
Model Water #2 _{174 1/s}	10	6.0	20	7.0	20	7.0
Model Water #2 _{LITF}	15	6.25	20	6.5	30	7.0
Model Water #3	30	6.25	30	6.25	30	6.25
Natural Water #2	20	6.0	25	6.5	25	6.5

Following hypothetical jar testing, bench-scale testing was evaluated at an initial coagulated pH of 6.5 for a fourth model water. This pH was selected due to the similarity of the results in this section and it being the median value of the contour plots. The previous series of hypothetical jar tests were applied in a manner that limited subjectivity, the concluding series of jar tests was performed in a more realistic manner that will mimic the subjectivity that staff at a water treatment facility would experience.

4.8.2 Bench-Scale Evaluation of the Alternating Single-Variable Method

A series of jar tests were conducted to find an effective coagulant dose for model water #4 (low turbidity, moderate-high DOC/SUVA model water). Low-intensity tapered flocculation with direct filtration was used. The initial jar test was conducted at a target coagulated pH of 6.5, across an alum dose range from 0 to 50 mg/L as Alum in 10 mg/L

increments. This was expanded from what was used in the hypothetical testing (Section 4.8.1) to cover a broader range of coagulant doses in the initial jar test.

Results from the initial jar test can be seen in Figure 4.65. The lowest filtered turbidity observed was 0.87 NTU. This turbidity occurred at a coagulant dose of 50 mg/L as Alum. This alum dose was selected and was evaluated from pH 5.75 to pH 7.0 in 0.25 increments in a subsequent jar test.

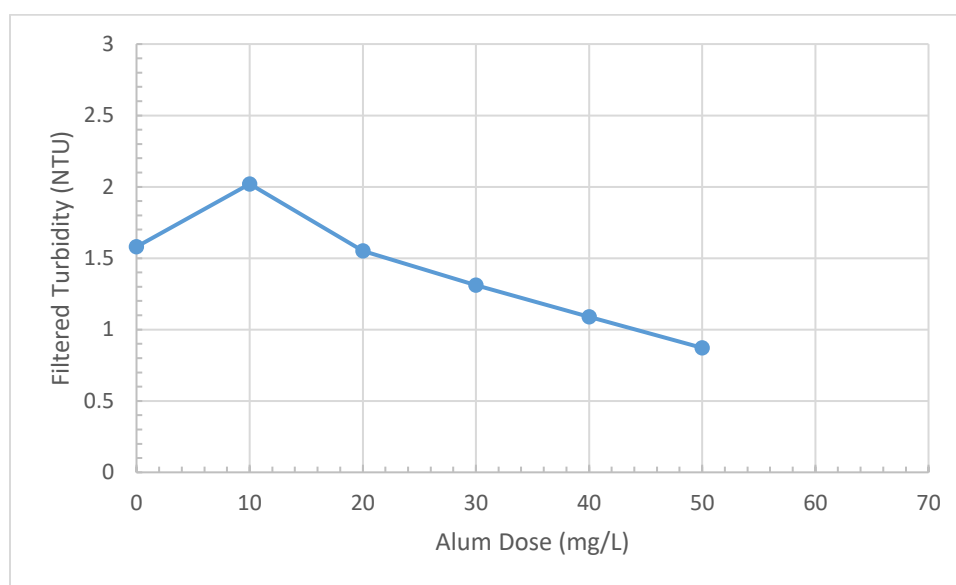


Figure 4.66. Jar test results at an alum dose of 50 mg/L for model water #4.

Results from the jar test at a target coagulated pH of 6.25, across the coagulant dose range of 25 to 50 mg/L as Alum can be seen in Figure 4.67. The lowest observed turbidity (0.39 NTU) occurred at an Alum dose of 40 mg/L. This turbidity value is higher than the 0.18 NTU observed at a coagulant dose of 50 mg/L as Alum and a coagulated pH of 6.17. The actual coagulated pH values for each jar during testing at a target coagulated pH of 6.25 were as follows: 6.20, 6.33, 6.34, 6.32, 6.36, and 6.32. This slight increase in turbidity and coagulated pH indicates that a target coagulated pH of 6.25 may be near or on a

boundary of changing treatment efficiency. Following this result, a jar test was conducted at Alum dose of 40 mg/L, across a target coagulated pH range of 5.5 to 6.75 in 0.25 increments.

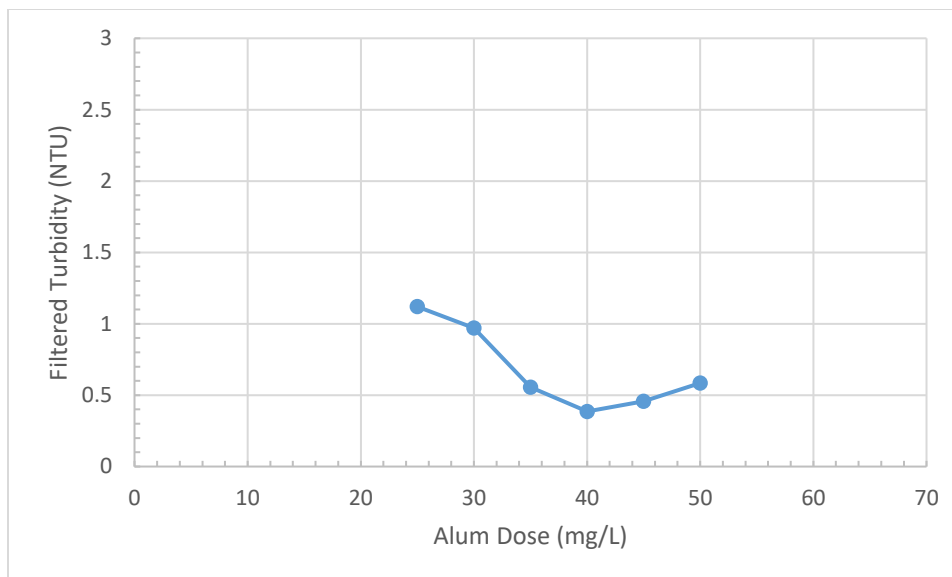


Figure 4.65. Jar test results at a target coagulated pH of 6.5 for model water #4.

Results from jar testing at a constant Alum dose of 50 mg/L, from pH 5.75 to pH 7.0 can be seen in Figure 4.66. The lowest filtered turbidity observed was 0.18 NTU, which occurred at a target coagulated pH of 6.25. The actual pH measured was 6.17. Following this result, a jar test was conducted at a target coagulated pH of 6.25 from a coagulant dose of 25 to 50 mg/L as Alum in 5 mg/L increments. A coagulant dose of 50 mg/L as Alum was selected as the maximum dose because it was shown to be an effective dose in Figure 4.66 at a coagulated pH of 6.25. There was no need to evaluate the effectiveness at a higher dose range because a coagulant dose of 50mg/L as Alum at a target pH of 6.25 resulted a filter turbidity (0.18 NTU) below 0.30 NTU.

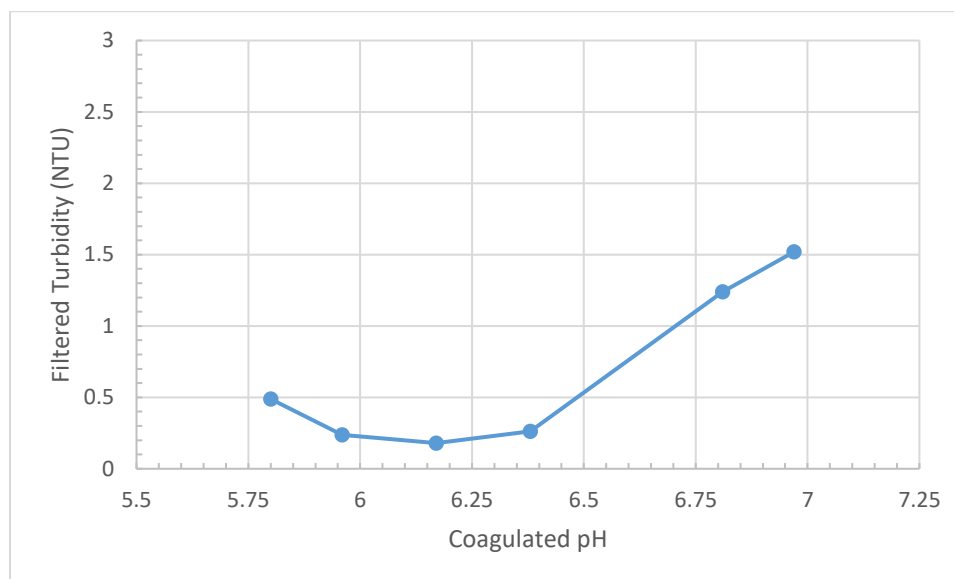


Figure 4.67. Jar test results at a target coagulated of pH 6.25 for model water #4.

Results from the jar test at an Alum dose of 40 mg/L from a target coagulated pH of 5.5 to pH 6.75 can be seen in Figure 4.68. The lowest observed turbidity was 0.29 NTU and occurred at an actual pH of 6.12. Following this result, a target coagulated pH of 6.00 was selected and a jar test was conducted across a coagulant dose range of 20 to 45 mg/L as Alum in 5 mg/L increments.

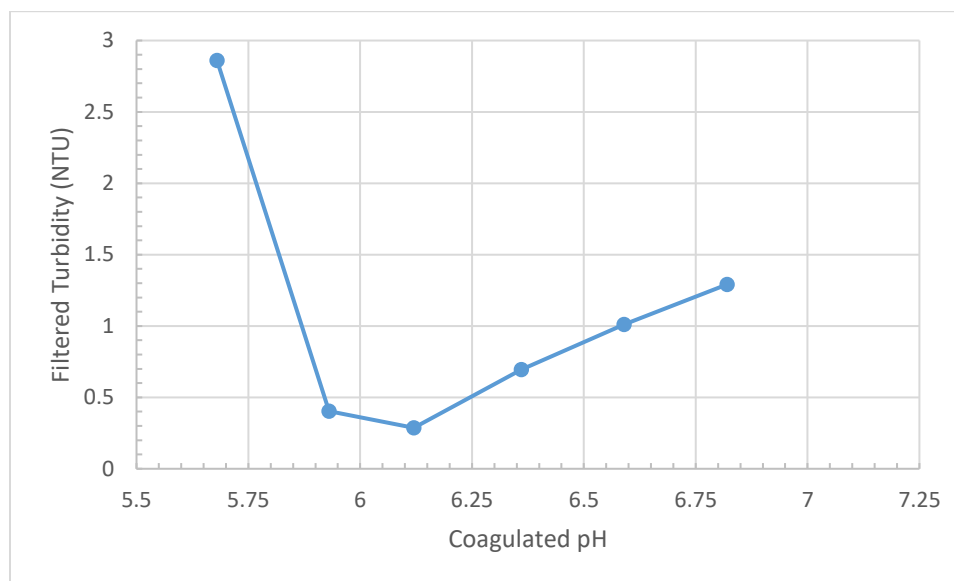


Figure 4.68. Jar test results at a coagulant dose of 40 mg/L as Alum for model water #4.

Results from the jar test at a target coagulated pH of 6.00, across the alum dose range of 20 to 45 mg/L, can be seen in Figure 4.69. The lowest observed filtered turbidity was 0.24 NTU. This result occurred at an alum dose of 40 mg/L.

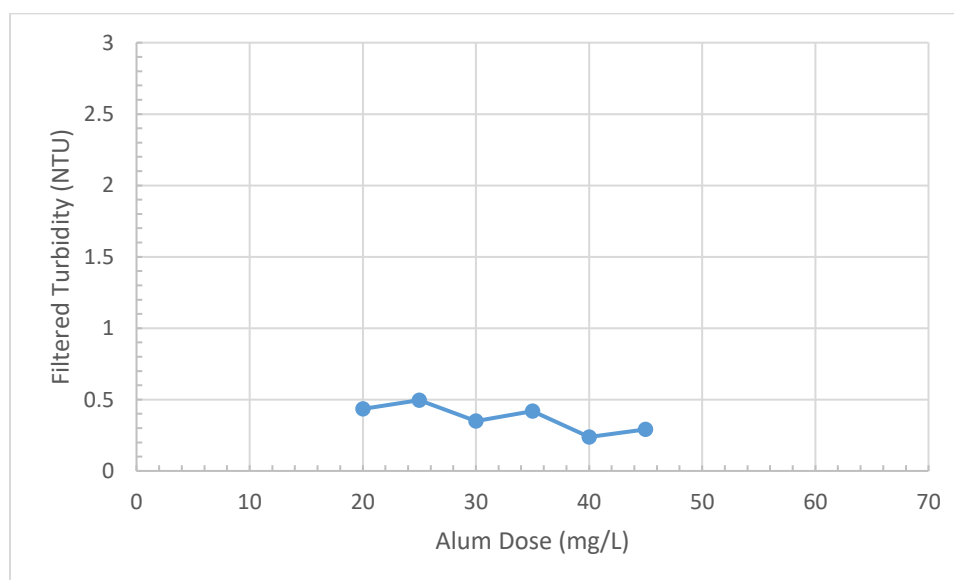


Figure 4.69. Jar test results at a target coagulated pH of 6.00 for model water #4.

Figure 4.70 is display of the target coagulated pH values and the alum doses used in each of the 5 previous jar tests. Each jar test in the series is labeled chronologically. The coagulant dose and pH combination that was selected is circled.

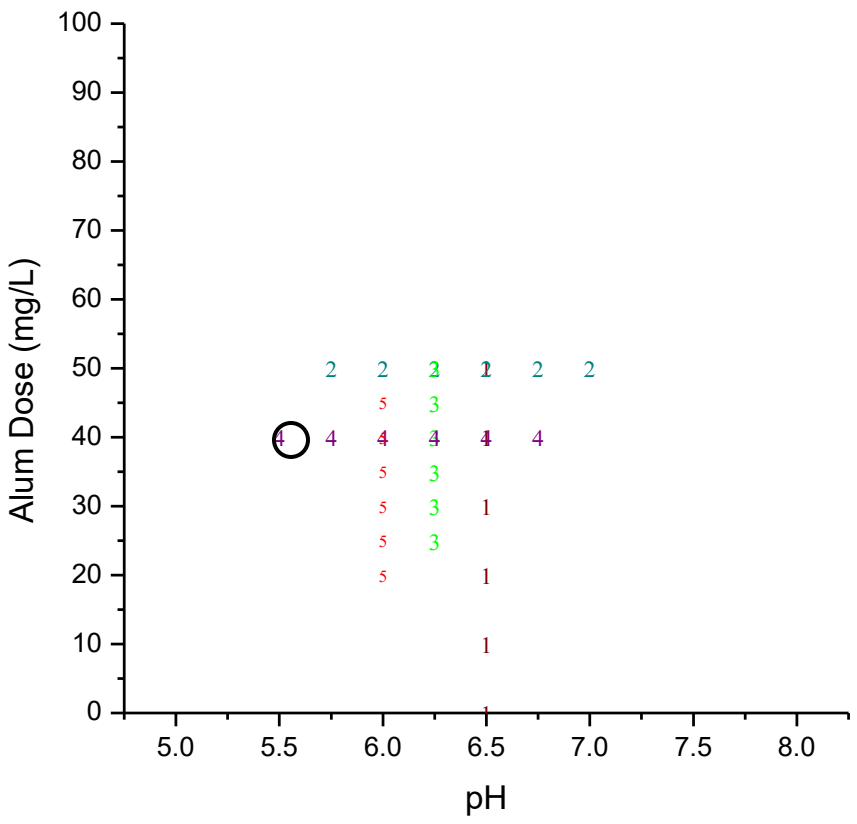


Figure 4.70. Target coagulated pH values and alum doses from the series of jar test used to determine effective coagulation conditions. Selected dose and pH has been circled.

Based on these results, it was determined that effective treatment conditions occurred an Alum dose of 40 mg/L and at a coagulated pH near a target of 6.0. A contour plot was created based on the previous results. A subsequent jar test was conducted to find the upper limit of the treatment zone and was also included in the contour plot. The jar test was conducted at a target coagulated pH of 6.0 from 40 to 65 mg/L as Alum in 5 mg/L

increments. The results for this jar test can be seen in Figure 4.71. Although this result was only to be used for the contour plot, it indicated lower filtered turbidity at a coagulant dose of 50 mg/L as Alum than at 40 mg/L. The mean filtered turbidity for an Alum dose of 40 mg/L at a target pH 6.0 was 0.30 with a standard deviation of 0.07. The mean filtered turbidity for an Alum dose of 50 mg/L at a target pH of 6.0 was 0.23 with a standard deviation of 0.04. This sample included the filtered turbidity from the coagulated pH target of 6.25 at a coagulant dose of 50 mg/L as Alum as the measured pH (6.17) was similar to that of measured pH values at a target of 6.0. The sample size for both alum doses was three. A t-Test resulted in a p-value of 0.23, which shows that the difference in the two samples is not statistically significant.

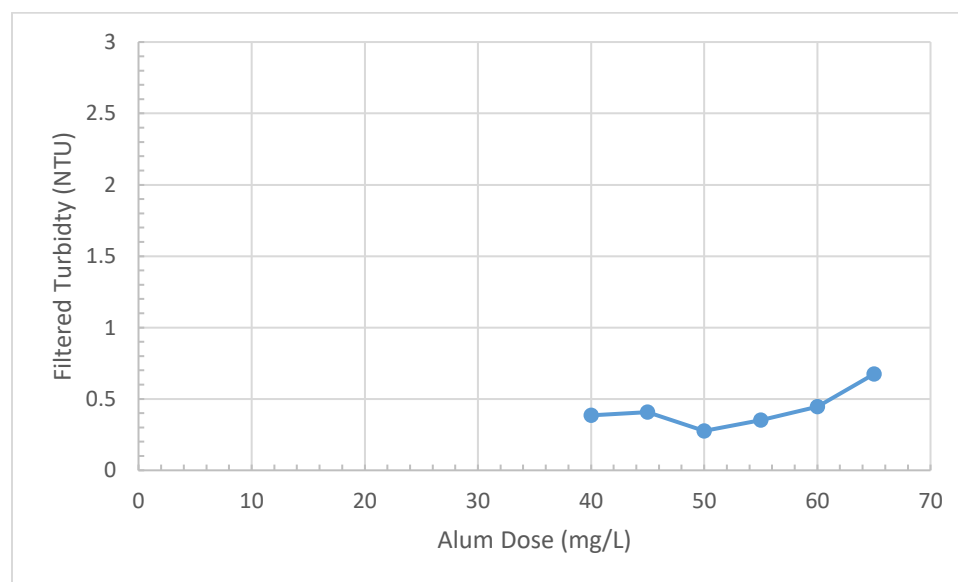


Figure 4.71. Jar test results at a target coagulated pH of 6.00, with an alum dose above selected effective dose, for model water #4.

The contour plot created from the previous series of jar tests for model water #4 can be seen in Figure 4.72. A centralized zone of maximum observed removals of 80% to 90% can be seen. The zone extends from an approximate coagulant dose of 38 to 55 mg/L as Alum. The zone is bound on the left between a coagulated pH value 5.75 and 6.00. The right bound of the zone is located near a coagulated pH of 6.25. The circled irregularity in the zone boundary is due to multiple results at similar points and the variability among those results. For the previous contour plots there was only one result for each point on the plot. At a coagulant dose of 40 mg/L as Alum, percent turbidity removals ranged from 79.6 to 85.6 in the area of this irregularity. Percent turbidity removals ranged 77.5 to 81.6 at a coagulant dose of 45 mg/L as Alum near this area of interest.

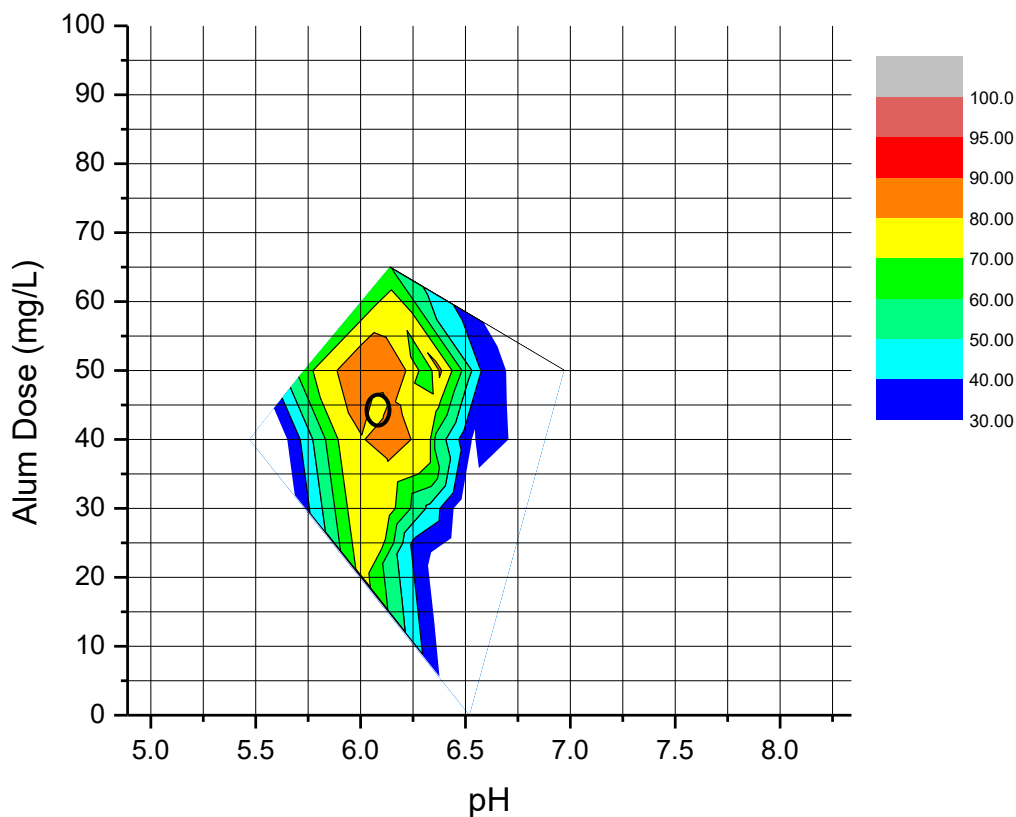


Figure 4.72. Contour plot created from a series of optimization jar tests for model water #4. A zone boundary irregularity has been circled.

The zone of maximum observed turbidity removal efficiency was $\geq 80\%$. The selected effective coagulation conditions fell within this zone. This can be seen in Figure 4.73. The alum dose and measured coagulated pH for each jar from the previous series of jar tests were graphed with the contour plot. Each jar test has been labeled numerically in the order of which it was performed. The maximum percent turbidity removals observed did not exceed the 95% threshold that was used in the previous contour plots. This is due, at least in part, to the low raw water turbidity ($Turbidity_{avg} = 1.66$ NTU) Table 4.3 is a summary of the minimum observed filtered turbidity from the data used to produce each

Table 4.3. Summary of the minimum observed filtered turbidity and its corresponding percent turbidity removal for each LITF with direct filtration contour plot.

Water	Raw Turbidity (NTU)	Filtered Turbidity (NTU).	Percent Removal (%)
Natural Water #2	3.38	0.10	97.1
Model Water #2	42.2	.269	99.4
Model Water #3	29.7	1.1	96.1
Model Water #4	1.66	.18	87.7

CHAPTER 5: SUMMARY AND CONCLUSIONS

5.1 Summary

Jar testing is among the most common tools that water treatment facilities use to determine the treatment conditions necessary to meet finished water goals. One study found that out of the eight methods identified for determining and monitoring coagulation conditions, jar testing was the second most prevalent method applied, following only the use of historical data (Logsdon & Hess, 2002). Of the 37 participating treatment facilities, 29 applied jar testing to their coagulation optimization process. Only 4 utilities surveyed used one method of coagulation monitoring and determination, with the majority of facilities applying three to five different techniques. Some treatment utilities are unable to use jar testing to determine optimal treatment conditions because the current jar test procedure does not indicate optimum full-scale treatment conditions for their water source. The objective of this research was to develop a new jar test procedure that could be used at all treatment facilities without site- specific customization to compare coagulation conditions based on filtration efficiency (instead of sedimentation efficiency) in a timely manner.

Following preliminary evaluation of filter loading rates and flocculation mixing procedures, a series of contour plots were created for three waters using low-intensity tapered flocculation and single-stage flocculation at mixing intensity of 174 s^{-1} (120 rpm). It was observed that turbidity removal by filtration (a new method modification) provided sufficient results without the need for sedimentation (the current standard practice for jar

testing). Through the evaluation of the contour plot for natural water #2, it was determined that the application of filters with the jar test apparatus has the potential to better replicate the plant operating conditions at the bench-scale.

An alternating, single-variable optimization method was developed and applied to a low turbidity, moderately-high DOC/SUVA model water. An area of effective treatment was identified using this optimization method that matched a contour plot created afterwards. It was also observed that using percent turbidity removal as a metric for evaluation of treatment effectiveness was dependent on raw water turbidity, which caused the turbidity removal targets to vary.

5.2 Conclusions and Recommendations

5.2.1 Conclusions

- Titrations are an essential step in the new jar test method when optimizing coagulation variables (coagulant dose and coagulated pH). Titrations prior to jar testing ensures that target coagulation conditions are being met during bench-scale evaluation. The use of titrations allows for a specific coagulated pH to be maintained in all jars or for different target pH values to be assessed accurately in each jar during jar testing.
- The adjustment of coagulant dose and coagulated pH is sometimes necessary to reach optimal treatment conditions. When water is treated with alum-only, the addition of the acidic coagulant causes pH and coagulant dose to change simultaneously. This provides only one diagonal path for treatment to occur across

a two-dimensional area, which sometimes misses the optimal treatment zones entirely.

- Filtration through 3 inches of granular media at a filter loading rate of ≈ 5 gpm/ft² was sufficient for coagulation optimization with jar testing while reducing testing time. It was shown that filter loading rate and filter design only affected jar test results when coagulation conditions were suboptimum. Low filter loading rates and deep-bed filters resulted in increased turbidity removals under suboptimum coagulation conditions. However, jar testing is intended to distinguish between relatively good and poor treatment, and having highly-efficient filters would make the distinction between these two conditions more difficult and less precise.
- Single-stage flocculation at 120 rpm for 10 minutes provided sufficient floc growth for jar testing with direct filtration for the waters and treatment conditions examined in this study.
- Comparing the jar test results from the Mt. Holly and Kannapolis natural waters to the full-scale coagulation conditions at each facility, it was shown that the new filtration-based jar test procedure better predicted actual plant performance over the traditional sedimentation method.
- Using contour plots to map jar test results was useful in identifying zones of coagulation conditions that could be applied at plant-scale.
- The results of the alternating, single-variable optimization method are affected by starting coagulant dose and pH. Starting at a pH of 6.0 versus 6.5 could result in different coagulant dose and pH recommendations. Using a median pH value of 6.5 when beginning a series optimization jar tests has been shown to result in a pH

and coagulant dose combination within a zone of maximum turbidity removals for the waters and treatment conditions examined in this study.

5.2.2 Recommendations

- A filtration-based jar test procedure using titrations and a standardized mixing protocol is recommended to identify effective coagulation conditions for drinking water utilities.
- The alternating, single-variable optimization method is recommended to identify the most effective coagulation conditions when contour mapping is not practical. This method allows for a systematic approach in determining the most effective coagulation conditions. Each jar test in the series builds on the previous ones to pinpoint an effective pH and coagulant dose combination.
- When applying the alternating, single-variable optimization method, it is recommended for the initial jar test be a dose optimization at a coagulated pH of 6.5.
- It is recommended that for existing treatment plants where an effective coagulant dose is known that the doses used in the initial optimization jar test be centered on the known dose in increments of 5 mg/L as coagulant.
- For waters where effective treatment conditions are unknown, it is recommended that the initial jar test cover a coagulant dose range of 10 to 60 mg/L as coagulant in 10 mg/L increments. These are minimum recommendations as the dose range and/or the increments could be increased if a high coagulant demand is expected.
- When applying the alternating, single-variable optimization method, it is recommended that the selection of coagulation conditions being evaluated be based

around the conditions that resulted in the maximum observed turbidity removals in the previous jar test.

- Optimum coagulation conditions as they were defined with this jar test procedure do not reflect plant-specific operational considerations (i.e. chemical cost, limitations in chemical feed locations, or solids disposal cost and restrictions).

5.3 Recommendations for Further Research

Future research is needed to investigate coagulation under the charge neutralization and sweep mechanisms. A better understanding of the individual mechanisms will allow for better interpretation of jar tests results and optimization predictions. Also, an investigation into individual water quality parameters and how each effect coagulant demand is needed. A better understanding of water quality parameters would improve coagulation condition predictions based on raw water characteristics and would better establish starting points for jar tests evaluation. Furthermore, water temperature effects on treatment efficiency should be investigated. It is established that alum is a poor coagulant for treatment of cold water, but this is a characteristic of the coagulant. It was shown with the research conducted on the natural water from the Kannapolis Water Treatment Plant that rising temperatures can cause a shift in effective treatment conditions. To counteract this, it was hypothesized that it would be necessary to adjust the target coagulated pH value by holding the pOH constant to ensure that reaction conditions remain similar.

REFERENCES

- American Water Works Association. (2011). *Operational control of coagulation and filtration processes: manual of water supply practices* (Third ed.). Denver, CO: American Water Works Association.
- Amirtharajah, A., & Mills, K. M. (1982). Rapid-mix design for mechanisms of alum coagulation *Journal (American Water Works Association)*, 74(4), 210-216.
- Au, K.-K., Alpert, S. M., & Pernitsky, D. J. (2011). Particle and natural organic matter removal. In *Operation control of coagulation and filtration processes* (Third ed., pp. 1-16). Denver, CO: American Water Works Association.
- Black, A. P., Buswell, A. M., Eidsness, F. A., & Black, A. L. (1957). Review of the jar test. *Journal (American Water Works Association)*, 49(11), 1414-1424.
- Black, A. P., Rice, O., & Bartow, E. (1933). Formation of floc by aluminum sulfate. *Industrial and Engineering Chemistry*, 25(7), 811-815.
- Bratby, J. (2006). *Coagulation and flocculation in water and wastewater treatment* (TechBooks Ed. Second ed.). London, UK: IWA Publishing.
- Brink, D. R., Choi, S.-I., AL-Ani, M., & Hendricks, D. W. (1988). Bench-scale evaluation of coagulants for low turbidity water. *Journal (American Water Works Association)*, 80(4), 199-204.
- Budd, G. C., Hess, A. F., Shorney-Darby, H., Neeman, J. J., Spencer, C. M., Bellamy, J. D., & Hargette, P. H. (2004). Coagulation applications for new treatment goals. *Journal (American Water Works Association)*, 96(2), 102-113.
- Cornwell, D. A., & Bishop, M. M. (1983). Determining velocity gradients in laboratory and full-scale systems. *Journal (American Water Works Association)*, 75(9), 470-475.
- Dempsey, B. A., Ganho, R. M., & O'Melia, C. R. (1984). The coagulation of humic substances by means of aluminum salts. *Journal (American Water Works Association)*, 76(4), 141-150.
- Eco Lawn & Garden. (2013). Retrieved from <http://www.ecolawnandgarden.com/eco-super-hume-humic-acid/>
- Edwards, G. A., & Amirtharajah, A. (1985). Removing color caused by humic acids. *Journal (American Water Works Association)*, 77(3), 50-57.

- Edzwald, J. K. (1993). Coagulation in drinking water treatment: particles, organic and coagulants. *Water Science & Technology*, 27(11), 21-35.
- Edzwald, J. K. (2014). Rapid-mixing tanks for coagulation: are they needed? *Journal NEWWA*, 128(1), 1-11.
- Edzwald, J. K., Becker, W. C., & Wattier, K. L. (1985). Surrogate parameters for monitoring organic matter and THM precursors. *Journal (American Water Works Association)*, 77(4), 122-132.
- Edzwald, J. K., & Van Benschoten, J. E. (1990). *Aluminum Coagulation of Natural Organic Matter*. Paper presented at the 4th Gothenburg Symposium, Madrid, Spain.
- Gregory, J. (2009). Monitoring particle aggregation processes. *Advances in Colloid and Interface Science*, 147-148, 109-123. doi:10.1016/j.cis.2008.09.003
- Hendricks, D. (2011). *Fundamentals of Water Treatment Unit Processes - Physical, Chemical, and Biological*. Boca Raton, FL: CRC Press.
- Hudson Jr., H. E. (1973). Evaluation of plant operating and jar-test data. *Journal (American Water Works Association)*, 65(5), 368-375.
- Hudson Jr., H. E., & Wagner, E. G. (1981). Conduct and use of jar tests. *Journal (American Water Works Association)*, 73(4), 218-223.
- Letterman, R. D., Quon, J. E., & Gemmill, R. S. (1973). Influence of rapid-mix parameters on flocculation. *Journal (American Water Works Association)*, 65(11), 716-722.
- Logsdon, G. S., & Hess, A. F. (2002). *Filter maintenance and operations guidance manual*. Denver, CO: AWWA Research Foundation and American Water Works Association.
- Mosher, R. R., & Hendricks, D. W. (1986). Rapid rate filtration of low turbidity waters using field-scale pilot filters. *Journal (American Water Works Association)*, 78(12), 42-51.
- Pernitsky, D. J. (2003). *Coagulation 101*. Paper presented at the P:\OFFICE\Conferences\2003TechTrans\Dave P\DAVE_paper.doc.
- Peterson, B. H., & Bartow, E. (1928). Effect of salts on the rate of coagulation and the optimum precipitation of alum floc. *Industrial and Engineering Chemistry*, 20(1), 51-55.

- Phipps & Bird. (2017). Jar test procedure. Retrieved from <http://www.phippsbird.com/pbinc/WaterWasteWater/jarpro.aspx>
- Randtke, S. J. (1988). Organic contaminant removal by coagulation and related process combinations. *Journal (American Water Works Association)*, 80(5), 40-56.
- Rank Brothers LTD. (2017). *PDA2000 Photometric Dispersion Analyzer*. In. Retrieved from <http://www.rankbrothers.co.uk/download/PDA2000.pdf>
- Reed, G. D., & Robinson, R. B. (1984). Similitude interpretation of jar test data. *Journal of Environmental Engineering*, 110(3), 670-677.
- Stumm, W., & O'melia, C. R. (1968). Stoichiometry of Coagulation. *Journal (American Water Works Association)*, 60(5), 514-539.
- Teefy, S., Farmerie, J., & Pyles, E. (2011). Jar Testing. In *Operational Control of Coagulation and Filtration Processes* (Third ed., pp. 17-57): American Water Works Association.
- Tintometer Group. (2016). *Floc-tester: ET 740 & ET 750*. In. Retrieved from http://dl.lovibond.com/instructions/floctest/ins_floctest_et740_750_gb_lovi.pdf
- Wagner, E. G., & Hudson, H. E. (1982). Low-dosage high-rate direct filtration. *Journal (American Water Works Association)*, 74(5), 256-261.
- Water Specialist Technologies LLC. (2017). Jar test procedure for precipitants, coagulants, & flocculants. Retrieved from http://waterspecialists.biz/wp/?page_id=120
- Yu, W.-z., Gregory, J., Campos, L., & Li, G. (2011). The role of mixing conditions on floc growth, breakage and re-growth. *Chemical Engineering Journal*, 171(2), 425-430 doi:10.1016/j.cej.2011.03.098
- Yukselen, M. A., & Gregory, J. (2004). The effect of rapid mixing on the break-up and re-formation of flocs. *Journal of Chemical Technology & Biotechnology*, 79(7), 782-788. doi:10.1002/jctb.1056

APPENDIX A: RESULTS FROM BENCH-SCALE FLOCCULATION ANALYSIS

Initially an Alum dose of 50 mg/L was selected and evaluated across the pH range previously mentioned. Percent turbidity removals are shown in Figure A.1. At a target pH of 6.0, significant turbidity removals were observed under all testing conditions. Filtered turbidities observed were 0.34 (99.2 %), 0.51 (98.8 %), and 0.16 (99.6 %) NTU for 174 s⁻¹, LITF, and LITF with a combination of sedimentation and filtration, respectively. Treatment effectiveness with LITF began to deteriorate above a coagulated pH of 6.0. The addition of sedimentation to the treatment process produced a filtered turbidity of < 0.2 from target pH 6.0 to 7.5. A minimum turbidity (0.16 NTU, 99.7%) while flocculating at an intensity of 174 s⁻¹ was observed around a target coagulated pH of 6.5 which was followed by less effective treatment at higher pH values. The pH limit (6.0) for charge neutralization (as defined in Section 4.5.1.2) is included in the graph and is indicated by a yellow line.

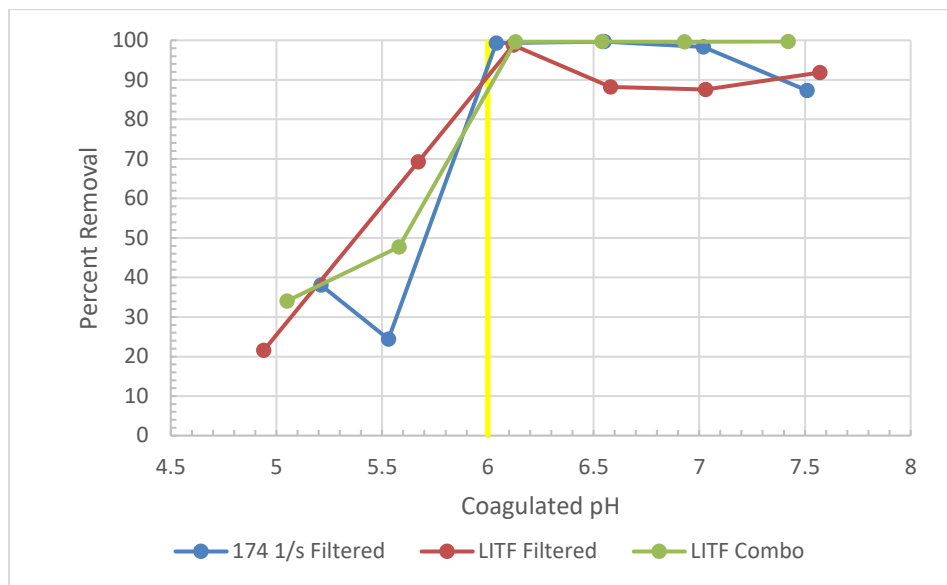


Figure A.1. The effects of different flocculation procedures on percent turbidity removals for model water #2 across a range of coagulated pH values at a constant coagulant dose of 50 mg/L as Alum.

Figure A.2 displays the results from flocculation testing at a target pH of 6.5 at select coagulant doses from 0 to 100 mg/L as Alum. LITF with combination particulate removal resulted in a filtered turbidity of 0.52 (98.9 %) at a coagulant dose of 10 mg/L as Alum. LITF with sedimentation and filtration (0.11 NTU, 99.8%), flocculation at velocity gradient of 174 s^{-1} (0.14 NTU, 99.7%), and LITF with direct filtration (0.70 NTU, 98.2%) all reached a filtered turbidity minimum at a coagulant dose of 30 mg/L.

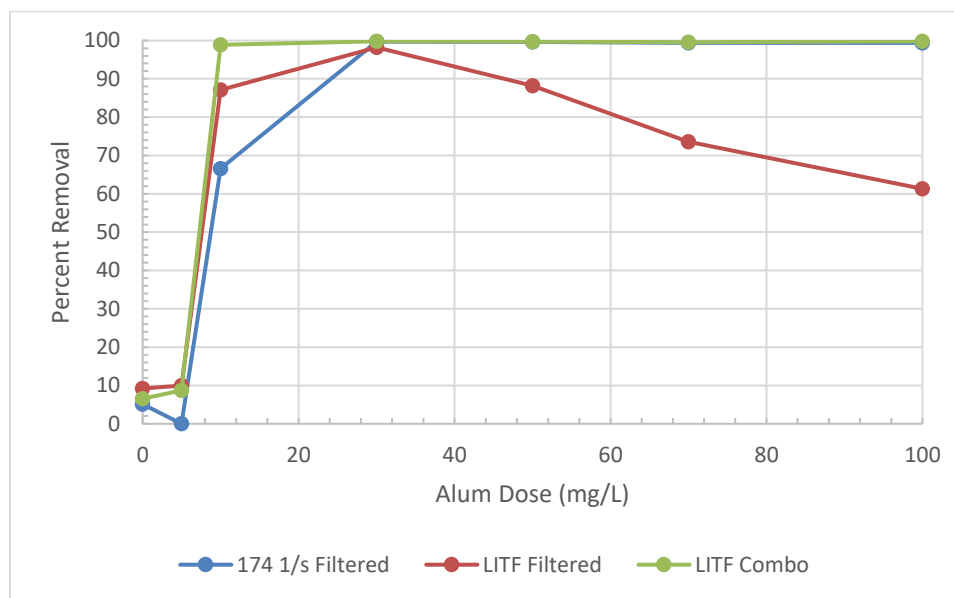


Figure A.2. The effects of different flocculation procedures on percent turbidity removals for model water #2 across a range of alum doses at a target coagulated pH of 6.5.

Testing with Alum at a constant dose of 10 mg/L, from pH 5.0 to 7.5 resulted in all three flocculation procedures producing graphs that were similar in shape. Regardless of applied flocculation procedure, it appears that the same conclusions could be drawn about potential zones of effective coagulation. Data from the three procedures evaluated were most similar about a target pH of 6.0. All turbidity removals at this target pH were > 93%. Results are shown in Figure A.3. Included in the graph is the upper pH limit (6.0) of charge neutralization limit.

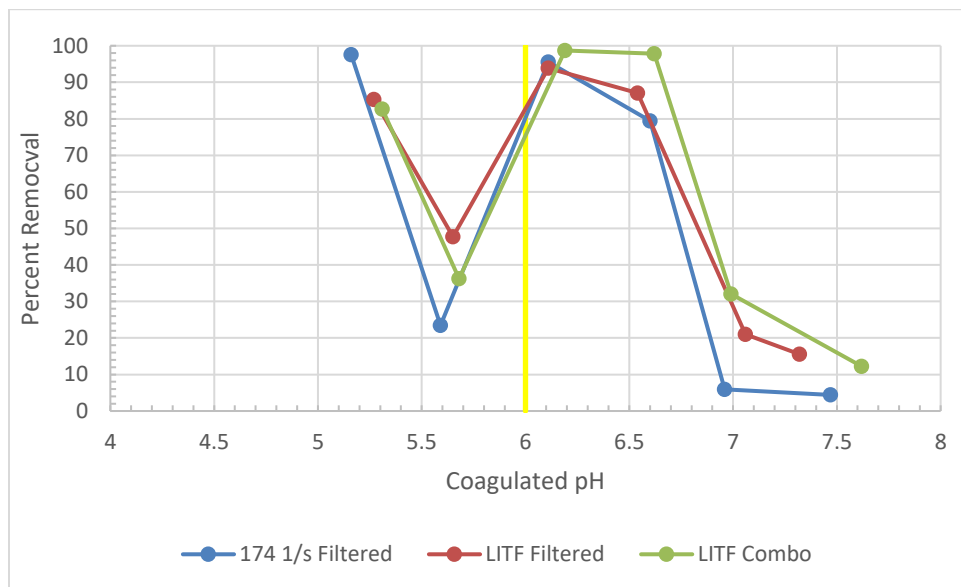


Figure A.3. The effects of different flocculation procedures on percent turbidity removal for model water #2 across a range of coagulated pH at a constant coagulant dose of 10 mg/L as Alum.

Results at a target coagulated pH of 5.5 had the same general trends as from previous testing, with flocculation at 174 s^{-1} and LITF with sedimentation and filtration resulting in the most similar results. An exception was observed at an Alum dose of 5 mg/L, where there was a difference of 11.3 NTU ($\approx 25\%$) in the filtered turbidities. At this dose, LITF with and without sedimentation provided the most similar results. It was observed that from an Alum dose of 10 mg/L to 70 mg/L LITF with direct filtration provided the greatest percent turbidity removals. Results are shown in Figure A.4.

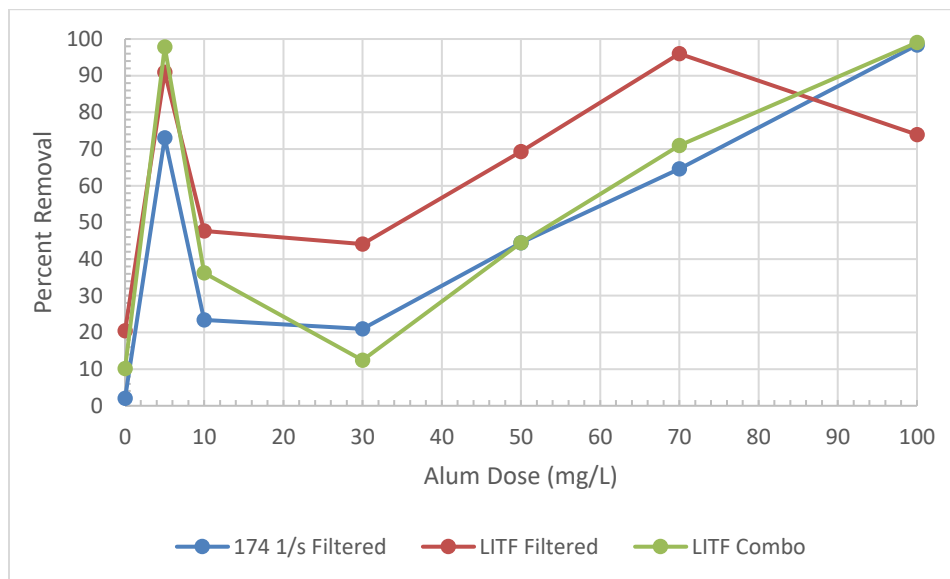


Figure A.4. The effects of different flocculation procedures on percent turbidity removal for model water #2 across a range of alum doses at a target coagulated pH of 5.5.

The following graphs are an individual comparison of the results from the different flocculation procedures. Direct comparisons of an individual flocculation procedure under different coagulation conditions should more easily allow for the identification of trends and effective coagulation conditions.

Figure A.5 shows the results from jar testing with flocculation at an intensity of 174 s^{-1} with direct filtration at coagulant doses of 10 and 50 mg/L as Alum. It was observed that at a coagulated pH of 5.16, a coagulant dose of 10 mg/L as Alum resulted in 97.6 % turbidity removals. At a coagulated pH near 6.0, single-stage flocculation indicates turbidity removals ≥ 95.0 % for both coagulant doses tested. This was the broadest range of effective alum doses observed at all coagulated pH values evaluated for this flocculation procedure. An Alum dose of 50 mg/L, resulted in turbidity removals ≥ 98 % from a coagulated pH of 6.0 to a coagulated pH of 7.0. Included in the graph is the upper pH limit (6.0) of charge neutralization.

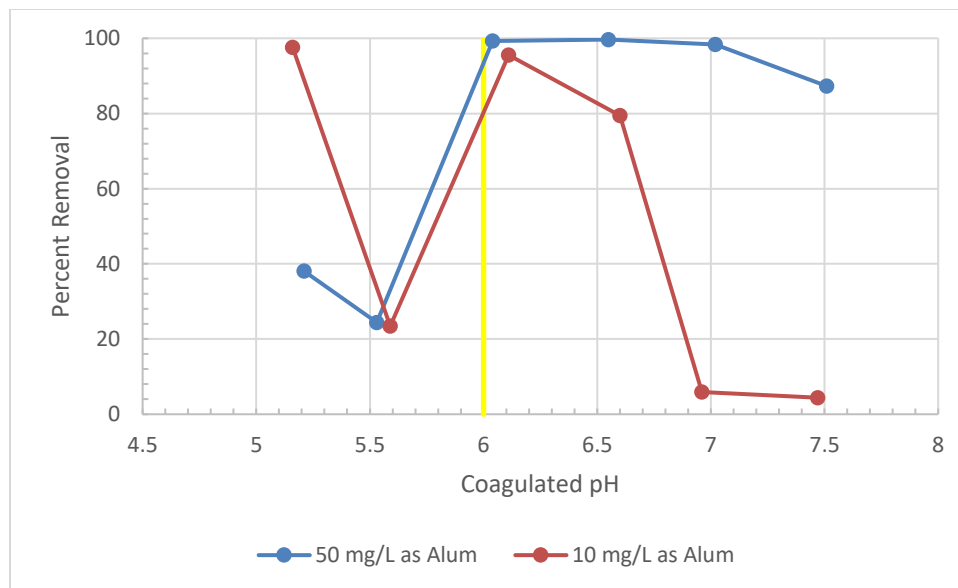


Figure A.5. Percent turbidity removal with flocculation at an intensity of 174 s^{-1} with direct filtration at Alum doses of 50 mg/L and 10 mg/L.

Figure A.6 is the results from jar testing with flocculation at an intensity of 174 s^{-1} with direct filtration at target coagulated pH values of 6.5 and 5.5. At a target coagulated pH of 6.5, turbidity removals were $\geq 98\%$ at a coagulant dose $\geq 30 \text{ mg/L}$ as Alum. Turbidity removals of this magnitude were only observed at an Alum dose of 100 mg/L for a target coagulated pH of 5.5. Based on the previous two figures, jar testing at a flocculation at intensity of 174 s^{-1} with direct filtration indicates a potential effective treatment zone between a coagulated pH of 6.0 and 6.5, with a minimum coagulant dose of 10 mg/L as Alum at a coagulated pH near 6.0.

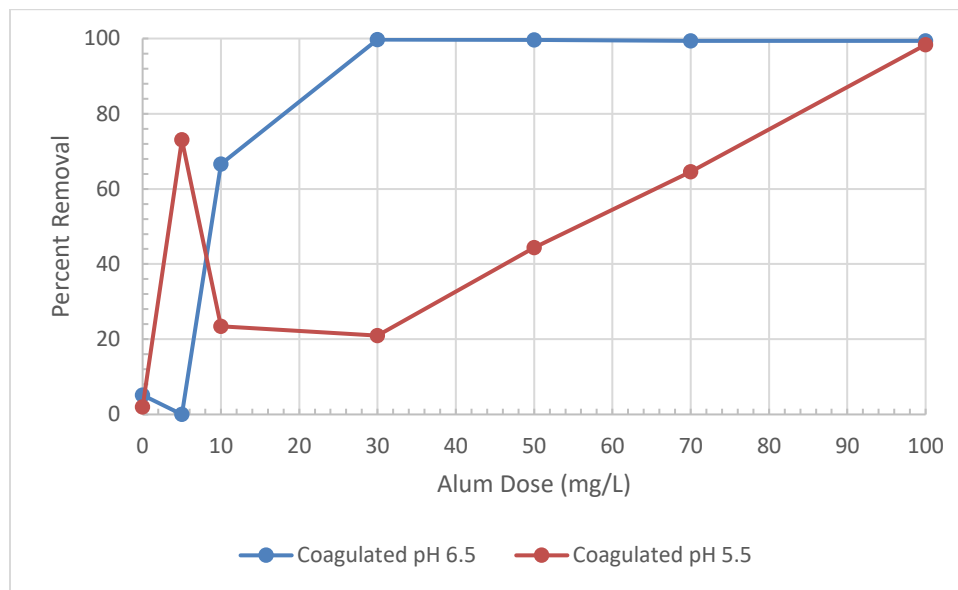


Figure A.6. Percent turbidity removal with flocculation at an intensity of 174 s^{-1} with direct filtration at target coagulated pH values of 6.5 and 5.5.

Figure A.7 shows the results from jar testing using LITF with direct filtration at coagulant doses of 10 and 50 mg/L as Alum. At a coagulated pH near 6.0 the most effective turbidity removals ($\geq 93\%$) for each alum dose was observed. These removals were not observed at any other treatment conditions evaluated. Included in the graph is the upper pH limit (6.0) of charge neutralization.

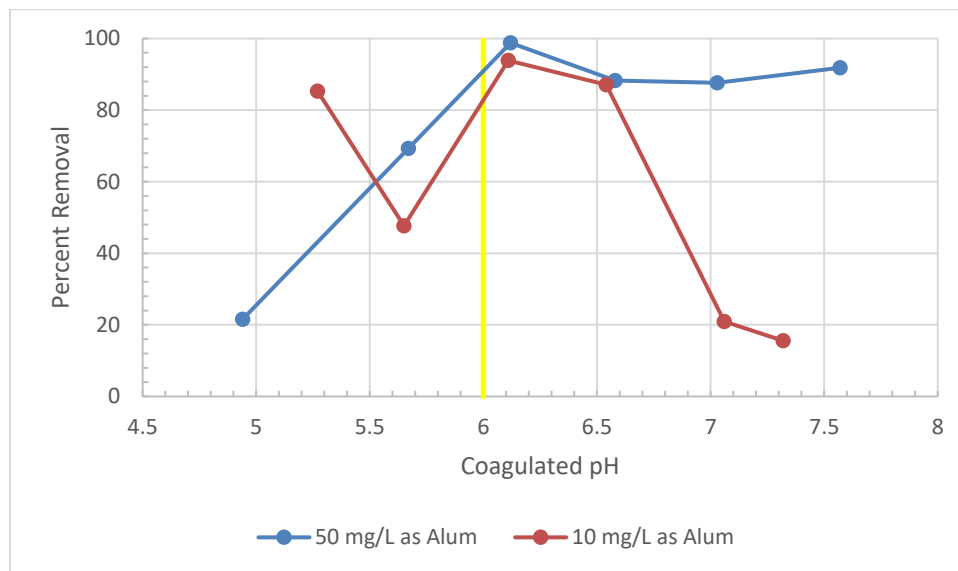


Figure A.7. Percent turbidity removal using LITF with direct filtration at coagulant doses of 50 and 10 mg/L as Alum.

Figure A.8 is the results from jar testing using LITF with direct filtration at target coagulated pH values of 6.5 and 5.5. At a target coagulated pH of 6.5, maximum treatment effectiveness was observed at a coagulant dose of 30 mg/L as Alum. Unlike jar testing with single-stage flocculation at a higher mixing intensity, treatment began to deteriorate beyond this point. Turbidity removals at a target coagulated pH of 5.5 peaked at an Alum dose of 70 mg/L, with removals of 96%. Data analysis for LITF with direct filtration indicates that there may be a zone of effective treatment similar to that indicated with flocculation at intensity of 174 s^{-1} , located between a coagulated pH of 6.0 and 6.5. A minimum effective coagulant dose appears to be located between 10 and 30 mg/L as Alum based on these results, but the zone appears to not extend to the higher coagulant doses evaluated.

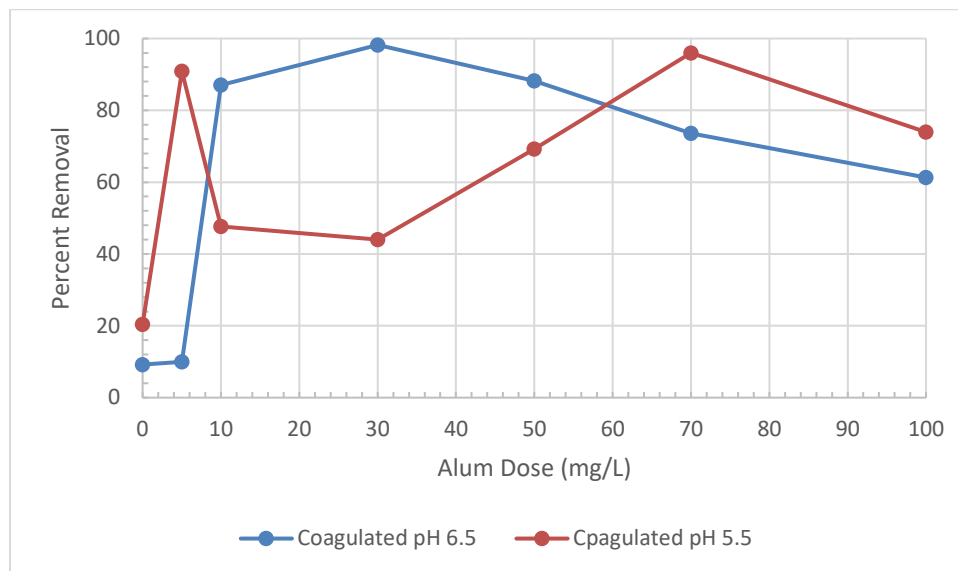


Figure A.8. Percent turbidity removal using LITF with direct filtration at target coagulated pH values of 6.5 and 5.5.

Figure A.9 shows the results from jar testing using LITF with sedimentation and filtration at coagulant doses of 10 and 50 mg/L as Alum. The application of sedimentation to the jar test procedure prior to filtration, showed that an effective treatment occurs at both coagulant doses evaluated at coagulated pH values near 6.0 and 6.5. Turbidity removals exceeded 97% under these treatment conditions. Beyond a coagulated pH near 6.5, treatment deteriorates with a coagulant dose of 10 mg/L as Alum. Included in the graph is the upper pH limit (6.0) of charge neutralization.

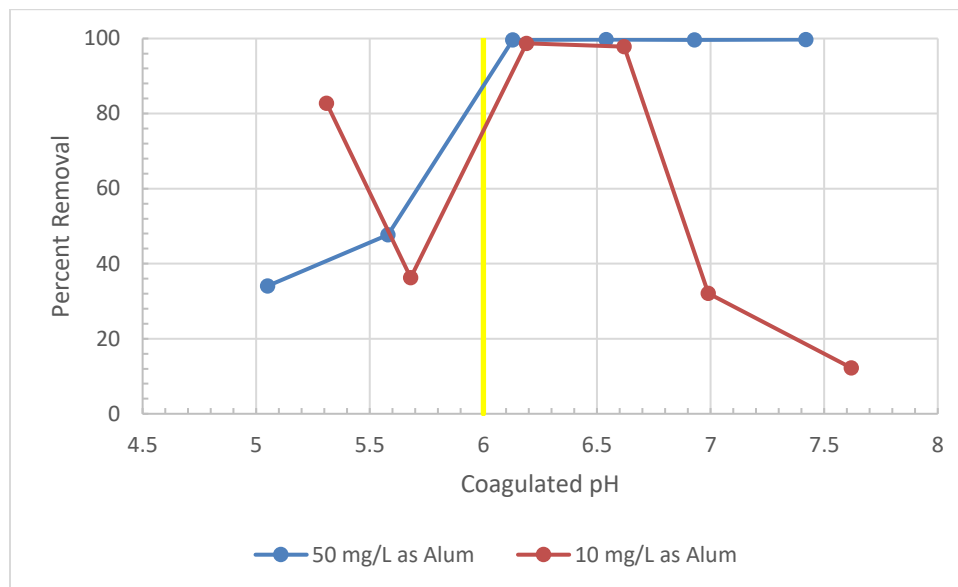


Figure A.9. Percent turbidity removal using LITF with sedimentation and filtration at coagulant doses of 50 and 10 mg/L as Alum.

Figure A.10 is the results from jar testing using LITF with sedimentation and filtration at target coagulated pH values of 6.5 and 5.5. For Alum doses 10 mg/L or greater, at a target coagulated pH of 6.5, turbidity removals overserved were $\geq 98.0\%$. At a target coagulated pH of 5.5, a coagulant dose of 5.0 mg/L as Alum resulted in turbidity removals of 97.8%. Removals exceeding 99% were observed at an Alum dose of 100 mg/L and a target coagulated pH of 5.5. Low-intensity, tapered flocculation with sedimentation and filtration indicates a potential point of treatment at coagulated pH near 5.5 and a coagulant dose of 5 mg/L as Alum. A treatment zone between a coagulated pH of 6.0 and 6.5 was also identified, with a minimum effective dose of 10 mg/L.

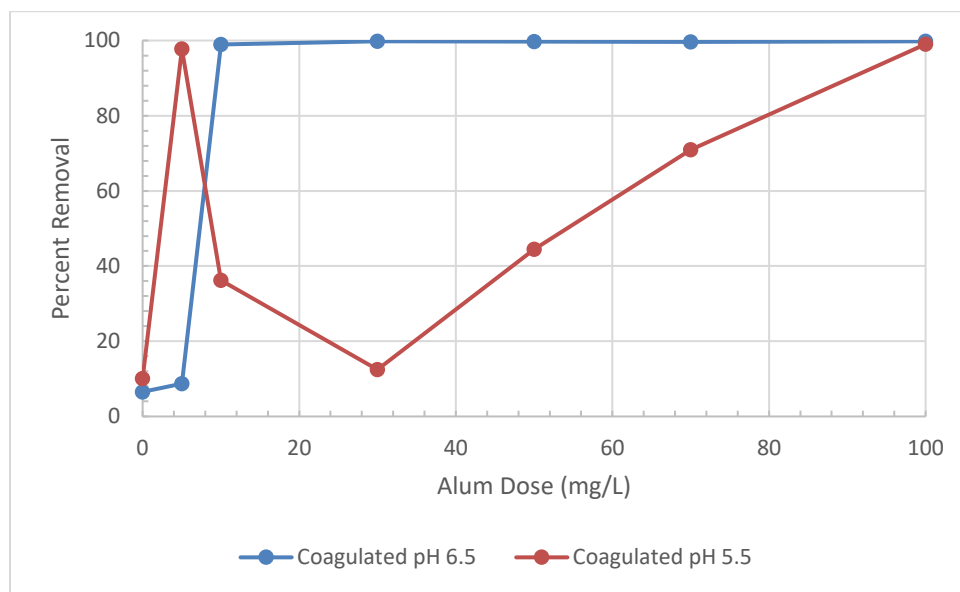


Figure A.10. Percent turbidity removal using LITF with sedimentation filtration at target coagulated pH values of 6.5 and 5.5.

APPENDIX B: JAR TEST PROCEDURE

NOTE: If the plant's jar test apparatus is programmable a sequential program should be set as follows:

Stage 1: 300 RPM for 1 Minute

Stage 2: 120 RPM for 20 minutes

Note: Flocculation is carried out for 10 minutes, the remaining time will be used for sampling and filtering

This procedure assumes titrations, if applicable, have been completed. Initial turbidity and pH values should have been measured and recorded.

1. Add 2 L of raw water to the jar tester jars and place on jar tester apparatus, centered below the mixers.
2. Lower the paddle mixer into each jar. Make sure to verify that each mixer is at the same height and centered in the jar.
3. Turn on the apparatus and set mixing speed to 100 RPM
4. Add the appropriate volume of pH adjusting chemical to each jar. If it is not possible to adjust operational pH, skip this step.
5. It is recommended that coagulant dosing be carried out with a syringe. There should be a syringe attached to the jar test apparatus above each jar. This aids in the optimal timing of each coagulant dose. Filling each syringe is as follows:
 - a. Pull the plunger out of the syringe.
 - b. Attach the syringe cap to the end of the syringe.
 - c. Pipette the appropriate volume of coagulant into the syringe.
 - d. Replace the syringe ensuring that it is in the locked position.
 - e. Invert the syringe and remove the cap.
 - f. Use the plunger to slowly push the air out of the syringe. Use care as not to eject any of the coagulant
 - g. Attach the syringe to the apparatus and repeat steps a – f for the remaining jars.
6. If using a programmable jar tester, start the sequential program and immediately dispense the coagulant into each jar. If using a manual jar tester, set the mixing speed to 300 RPM and then dispense the coagulant into each jar.

7. The rapid mix phase of testing will be carried out for 1 minute, during this time there should be a 250-mL beaker placed at each jar for pH sampling.
8. Upon completion rapid mixing, a 200-mL sample should be taken from each jar. A pH measurement should be taken and recorded as “coagulated pH”. This sample can now be discarded.
9. Flocculation should immediately follow rapid mix and initiate before taking the 200-mL pH sample. For plants without a programmable jar test apparatus the following applies:
 - a. Flocculate at 120 RPM for 10 min
 - Leave mixers running at 120 RPM after the final flocculation stage is over
10. After the pH measurements have been obtained, the spigot of each jar should be connected to its corresponding filter and a turbidity cell should be placed at each jar.
11. Immediately following 10 minutes of flocculation at speed of 120 RPM, the spigot of each jar should be opened one at a time in 15 second intervals.
12. Filter 800 mL of coagulated water through the filter. The water level should be at the 1 L mark on the jars.
13. After 800 mL of water has passed through the filter, a turbidity sample can be taken and recorded. The time interval between the openings of each spigot should allow for ample sampling time.
14. When turbidity measurements are complete, a final pH measurement needs to take from each jar.
15. Jar test is complete.